NONDESTRUCTIVE LOAD TESTING and COMPARISON OF APPROACHES
FOR BRIDGE LOAD RATING USING ASD, LFD, and LRFD METHODS

A thesis submitted by

Merve Iplikcioglu

In partial fulfillment of the requirements

for the degree of

Master of Science

in

Civil and Environmental Engineering

Tufts University

May 2012

ADVISOR: Masoud Sanayei, Ph.D.

Tufts
UNIVERSITY

OFFICE OF GRADUATE STUDIES

CERTIFICATE OF FITNESS

This certifies that the undersigned, appointed to determine the fitness of

Merve Iplikcioglu

for the degree of   Master of Science   in Civil and Environmental Engineering

have examined the candidate's thesis/dissertation (or papers) on the subject:

Nondestructive Testing and Comparison of Approaches for Bridge Load Rating

and have found it satisfactory.

March 17, 2012

Date of Defense

This certifies further that the candidate this day has successfully passed the customary examination.
We recommend, therefore, that the degree be awarded under the usual conditions.

SIGNATURES   NAMES

_____   Masoud Sanayei

Chairperson, Examining Committee   *Chairperson, Examining Committee*

                                            Brian Brenner

                                            Erin Santini Bell

                                            Gregory R. Imbaro

Medford, Massachusetts 02155
617.627.3395

Acknowledgments

This research would not have been possible without the guidance and the help of several individuals who in one way or another contributed and extended their valuable assistance in the preparation and completion of this study.

Firstly, I would like to emphasize that I am most grateful to have been a part of the NSF support research project "Whatever Happened to Long Term Bridge Design?". This experience provided me with the unique opportunity to gain a wider breath of experience in structural health monitoring and bridge design.

I am grateful and wish to express my gratitude to my first advisor Masoud Sanayei who was abundantly helpful and offered invaluable assistance, support and guidance. Deepest gratitude is also due to Brian Brenner for making me part of this project and giving me the opportunity. I am thankful to Erin Bell for the excellent example she has provided as a successful woman engineer and professor. I also would like to acknowledge Gregory R. Imbaro without his knowledge and assistance this study would not have been successful.

Special thanks also to all my graduate friends, especially my officemates; Jesse Sipple, Paul L. Rosenstrauch, Chris Paetsch, Peeyush Rohela, Wenjian Lian and my dear friend Pradeep Maurya for sharing the literature and invaluable assistance.

I would also like to convey my thanks to Fay, Spofford and Thorndike Inc for providing the opportunity to utilize their facilities.

I finally, wish to express my love and gratitude to my beloved family and Erman Kirtan; for their understanding and endless love and support, through the duration of my studies.

<div align="right">

Merve Iplikcioglu
March 9, 2012

</div>

I

Table of Contents

List of Figures

List of Tables

CHAPTER 1

Introduction

The Powder-Mill Bridge over the Warre River in Barre, Massachusetts was used as a pilot bridge for this study. The bridge was instrumented during the construction of the bridge, between June 2009 and October 2009 as part of a National Science Foundation Partnership for Innovation Project entitled, "Whatever Happened to Long-Term Bridge Design?" The project's title is inspired by the paper written by Thomos R. Kuesel (1990), "Whatever Happened to Long-Term Bridge Design?" Over the past three years of Powder-Mill Bridge service life, three diagnostic load tests were performed during the summers of 2009, 2010 and 2011.

In this study, rating factors of the Powder-Mill Bridge (PMB) are calculated using two methods of Allowable Stress Rating (ASR) and Load Factor Rating (LFR) using four different approaches. These four approaches are (1) conventional bridge load rating with hand calculations, (2) load rating using AASHTOWare® program Virtis 6.3, (3) load rating using nondestructive load test data, and (4) load rating using a calibrated 3D finite element model (FEM) with NDT data. In addition to calculating the load ratings using the four approaches mentioned above, a brief description is given on how the nondestructive test data was obtained as well as how the finite element model was calibrated. The comparison of these four approaches

will provide a better understanding of these methods. It will not only provide a comparison of the conventional load rating methods using ASR and LFR, but will also show the potential of using advanced rating techniques such as using NDT data and a calibrated FEM.

The main contribution of this research, shown in chapter 2, will be submitted for publication as a journal paper. The remaining chapters are supporting documents such as detailed explanations of instrumentation, load testing, DAQ and load rating calculations.

CHAPTER 2

Nondestructive Testing and Comparison of Approaches for Bridge Load Rating[1]

The Powder Mill Bridge in Barre, Massachusetts (Vernon Avenue over Ware River, Bridge No. B-02-012) was instrumented during construction and diagnostic load tests were performed. Bridge load ratings were calculated using the Allowable Stress Design, Load Factor Design, and Load and Resistance Factor Design methods with four different approaches. Initially, the rating factors of the Powder Mill Bridge were calculated by hand. The second approach used the bridge load rating program Virtis 6.3, developed by the American Association of State Highway and Transportation Officials, and the results were compared with the hand calculations. The third approach consisted of using the data collected during the diagnostic load tests to modify the load rating factor calculated by hand. The diagnostic load test data was also used to calibrate a finite element model of the Powder Mill Bridge. Finally, the fourth approach used a calibrated finite element model to determine load rating factors of Powder Mill Bridge. The rating factors obtained by using nondestructive test data and the finite element model were higher than the conventional load rating factor since both of these methods take advantage of the true three dimensional system behavior of the structure. The comparison and explanation of the

---

[1] Masoud Sanayei, Merve Iplikcioglu, Jesse D. Sipple, Erin S. Bell, Brian R. Brenner, Gregory R. Imbaro

aforementioned methods for calculating rating factors provide bridge owners with insight into the different approaches for calculating bridge load rating factors for maintenance and management decisions.

2.1   <u>Introduction</u>

Highway bridges in the United States are at risk due to age and deterioration. U.S. bridges are, on average, greater than 43 years old (AASHTO, 2008). According to Bridging the Gap, the five major problems for our nation's bridges are age and deterioration, congestion, soaring construction costs, maintaining bridge safety, and the need for new bridges (AASHTO, 2008). Based on the Federal Highway Administration (FHWA) data 71,177 (11.8%) bridges out of 604,460 bridges were rated structurally deficient and 78,477 (13.0%) were rated functionally obsolete (FHWA, 2010).

Existing bridges are required to be inspected at least once every two years. In some cases, more frequent inspection may be warranted based on advancing deterioration. Inspection reports include a numerical evaluation of bridge components, numbered on a scale from 0 to 9. A lower number indicates the inspector's evaluation that the structural component shows distress. The numerical evaluations are, to a degree, subjective, based on the inspector's experience.

In addition to regular inspections, owners may perform load ratings. This process requires a more detailed inspection, as well as a structural analysis to quantify specific capacities of bridge structural elements. The result of a load rating analysis may be a posting of the bridge for reduced allowable truck loading. Computing bridge load ratings is a tool that owners may use to determine the maintenance needs of the bridges, including load posting for public safety and/or scheduling its retrofit or replacement (Ellingwood et al., 2009). Therefore, having accurate load rating techniques and calculations are important for effective bridge management.

Improving technologies and approaches in structural instrumentation, analysis, and data management provide opportunities to address old problems in new ways. The traditional approach for bridge analysis has been developed long before the widespread use of computers. This approach seeks to isolate individual elements of a bridge structure and analyze them for

enveloped maximum demand conditions. For example, individual girders in a beam bridge are isolated in analysis and are subjected to the maximum loads and demands. This approach does not take advantage of, or consider, overall structural system behavior. The resulting analysis and design is appropriately conservative. But it is not an attempt to model in-situ structural behavior. More robust structural analysis models, structural instrumentation, sensing, and remote data reporting via wireless systems provide the opportunity to develop more realistic analyses and design approaches that can better model the true behavior. Load rating existing bridges with these new methods may help with the enormous challenge of evaluating and managing our nation's aging bridges.

Walter and Chase (2006) discussed how long term and short term bridge monitoring provide an objective and quantitative assessment basis leading to a better understanding of structural behavior and deterioration. Barr et al. (2006) presented an approach for using load test data in in conjunction with a finite element model (FEM) to determine the load rating of a bridge. Yost et al, (2005), found that the accuracy of load rating can be significantly improved through the use of a calibrated FEM. Alampalli and Kunin (2001) used load testing in order to calculate the load rating factors of a fiber reinforced polymer (FRP) bridge deck on truss bridge. This study showed that load rating factors, which were calculated using STADD software, closely agreed with the load rating factors calculated using the test data. DeWolf (2009) demonstrated to the Connecticut Department of Transportation (ConnDOT) that nondestructive field monitoring can be used to evaluate structural steel bridges that have been reported to have structural problems based on visual inspection and concerns related to increased traffic volume and increased loads. Kukay et al. (2010) developed nondestructive test methods in order to obtain the in-service residual prestressed force to evaluate eight AASHTO Type II bridges with 0.914m (36in) depths girders that were in service for approximately 40 years. Catbas et al. (2001) used three methods for load rating of a concrete T-beam bridge; the first method used the rating program BAR7, the second method was based on the load test result, and the third method used a FEM. In the National Cooperative Highway Research Program NCHRP Report 700 (2011) 1,500 bridges were analyzed using AASHTOWare® program Virtis 6.1. Both the Load Factor Design (LFD) and the Load and Resistance Factor Design (LRFD) methods were used to calculate critical shear and

moment load rating. Lessons learned from these previous exercises in load rating were incorporated into the calculation of rating factors for the Powder Mill Bridge.

In this study, rating factors of the Powder Mill Bridge (PMB) were calculated using Allowable Stress Rating (ASR), Load Factor Rating (LFR), and Load and Resistance Factor Rating (LRFR) through four different approaches. These four approaches were (1) conventional bridge load rating with hand calculations, (2) load rating using the AASHTOWare® program Virtis 6.3, (3) load rating using hand calculations modified by nondestructive test data (NDT), and (4) load rating using a 3D FEM calibrated with NDT data. In addition to calculating the load rating factors using the above four approaches, a brief description of NDT and model calibration procedure is presented. The comparison of these four approaches will provide a better understanding of load rating methods. It will not only provide a comparison of the conventional load rating methods using ASR, LFR, and LRFR, but will also show the potential benefit of using advanced rating techniques such as using NDT data and a calibrated FEM for objective bridge load rating.

2.2 **Powder Mill Bridge**

The PMB, Figure 1, is a three span continuous steel girder bridge with a composite reinforced concrete deck, located in Barre, MA. The bridge is 47 m (154 ft) long with a 23.5 m (77.1 ft) main span and two 11.75 m (38.55 ft) end spans.

Figure 2.2.1 Powder Mill Bridge (PMB)

6

Owned by the Town of Barre, the PMB was designed by Fay, Spofford, and Thorndike (FST) using the ASD method in 2004 and was constructed by ET&L Corporation in 2009. The bridge was designed for the HS-25 truck loading. Although it is at a rural location, the PMB supports a flow of heavy trucks from the Barre-Martone regional landfill and recycling facility near the bridge.

The PMB was instrumented as part of a National Science Foundation Partnership for Innovation project, "Whatever Happened to Long Term Bridge Design", which was awarded to a team of researchers and engineers by Tufts University and the University of New Hampshire. Instruments on the bridge were installed during the construction of the bridge, between June 2009 and October 2009. Six different types of sensors were installed: 100 strain gauges, 36 steel temperature sensors, 30 embedded concrete temperature sensors, 3 ambient temperature sensors, 16 uniaxial-accelerometers, 16 biaxial tiltmeters, and 2 pressure plates (Sanayei et al, 2012). All sensors are connected to data acquisition boxes located near the South Abutment shown in Figure 2. Collected static strain data were used for the NDT based load rating.

Figure 2.2.2 Data Acquisition System under the PMB

2.3   Diagnostic Load Tests

The instrumentation on the PMB allows for the bridge to be an excellent test bed of various types of nondestructive testing techniques. Data collected from three diagnostic load tests in 2009, 2010, and 2011PMB were used in this study. The following section will provide a

summary of the three load tests as related to their use in load rating calculations discussed here within.

2.4   2009 Diagnostic Load Test

The September 3, 2009 crawl-speed load test applied three load patterns running along the length of the bridge, paths X1, X2 and X3, as shown in Figure 3. The cross-section is shown facing north with the six girders numbered G1 to G6 from left to right. As shown in the annotations, load path X1 was 0.61 m (2 ft) off of the northwest curb and X3 was 0.76 m (2.5 ft) off of the southeast sidewalk. In path X1 the right tire was placed over girder G2; for path X3, the right tire was placed over girder G5. Load path X2 was centered over girder G3. For the crawl speed load test the truck speed was approximately 1.34 m/s (3 mph).
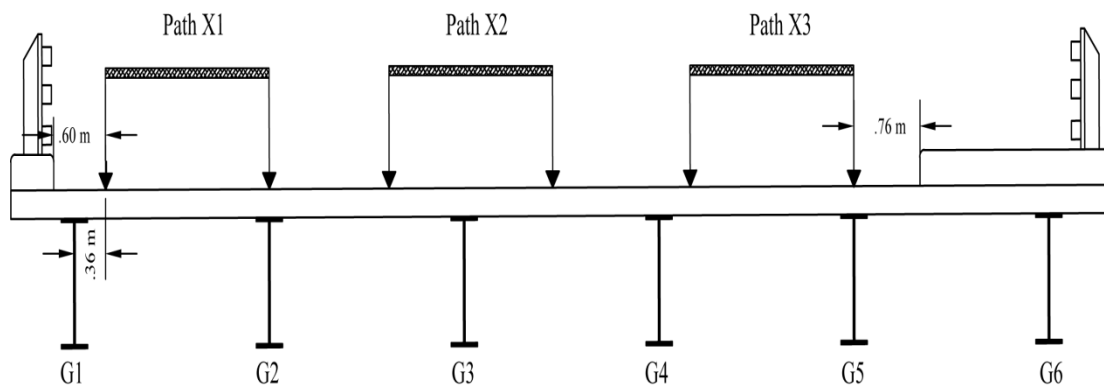
Figure 2.4.1. 2009 Truck Load Test Paths

A tri-axle dump truck was used for all load tests, Figure 4. The loaded truck had a total weight of 323.80 kN (72.78 kips). The axle loads for the first, second, and third axles were 87.31 kN (19.62 kips), 118.42 kN (26.62 kips) and 118.07 kN (26.54 kips), respectively for 2009 test truck.
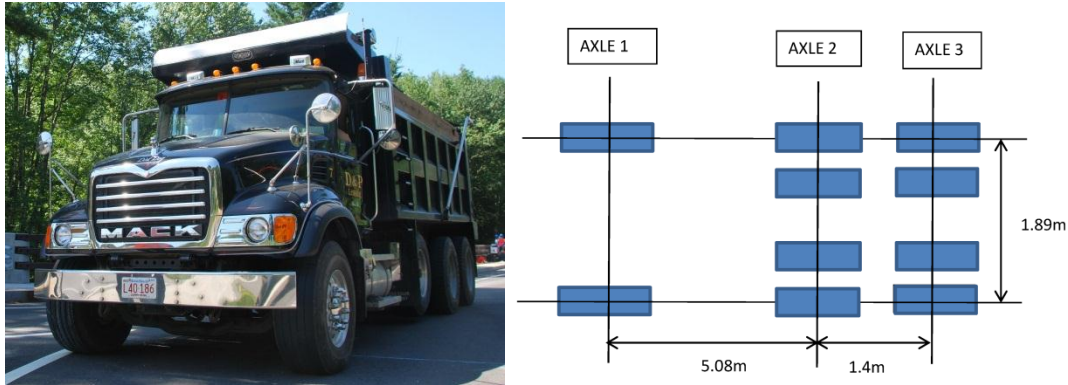
Figure 2.4.2 Test Truck and Dimensions

Sanayei et al (2012) presented updating the FEM using 2009 diagnostic load test static strain data. Ultimately, analysis of the 2009 load test data showed that this particular set of nondestructive test data could be used only to evaluate the load factors of girders G2, G3, and G5 because the strain gauges on girders G1, G4, and G6 did not exhibit a high enough response. Lessons learned from the 2009 load test and the calibrated FEM were incorporated into the design of the 2010 load test. The truck loading lanes were modified to excite each girder for NDT-based load rating.

2.5 2010 Diagnostic Load Test

During the July 31, 2010 load test, the truck paths were adjusted by positioning the test truck at the center of each target girder in order to induce higher stresses. As seen in Figure 5, truck paths were not able to be positioned directly above girders 1 and 6 due to the location of the safety curb and sidewalk. The total weight of the 2010 load test truck was 328.28 kN (73.79 kips) with the axle load for the first, second and third axles were 86.23 kN (19.38 kips), 121.71 kN (27.36 kips) and 120.34 kN (27.05 kips) respectively.

9
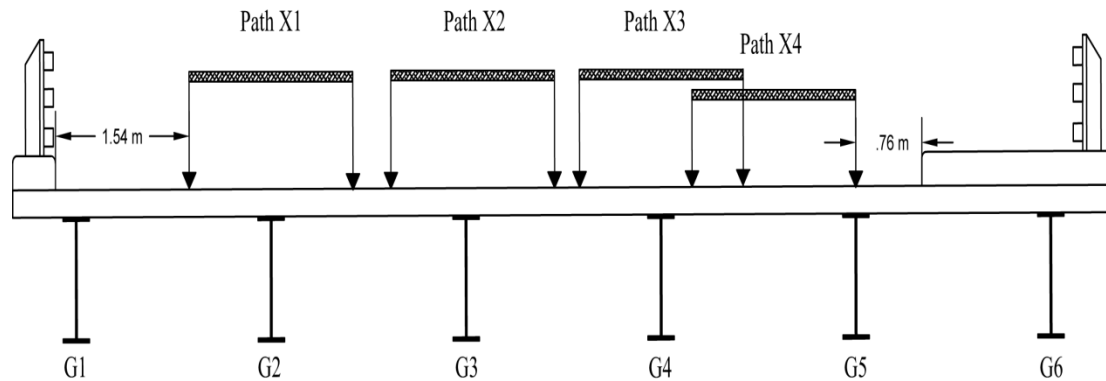
Figure 2.5.1 2010 Truck Load Test Paths

2.6   **2011 Diagnostic Load Test**

During the September 25, 2011 load test, the truck paths were once again modified to position the truck to effectively stress all of the girders and generate a sufficient response for load rating using NDT data, Figure 6. In the 2010 load test, even though the trucks were repositioned, stress levels in girders 1 and 6 were not high enough to be able to be included in the load rating. In order to avoid that same problem, two more truck paths were added in the 2011 test plan as close as possible to girders G1 and G6 to induce sufficient stress in them for use in load rating. The total weight of the 2011 load test truck was 353.59 kN (79.48 kips).The first, second, and third axle loads were 84.79 kN (19.06 kips), 134.79 kN (30.30 kips), and 134.01 kN (30.12 kips), respectively.
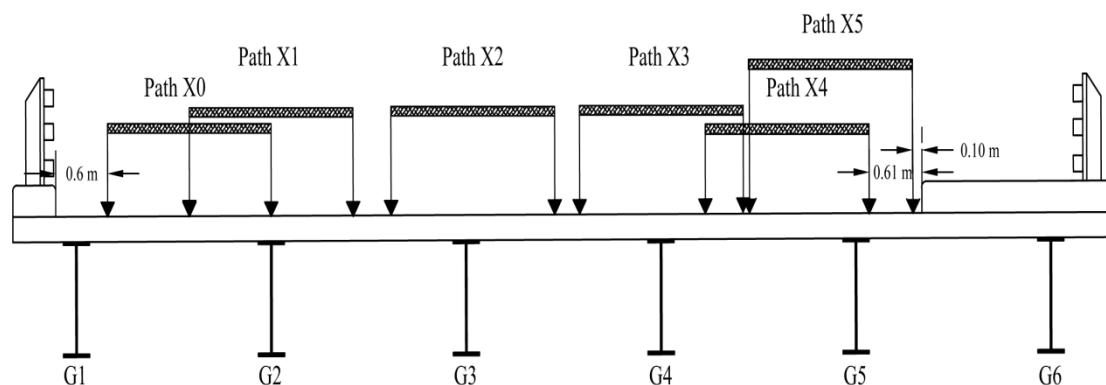
Figure 2.6.1 2011 Truck Load Test Paths

In summary, Figures 3, 5, and 6 illustrate the improvements to the load test plan. The truck paths for each year were modified to adequately stress all bridge girders to meet the requirements for load rating using NDT data. The increase in the weight of the test truck in 2011 to its maximum capacity was to further increase the stress levels in the exterior girders G1 and G6 for load rating. Most other aspects of the load test were kept consistent for each of the three load tests.

2.7   Load Rating Techniques and Methods

In the AASHTO Manual for Bridge Evaluation (MBE) (2011), three different methods for calculating load rating are presented: ASR, LFR, and LRFR. According to the FHWA Bridge Load Ratings for the National Bridge Inventory (NBI) policy (2006), load rating factors of the members should be based on the LRFD or LFD method if the bridge was designed using either the ASD or LFD methods. Additionally, the PMB falls under the guidelines of the Massachusetts Department of Transportation (MassDOT) Bridge Manual. According to the MassDOT Bridge Manual (MassDOT, 2007), if a bridge was designed using a method other than the LRFD specifications, it should be rated using the June 2007 Chapter 7 Bridge Load Rating Guidelines (MassDOT, 2005) and both ASR and LFR methods should be included. In order to represent all methods, ASR, LFR, and LRFR methods were applied using four different approaches.

The first approach of load rating used was conventional hand calculations. The second approach involved using a program developed by AASHTOWare® called Virtis. The 2011 version of Virtis (6.3) mimics and automates the first approach that is based on girder-by-girder analysis methods. The third approach of load rating takes advantage of bridge NDT data. This data captures the in-situ behavior of the bridge and is used to improve the conventional rating factors of the first approach. The fourth approach was to use an NDT calibrated 3D FEM. The first two approaches, hand calculations and Virtis, are typically used by bridge engineers, while the other two methods, NDT and FEM, are advanced approaches used less by rating engineers today, but which may be used more in the future. It should be noted that as long as the bridge exhibits linear behavior, diagnostic load test data can be used to validate and update the analytical model (AASHTO, 2011a).

While load rating using hand calculations and Virtis are most frequently used by bridge engineers, the, the MBE (2011a) provides criteria for load rating using advanced methods including *"analytical and empirical methods for evaluating the safe maximum live load capacity of bridges"*. The MBE also defines empirical methods as load rating by load testing and details a NDT based load rating procedure (NCHRP, 1998) Both the MBE and NCHRP were used as roadmaps for load rating using NDT data for the PMB.

The MBE (2011a) provides further options to the bridge engineer for methods of structural analysis suitable for the evaluation of bridges according to AASHTO 2010. AASHTO 2010 states that the finite element method is an acceptable method of analysis, therefore allowing the use of finite element models in load rating.

This trend towards using FEM in load rating can also be seen by AASHTOWare® which has been developing enhancements to create a Virtis finite element analysis engine (AASHTO Task Force Meeting, 2011). The FEM used for PMB goes a step further, as it is was field-calibrated using NDT data, and thus it provides more confidence that the analytical model is accurately representing the true behavior of the bridge. The fourth approach took advantage of NDT data and 3D finite element analysis.

2.8 Allowable Stress Rating, Load Factor Rating and Load Resistance Factor Rating

The Allowable Stress Rating and Load Factor Rating methods have two different levels of load rating, inventory and operating. The inventory rating level corresponds to the routine live load capacity for bridge traffic for an indefinite period of time. The operating rating level describes the live load capacity for less frequent vehicles. The operating rating is commonly used to decide the maximum permissible live load that the bridge could be allowed to carry.

The general expression to determine ASR and LFR load rating factor (RF) is (AASHTO, 2011a):

$$RF = \frac{C - A_1 D}{A_2 L (1+I)} \tag{1}$$

RF is the rating factor for the live load carrying capacity, *C* is the capacity of the member, *D* is the dead load effect on the member, *L* is the live load effect on the member and *I* is the impact factor. A_1 and A_2 are the dead and live load factors, respectively.

The ASR method considers the service condition only, and uses linear elastic method of analysis. The dead load factor, A_1 and live load factor, A_2, are both equal to 1.0 for inventory and operating levels. For inventory level, the capacity of a steel member is equal to an allowable stress of $0.55F_y$, where F_y is the yield stress of the steel. For operating level, the capacity of a steel member is equal to 0.75Fy.

The LFR method is based on the ultimate member capacity. The dead load factor A_1 and live load factor A_2 are equal to 1.30 and 2.17 at the inventory level and 1.30 and 1.30 at the operating level. The capacity of bridge members were calculated at the plastic moment.

Load Resistance Factor Rating has three levels of bridge ratings: design load rating, legal load rating, and permit load rating. Inventory and operating level load rating are determined from design load rating. Therefore, only design load rating will be calculated for the LRFR method.

The general expression to determine LRFR load rating factor (RF) is (AASHTO, 2011a):

$$RF = \frac{C - \gamma_{DC} \times DC - \gamma_{DW} \times DW - \gamma_P \times P}{\gamma_{LL} \times (LL + IM)} \tag{2}$$

The load factors for load rating calculation change based on the type of bridge and limit state, which is defined in AASHTO 2010. According to the MBE, strength is the primary limit state for load rating (AASHTO, 2011a).. At the inventory level, the dead load factor, γ_{DC}, is equal to 1.25, the superimposed dead load factor, γ_{DW}, is equal to 1.5, and the live load factor, γ_{LL}, is equal to 1.75. At the operating level, the dead load factor, γ_{DC}, is equal to 1.25, the superimposed dead load factor, γ_{DW}, is equal to 1.5, and the live load factor, γ_{LL}, is equal to 1.35.

Because the PMB is a three span continuous bridge, load rating factors were calculated separately for both the positive and negative moment regions; middle of the center span, and at the piers. The rating factors at the negative moment regions were found to be less than the

positive-moment load rating factors, therefore they are the controlling rating factors. Due to this reason, only negative moment region rating factors are presented in this paper.

2.9   Properties Used for Bridge Load Rating

Several assumptions about the properties of the structure were kept constant throughout the different approaches of load rating. The structure has three continuous spans and a composite concrete deck. For the calculation of live load stresses in the positive bending region, the steel girder and concrete deck were considered and the reinforcing steel conservatively neglected. For the negative bending region, the moment of inertia was calculated assuming no strength of concrete in tension, but taking into account the strength of the reinforcing steel. For the calculation of dead load stresses, the only resisting components included were the steel girders due to the use of stay-in-place forms with no shoring during construction. Therefore, only the weight of wet concrete was included, not the stiffness. For the superimposed dead and the live load, the composite structure for the positive moment region was used with a long-term composite section factor of *3n* for superimposed dead load, and short term composite section factor of *n* for live load (AASHTO, 2011a). In the calculation of section properties, the thickness of the haunch was included while the strength of the material was not used due to its small area. The modulus of elasticity for concrete was calculated using AASHTO, 2002. The structural steel is AASHTO M270M Grade 345W with the yield strength of 344.74 MPa (50 ksi).

There were several important assumptions made in calculated the load calculations, which were kept consistent between the different approaches. Elements included in the superimposed dead load calculations include the weight of the wearing surface, curb, sidewalk, and railing. The density of concrete used was 23.6 kN/m^3 (150 pcf), while the density for the wearing surface was 25.2 kN/m^3 (160 pcf). Based on MBE (AASHTO, 2011a) for LRFR method, the HL-93 design truck should be used; however, for consistency in comparison of load ratings, the HS-25 design truck was used for all methods. Two lanes were loaded with HS-25 trucks, axles weighing 44.5 kN (10 kips), 177.9 kN (40 kips), and 177.9 kN (40 kips), and no lane loads were used in the calculations. The distance between the axles was kept the same as the AASHTO Standard HS Truck, figure 6B.6.2-1 (AASHTO, 2011a). The distribution factors (DF) and impact factor (IM)

for ASR and LFR are same; however, the distribution factors and impact factors are different for the LRFR method, as shown in Table 1. These three distribution factors show the wheel loads as the full axle loads (Santini-Bell et al, 2012)

Table 2.9.1 PMB distribution and impact factors

Interior Girders	ASR	LFR	LRFR
DF	0.67	0.67	0.59
IM	25%	25%	33%

2.10   Rating Factors using Hand Calculations

To simplify hand analysis, a continuous 3-span beam model built from frame elements with member properties of the transformed bridge section was created in CSiBridge 15 (Computers and Structures Inc., 2011). This method allowed the live load and dead load moments to be easily obtained. A truck ran along the length of the bridge model to generate both the maximum positive and maximum negative live-load moments for load rating.

2.11   Rating Factors Using Virtis

In Virtis, the rating factors were computed based on flexural stresses for a beam member (Virtis 6.3, 2011). To calculate the rating factors using Virtis, detailed bridge geometry was input into the program and the HS-25 design truck was selected for analysis. The current version of Virtis essentially follows the same approach as hand calculations. It creates a continuous beam model using a transformed section of an individual girder and the deck using the bridge geometry. Then Virtis runs an analysis to determine minimum and maximum response values, which it uses for load rating (AASHTO, 2011b). The method used for analyzing the live load is an influence line for the maximum live load effect. Based on the moment and shear capacities and demands, the program calculates the rating factors using the ASR, LFR, and LRFR methods.

2.12 <u>Comparison of Hand Calculations with Virtis</u>

As discussed in the previous two sections, the rating factors for the PMB were evaluated by two conventional approaches; hand calculations and Virtis 6.3, each using the three methods, ASR, LFR, and LRFR. The conventional inventory and operating rating factors using hand calculations and Virtis 6.3 for the ASR method are shown in Figure 7.

(a) Inventory RFs   **(b)** Operating RFs
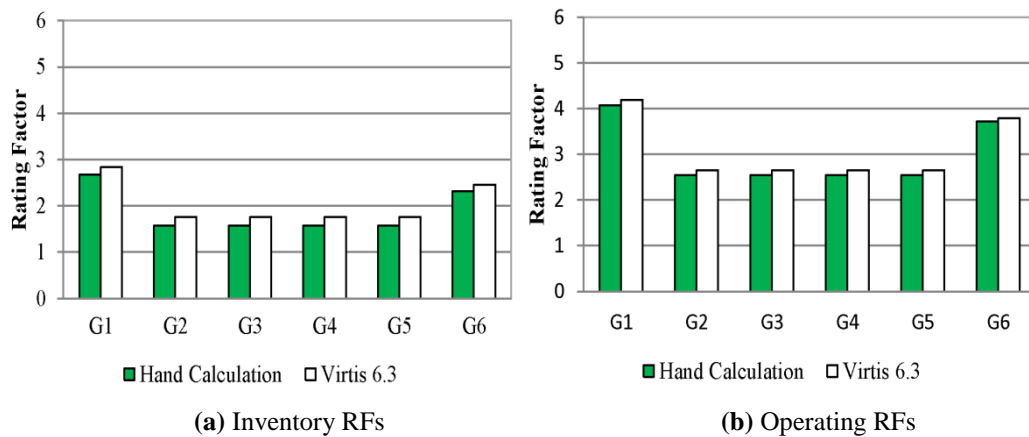
Figure 2.12.1 PMPB Design Office Rating Factors with ASR Method

Ratings performed by hand and Virtis follow the same principles, but there are slight differences between the two. For both, the superimposed dead loads of sidewalk, safety curb, and railing were distributed to the beams using a 60/40 exterior/interior distribution, while the dead loads of the concrete deck, haunch, and diaphragms were equally distributed to the beams according to MassDOT Bridge Manual (MHD, 2005). Also, as observed in Figure 7, the exterior girders have higher rating factors than the interiors girders for both hand and Virtis calculations. The reason for this is that exterior girders section modulus was approximately 1.5 times higher than the interior girders section moduli for live load plus impact stresses carried by long term composite. This translates into a higher capacity of the exterior girders. The maximum critical moment at the center of the middle span was 897 kNm by hand calculations and 888 kNm by Virtis, which is only slightly different.

In the following sections, the hand calculated rating factors for ASR, LFR, and LRFR methods are used to evaluate the load rating factors instead of Virtis, since all the details that went into these calculations are known exactly and all assumptions are clear. Load rating factors using hand calculations alone are compared with load rating factors using hand calculations

modified by NDT data and load rating factors calculated using a calibrated FEM. Virtis rating will not be shown in subsequent graphs since they are close to the hand calculations.

2.13   Rating Factors using Diagnostic Load Test Data

The third approach of load rating for the PMB uses data from nondestructive tests to enhance the ratings already determined by hand calculations. Based on the MBE (AASHTO, 2011a), diagnostic load tests are used to observe the bridge system behavior and to reduce uncertainties. Furthermore, based on the MBE, if the bridge exhibits linear-elastic behavior during the diagnostic load test, the NDT results can be used for model calibration and load rating (AASHTO, 2011a).

While the bridge test is performed on the actual bridge structure, which has true 3D behavior, load ratings using NDT data are achieved by modifying the load ratings calculated using hand calculations, which are determined using AASHTO distribution factors. Therefore, this combination of true 3D bridge behavior and hand calculations, which are girder-by-girder based, can be seen as closer to the actual bridge behavior although not fully capturing the true behavior of the bridge since the initial values that are modified are based hand calculations.

A sample of the strain data from the 2009, 2010 and 2011 static load tests, for load path X2 are shown in Figure 8 with truck location along the bridge on the x-axis and strain on the y-axis. The truck location along the x-axis of the graphs was measured by tracking the truck during the load test using an Automated Motorized Total Station. For this sample data, the strain gauges are located at the south side of the north pier, which is in the negative bending moment region of the girder. Strain gauge 43 is at the right side of the top flange, strain gauge 44 is at the left side of the top flange, strain gauge 45 is at the right side of the bottom flange, and strain gauge 46 is at the left side of the bottom flange. Each year the truck weights were different and in order to compare the results, the 2010 and 2011 test data were scaled linearly for better comparison with 2009 test data.
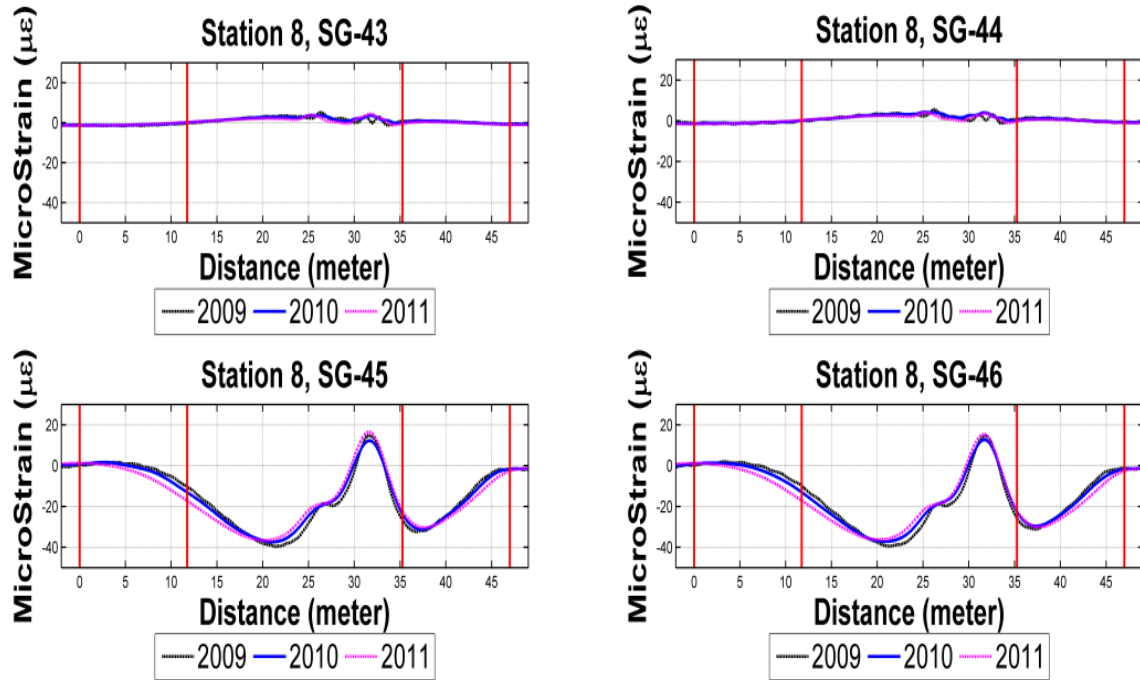
Figure 2.13.1 Girder 3 Strains at South Side of North Pier

The Research Digest (NCHRP, 1998) recommends using legal load vehicle for nondestructive test, however acknowledges that *"test vehicles representative of AASHTO legal and rating vehicles are seldom available"*. NCHRP (1998), which describes how to use a test truck that is not considered an AASHTO legal vehicle for load rating with NDT data. The following equation provides the load rating based on the static load test results (AASHTO, 2011a):

$$RF_T = RF_c * K \qquad (3)$$

The variable RF_C is the analytical rating factor, which was calculated by hand. RF_T is the adjusted rating factor for the live-load capacity based on the static load tests. The variable K is defined in NCHRP (1998) as an adjustment factor that allows the comparison of the measured behavior, from NDT, with the analytical behavior from hand calculations. The adjustment factor K can provide a benefit by increasing the rating factor calculated by hand and is defined as (NCHRP, 1998):

$$K = 1 + K_a \times K_b \qquad (4)$$

18

The term K_a considers both theoretical and measured differences, while K_b considers only theoretical differences. The term K_a specifically looks at the ratio between the theoretical strain and measured strain defined as (NCHRP, 1998):

$$K_a = \frac{\varepsilon_C}{\varepsilon_T} - 1 \tag{5}$$

where ε_T is the maximum measured member strain during the load test and ε_C is the theoretical value calculated from the test vehicle in the same position as the truck in ε_T.

ε_C, live load lateral distribution factors were calculated based on the actual truck position using the lever rule. The bridge section properties are based on the AASHTO Standard Specifications (AASHTO, 2002) and separate values are calculated for positive and negative regions. The truck load is then applied to a continuous 3-span beam model to determine moments which are then converted to strain. The K_a factor provides the connection from the measured data to the theoretical assumptions that were used in the hand-calculated rating and accounts for the benefit derived from the load test. The K_b factor takes into account the understanding and explanations of the changes in load carrying capacity, the ability of the inspection team to find problems, and the critical structural features of the bridge. One important factor in determining K_b, defined as K_{b1} in the Research Digest (NCHRP, 1998), is the *T/W* factor.

According to NCHRP (1998), the test truck should be large enough and placed in multiple positions on the bridge so that all critical members are sufficiently stressed, (AASHTO, 2011a). Ensuring that the ratio between the theoretical moment produced by the test truck, *T,* and the maximum live load moment plus impact due to the design truck, *W*, is greater than 0.4. Both of these values are calculated using a simple beam model with an effective moment of inertia and are both analytic values. The T/W ratios are used to determine K_b values based on MBE (AASHTO, 2011a). In the MBE the factor K_b is a value between 0 and 1, which indicates the level of confidence in the load test. Tables 2 through 4 show the *T/W* values for the PMB. The values found here are then combined with the values for K_a to determine K as shown in equation (4). *K* serves as a multiplier. If it is greater than one, the rating factors are higher than the hand calculation, which indicates that the bridge capacity is higher than conventionally calculated rating factors. Conversely, if it is less than one, the rating factor is lower than the hand

calculation, which means the capacity of the bridge is lower than the conventionally calculated rating factors. The *K* factors for the PMB were calculated in accordance with the MBE (AASHTO, 2011a). Calculated *K* factors for the three years are shown in Tables 2 through 4.

Since load rating deals with maximum response compared with capacity, it is best for the strain gauge to be installed at the maximum bending moment locations. However, this was not the case for the PMB. Therefore, the NDT strain reading of the nearest strain gauge was adjusted to the location of maximum strain. For the theoretical values, the test truck axle loads were multiplied by distribution factors which were calculated based on the test truck position during the diagnostic load test and run on a simple 3-span continuous beam model to calculate maximum bending moments caused by the test truck.

Table 2.13.1 Rating Factor with 2009 NDT Data using ASR method

G #	Strain Gauge #	Measured (µε)	Max Measured Strain (µε)	Max Theoretical Strain (µε)	Truck Path	T/W	K	Inv. RF	Opr. RF
1	SG6	92.91	104.99	88.23	X1	0.38	1	2.67	4.07
2	SG22	96.94	109.54	175.94	X1	0.53	1.49	2.34	3.80
3	SG42	93.06	105.19	175.94	X2	0.53	1.54	2.42	3.93
4	SG61	81.56	92.16	127.53	X3	0.38	1	1.57	2.55
5	SG82	88.43	99.98	175.94	X3	0.53	1.61	2.53	4.11
6	SG96	60.63	68.52	N/A	X3	N/A	N/A	N/A	N/A

Table 2.13.2 Rating Factor with 2010 NDT Data using ASR method

| G #	Strain Gauge #	Measured (µε)	Max Measured Strain (µε)	Max Theoretical Strain (µε)	Truck Path	T/W	K	Inv. RF	Opr. RF
1	SG6	70.98	80.21	44.84	X1	0.19	1	2.67	4.07
2	SG22	101.46	114.65	179.04	X1	0.53	1.45	2.28	3.70
3	SG42	91.66	103.58	179.04	X2	0.53	1.58	2.48	4.03
4	SG61	94.59	106.97	179.04	X3	0.53	1.54	2.42	3.93
5	SG81	84.32	95.28	179.04	X4	0.53	1.64	2.57	4.18
6	SG96	51.62	58.33	N/A	X4	N/A	N/A	N/A	N/A

Table 2.13.3 Rating Factor with 2011 NDT Data using ASR method

G #	Strain Gauge #	Measured (με)	Max Measured Strain (με)	Max Theoretical Strain (με)	Truck Path	T/W	K	Inv. RF	Opr. RF
1	SG6	91.25	103.11	97.46	X0	0.42	1	2.67	4.07
2	SG21	104.56	118.15	194.34	X1	0.58	1.52	2.39	3.88
3	SG41	100.20	113.23	194.34	X2	0.58	1.58	2.48	4.03
4	SG61	103.46	116.91	194.34	X3	0.58	1.53	2.40	3.90
5	SG81	71.02	80.25	143.35	X5	0.41	1.63	2.56	4.16
6	SG96	71.12	80.37	34.80	X5	0.15	1	2.32	3.72

Using the three years of load test data from the PMB, the hand calculated load rating factors were modified. Load rating factors for all interior girders were increased as shown in Figure 9. However, exterior girders G1 and G6 did not increase due to geometric limitations imposed by the sidewalk and curb, respectively. The test truck could not be positioned close enough to G1 and G6 to sufficiently stress these exterior girders. This resulted in the *K* factor being set to one and the analytical rating factors were used for these girders.

(a) Inventory RFs **(b)** Operating RFs
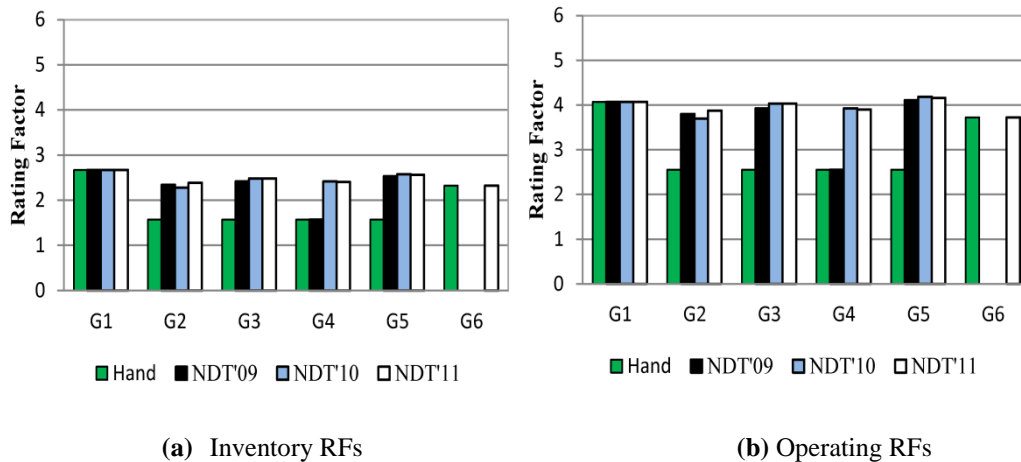
Figure 2.13.2 PMB Rating Factors with ASR Method using NDT Data

Overall Figure 9 shows an increase in rating factors calculated using NDT data, as compared the values from conventional hand calculations, for all interior girders for all three load tests. The reason for this increase is that since the position of the truck and the weight of the truck created higher stresses in the girders, both ε_T and *K* values were increased, thus resulting in higher rating factors. The overall increase of the load ratings in the interior girders shows the

21

benefit of performing NDTs for exploring the reserve capacity of bridges. Note that this increase was not observable using 2009 NDT data for G4 due to the selected truck path. Therefore, in this type of nondestructive testing for bridge load rating, it is paramount to select truck load paths and truck weight to sufficiently stress the target girders. Also, strain gauges should be mounted in the vicinity of the predicted maximum strain locations.

2.14   Rating Factors Using Calibrated FEM Model of PMB

The fourth and final method used in the load rating comparison of the PMB was performed using an FEM calibrated with NDT data to evaluate bridge girder load rating factors. The accuracy of conventional load ratings might be improved by capturing the system behavior of the bridge by using a 3D FEM that is calibrated with NDTs performed on the bridge.

A 3D FEM was created at Tufts University (Sanayei et al., 2012). The bridge deck was modeled with solid elements and the steel girders were modeled with shell elements. The bridge supports were modeled with springs representing the steel reinforced elastomeric neoprene bearing pads. Due to high flexibility of these supports compared with the substructure and foundation, only the bearing pads and superstructure was modeled. The neutral axis of the PMB superstructure was calculated with and without reinforcement. Since the difference was not significant, the reinforcement was not included in the model. The bridge model was successfully calibrated and verified using the 2009 NDT truck load test data.

During these three years of load testing, the path X2 over girder 3 was kept consistent to more easily compare the bridge behavior over the three years. Since the truck weights were slightly different, the 2010 and 2011 NDT data were scaled with respect to the 2009 NDT data. Scaled test data responses for 2009, 2010, and 2011 are compared with the calibrated FEM response in Figure 10. For this sample data, the location of the strain gauge 42 is at the center span girder 3, which is in the positive bending moment region of the girder.
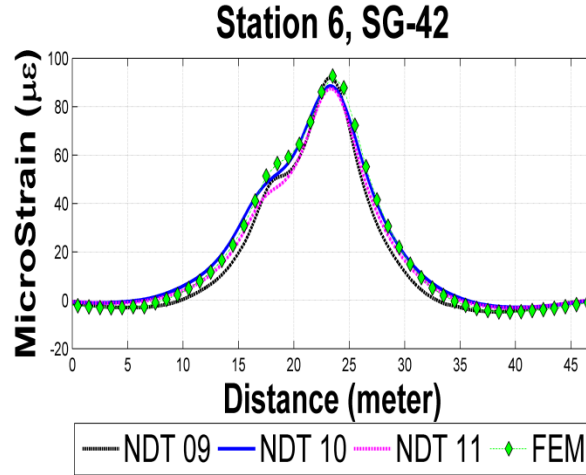
Figure 2.14.1 Girder 3 Strains at Center Span

Longitudinal (normal) stresses were used to calculate the PMPB rating factors using the FEM. For this purpose, equation 1 was modified using longitudinal stress components (AASHTO, 2011a),

$$RF = \frac{\sigma^C - A_1(\sigma^{DL} + \sigma^{SDL})}{A_2\sigma^{LL}(1+I)} \qquad (5)$$

where σ^C is the longitudinal stress capacity of the individual girder, σ^{DL} is the longitudinal stress caused by dead loads, σ^{SDL} is the longitudinal stress caused by superimposed dead loads, and σ^{LL} is the stress value resulting from live loads. Longitudinal stresses caused by dead load, superimposed dead load, and live load were extracted from the FEM. The longitudinal stress capacity was calculated by hand using MBE (AASHTO, 2011a).

The calibrated FEM is used to simulate assumptions made in the hand rating calculations and obtain rating factors for the bridge. To replicate these assumptions, the bridge was loaded in two lanes with the HS-25 trucks positioned to apply the greatest load to the girder of interest according to AASHTO, 2002. A linear multi step static case was created as a load case in SAP2000 (Computers and Structures Inc, 2010) and for each step, longitudinal shell stresses were output and converted to strains.

The longitudinal stress values were obtained from runs in the FEM with each set of two lanes loaded applied individually for each girder. The critical stress value used for the calculation

of load rating factors was obtained from either the maximum positive or maximum negative stress. The locations of these stress values were at the areas of actual maximum positive and negative stresses, and are not limited to location of sensors since they are obtained from a FEM.

2.15   Remarks for Three Years of Load Ratings

Results from all four methods used to evaluate the load rating of the PMB are shown in Figures 11, 12 and 13. The NDT rating factors of PMB are higher than the conventional design office hand calculations. The reason for this increase is that NDT data more accurately captures the in-situ system behavior and lateral live load distribution of the bridge structure caused by the stiffness of the diaphragms and the continuous deck across the girders. Therefore the distribution of loads is more realistic than the hand-calculated, approximate distribution factors.
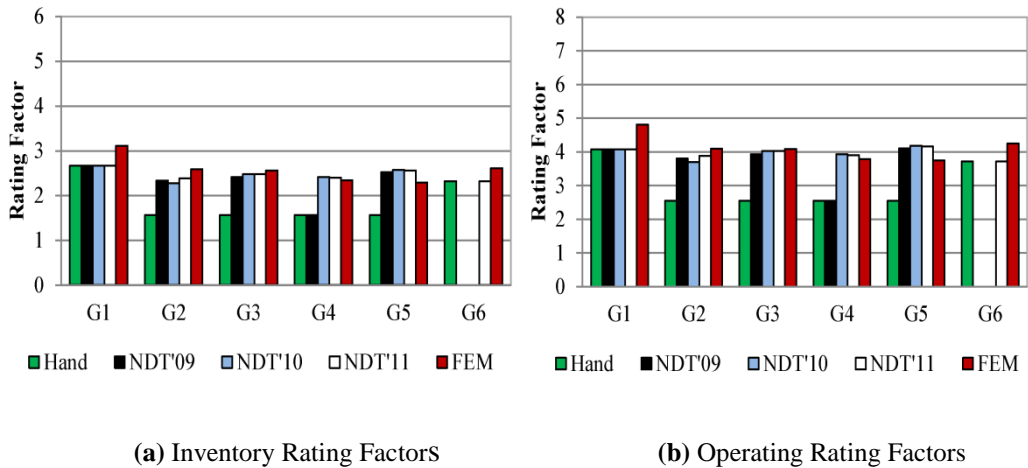

(a) Inventory Rating Factors   (b) Operating Rating Factors

Figure 2.15.1 PMB Rating Factors with ASR Method

(a) Inventory Rating Factors   (b) Operating Rating Factors

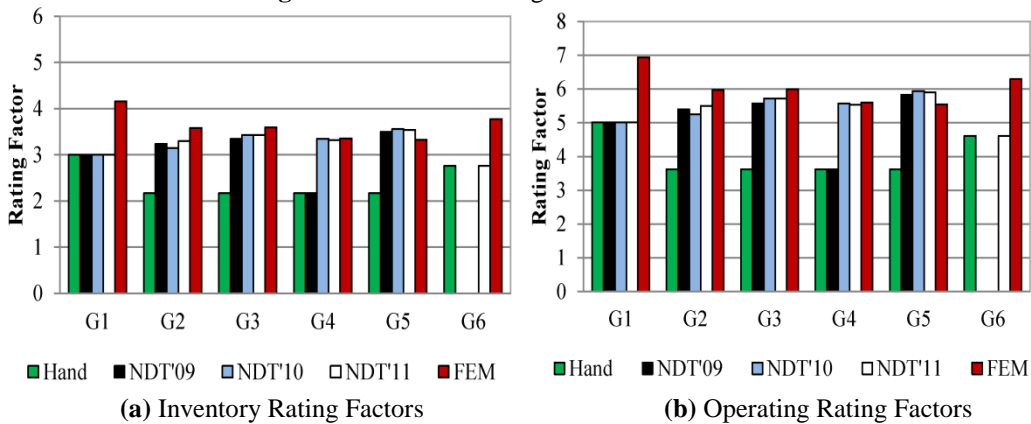**Figure 2.15.2** PMB Rating Factors with LFR Method

24

(a) Inventory Rating Factors   **(b)** Operating Rating Factors
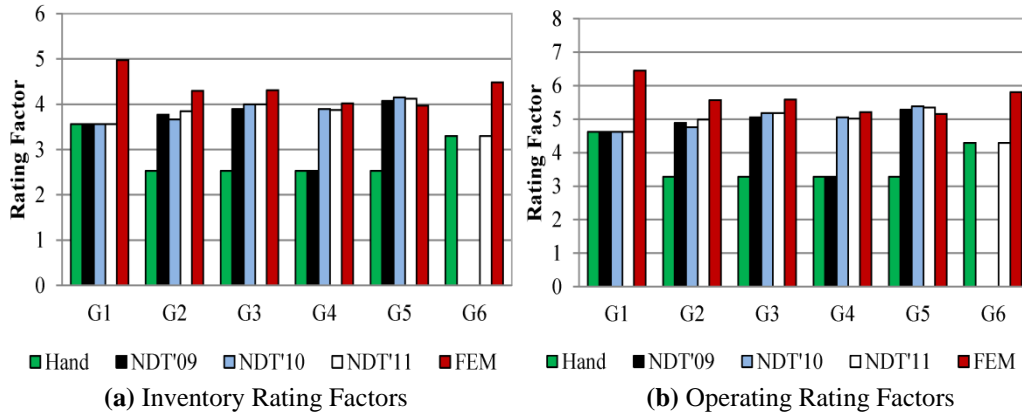
Figure 2.15.3 PMB Rating Factors with LRFR Method

The LFR method showed more capacity than did the ASR method. This behavior is expected for shorter span bridges when using the LFR method. The LFR method tends to result in more capacity for shorter spans. When the span length gets longer, the difference slightly decreases (Kulicki, 2000). The LRFR method shows a higher capacity than the LFR method. The reason for this difference is that the live load factor for LRFR is less than LFR, i.e. 2.17 and 1.75, respectively.

Furthermore, it is noted that the load rating factors obtained using the calibrated FEM were found to be similar to the rating factors calculated using NDT data. The NDT rating observes only in-situ 3D system behavior from the measured data and modifies the hand calculations which have no 3D system behavior. However, the calibrated FEM observes both the in-situ 3D system behavior as well as the analytical 3D system behavior since the model is calibrated with actual test data. Therefore the FEM response is closer to the true behavior of the structure and is based on more accurate live load distribution factors as compared to AASHTO methods.

In the hand calculations, superimposed dead loads were distributed using a 60/40 distribution as stated previously and hand calculated rating factors were modified by NDT data. However, in the FEM, superimposed dead load, locations were the same on the actual structure; therefore girders G4, G5 and G6 were under the effect of the sidewalk weight. As a result, the FEM load rating factors of those girders were slightly lower rating factors than the NDT rating factors. In addition, girders 4 and 5 support a water pipe under the bridge, which uses different

25

set of diaphragms with different stiffnesses, leading to lower load rating factor in the FEM rating.

The 3D behavior of the PMB is well represented in the FEM, because the model itself determines the distribution of loads based on stiffness, connectivity, geometry, and internal indeterminacies of the structural system. Using the calibrated FEM to determine load rating of the PMB resulted in rating factors that were higher than those obtained through analytical calculations. This analysis method which more closely models the actual behavior of the bridge suggests that the structure has additional capacity than what would be reported by the traditional, element-by-element approach. However, the bridge rating engineer should use judgment under the guidelines of AASHTO to determine how much additional capacity should be reported and relied upon.

It was observed that the load rating factor are sensitive to the differences between the capacity and dead load moments in the numerator of (1) and are also influenced by the changes in live load moments in the denominator. Therefore, all loads should be calculated carefully in order to rate the bridge accurately.

Once the bridge is load rated, this rating can be converted into tons, represented as *RT* in equation 6, with *RF* being the rating factor from tables shown in Figure 11 and *W* being the weight of the truck in tons that was used to compute the live load effects (AASHTO, 2011a).

$$RT = RF \times W \tag{6}$$

For example, looking at the ASR ratings from the hand calculations, the lowest rating level for both inventory and operating, 1.57 and 2.55, are multiplied by the gross weight of the HS-25 truck to obtain a total weight of 70.65 US Tons and 114.75 US Tons for inventory and operating, respectively. It should be noted that this weight is just a scaling for the same axle configurations of the HS25. If the truck load rating is desired for a truck with different axle configuration and distribution, then the rating factors must be computed for that specific configuration.

2.16   Conclusions

The Powder Mill Bridge in Barre, Massachusetts was instrumented as part of a National Science Foundation research project. Instrumentation included strain gauges, and strain data was used for this study. Three load tests have been performed during each of the first three years of bridge service. Load rating calculations were done for the PMB using the methods of ASR, LFR, and LRFR with four different approaches: (1) by hand calculations; (2) using Virtis 6.3; (3) using NDT data; and (4) using a calibrated FEM. These four approaches provide different load ratings for each of the three methods. Overall, the NDT and FEM approaches showed more load rating capacity than the conventional calculations.

The conventional hand calculation methods using ASR, LFR, and LRFR are often based on simplified 2D girder-by-girder analysis that does not take into account the full 3D bridge system behavior. The rating factors calculated using NDT data more closely captures the in-situ 3D system behavior. Furthermore, the rating factors calculated using the calibrated FEM take into account both the 3D analytical and in-situ system behavior of the bridge. A comparison of the load rating factor from hand calculation, three years of NDT data, and the calibrated FEM were successfully performed for ASR, LFR, and LRFR methods. Overall, the LRFR method showed higher load ratings than the LFR and ASR methods. The PMB was designed using the ASD method. However, the same large reserve capacity increases depicted may not be realized for bridges designed by LRFD.

Evaluation of bridge performance, using measured test data and a calibrated FEM, may provide bridge owners a better understanding of true bridge performance, and help lead to more informed and objective bridge management decisions. The alternate load ratings can play different roles based on the objectives and needs of the bridge owners in various phases of bridge service life, such as the initial design, load ratings, permit loadings, load postings, retrofits, revised load ratings, and replacements. The main question is that whether or not if the reserved loading capacity of bridges, as demonstrated in this paper, should be relied upon. The final decision of which load rating methods and which approaches of bridge load ratings should be used is left to the judgment of bridge engineers, bridge owners, and state officials.

2.17 <u>Acknowledgments</u>

CHAPTER 3

Powder-Mill Bridge

Powder-Mill Bridge (PMB) over the Warre River connects MA route 122 with the Barre Depot Road. Also Powder-Mill Bridge directly connects Barre state forest and Barre –Martone regional landfill and recycling facility to the downtown Barre and the location of the bridge can be seen in Figure 3.1 Annual average daily traffic (ADT) of PMB counted 2,000 vehicles per day (VPD) and bridge is expected to see about 2,500 by 2015 (FST, 2007).

Figure 3.1 Powder-Mill Bridge Location

(Source: Google Inc. Google Map)

The old Powder-Mill Bridge was in service until June 2008. It was structurally deficient, Figure 3.2(a). The new bridge was designed by Fay, Spofford, and Thorndike (FST) in 2004 and constructed by ET&L Corporation in 2009, Figure 3.2(b). The replacement bridge was opened to traffic in September 2009 with a Structural Health Monitoring (SHM) system. The major reason to select this bridge for instrumentation and testing as a research project is that the bridge daily traffic is mostly truck because of the proximity of Barre-Martone Landfill.

(a) Old Powder-Mill Bridge   **(b)** New Powder-Mill Bridge

Figure 3.2 Powder-Mill Bridge

3.1 <u>Structural and Geometric Properties</u>

The Powder-Mill Bridge is a three span continuous steel girder bridge with composite reinforced concrete deck located in Barre, MA. The bridge is 47m (154ft) long with two 11.75m (38.55ft) outer spans and a 23.5 (77.1ft) center span. There is a field splice located in the middle span, 4.4m (14.44ft) from the North Pier. The girders between south abutment to field splice are rolled section and between field splice to north abutment are plate section. The plate girders were designed in similar section properties with rolled girder, Figure 3.1.1. The steel girders and diaphragms on the bridge are weathering steel and were made of AASHTO M270M Grade 345W (50ksi). There are six girders through the length of the bridge, equally spaced at 2.25m (7.4ft), Figure 3.1.2. The exterior girders are W920×345 (W36×232), the interior girders are W920×238 (W36×160) and the fascia girders are W920×201 (W36×135).
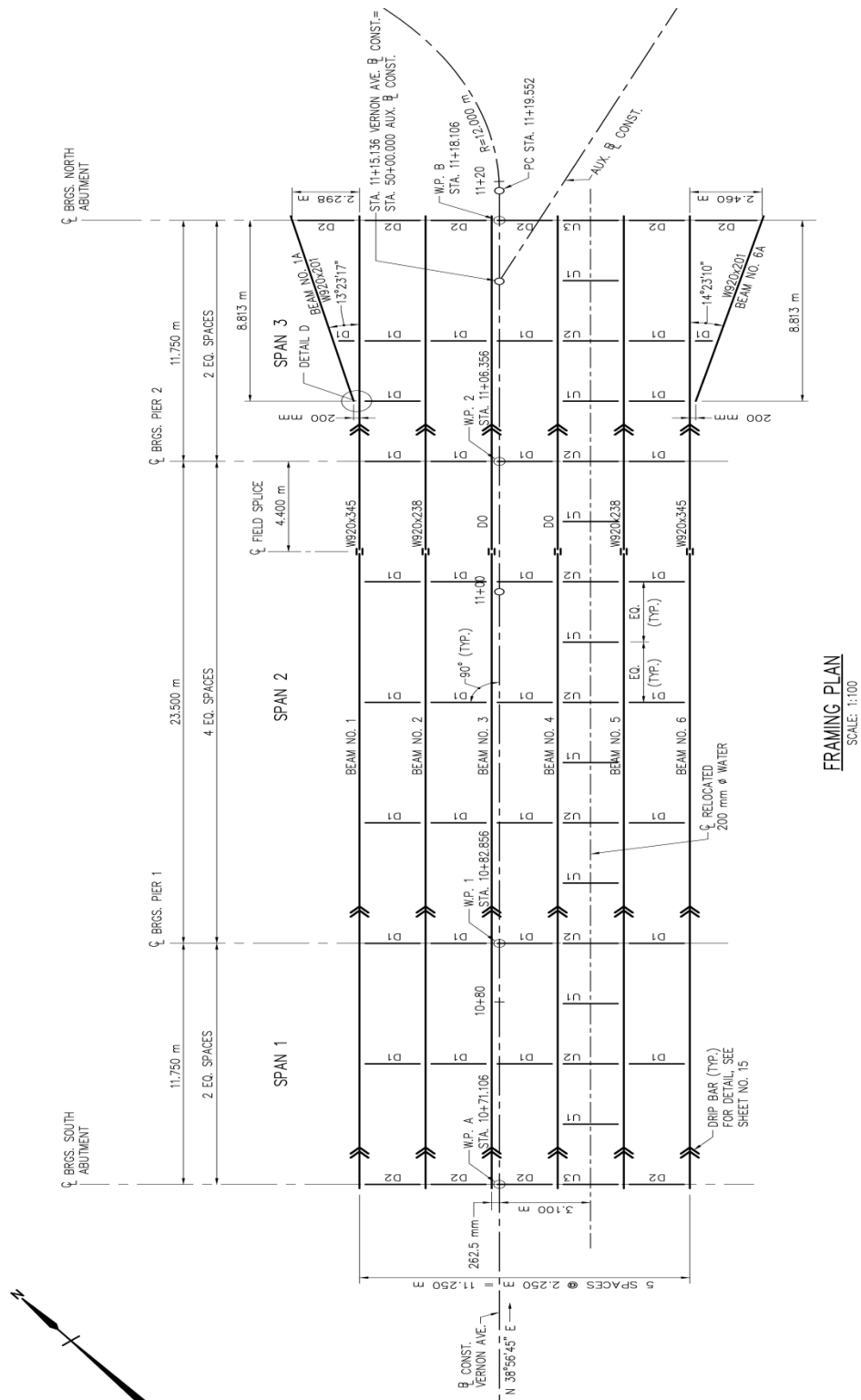
Figure 3.1.1 PMB Framing Plan

Figure 3.1.2 Typical Deck Section, Span 1 and 2
(Source: Fay, Spofford & Thorndike, Inc)

There is a utility pipe between girder 4 and 5 which is supported with extra diaphragms. PMB steel girders were fabricated at the facilities of High Steel Structures Inc. in Lancaster, Pennsylvania.

The Powder-Mill Bridge is owned by the Town of Barre. The bridge was instrumented by researchers at Tufts University and the University of New Hampshire with instrumentation consultant from Geocomp Corporation.

3.2 Instrumentation

Instrumentation of Powder-Mill Bridge was completed between June 2009 and October 2009 during the construction. Six different types of sensors were installed; 100 strain gauges, 36 steel temperature sensors, 30 concrete temperature sensors, 3 ambient temperature sensors, 16 uniaxial-accelerometers, 16 biaxial tiltmeters, 2 pressure plates, 1 UPS (Uninterrupted Power Supply), and one onboard computer. Table 3.2.1 summarizes the type of instruments that was installed.

Table 3.2.1 Instrumentation Summary

Instrumentation	Type	Quantity	Place of Instrumentation
Strain Gauge	Omega 3-wire uniaxial model # KFG-5-350-C1-11L3M3R	100	Steel Fabrication Facility
Steel Temperature Sensors	YSI 44000 series	36	Steel Fabrication Facility
Concrete Temperature Sensors	YSI 44000 series	30	On Site
Ambient Temperature Sensors	YSI 44000 series	3	On Site
Accelerometers	Dytran uniaxial model # 7521A1	16	On Site
Tiltmeters	VTI Technologies biaxial model # SCA121T	16	On Site
Pressure Plates	Geokon series 3500	2	On Site
UPS	APC Smart-UPS 1000VA LCD 120V	1	On Site

Powder-Mill Bridge was instrumented in 13 different stations from 0 to 12; instrumentation plan can be seen in Figure 3.2.1.

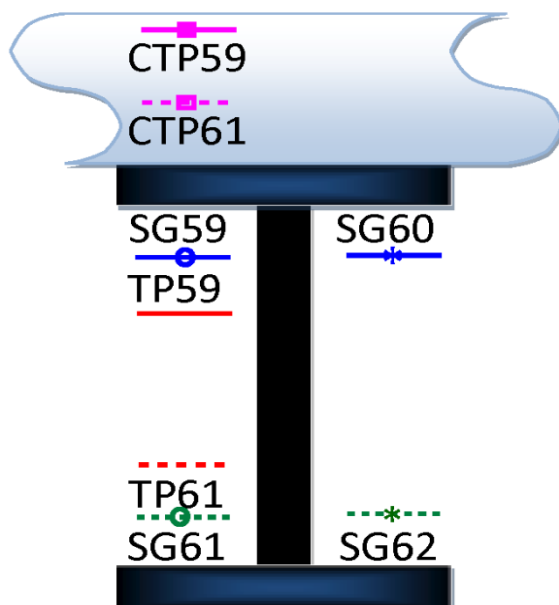**Figure 3.2.1** Instrumentation Plan
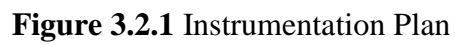
All sensors were connected with cables which run along the length of the bridge then connect to iSite data acquisition boxes located near the south abutment, Figure 3.2.2. In the PMB both high speed and low speed boxes, which were designed and manufactured by Geocomp Inc, were used. Each low speed box supports 32 channels and used for only temperature sensors. Each high speed box supports 8 channels and used for all other sensors.

Figure 3.2.2 ISite Boxes Near South Abutment

The strain gauges were installed on six girders at five different stations which have largest bending moments. Each interior girder was instrumented with four gauges, two on the top of the bottom flange, and two on the bottom of the top flange, as seen in Figure 3.2.3. The exterior girder was instrumented with two gauges, only on the inner side of the girder in order to discourage vandalism and visual impact.

The reason having strain gauges on both top and bottom flange is for determining the location of neutral axis. In addition, having strain gauges on both sides of the girder can help to determine axial, bending, and torsional effects on the girder. At stations 2, 4, 6, 8 and 10, strain gauges were installed for girders 1 through 6.

Figure 3.2.3 Location of Gauges on the Girder 4, Station 6

Thirty-six steel temperature sensors were placed on six girders at station 2, 6, and 10. Since the temperature does not differ on either side, two temperature gauges were installed, one of underneath the top flange and one on the top of the bottom flange, Figure 3.2.3. The temperature sensor location on the steel girder flange is at a distance of a quarter of an inch off of the surface of the web since the plumbers putty were used to install the gauges. Therefore, these sensors do not report the actual steel temperature, however, there are close to the values with a small delay.

Three of two ambient temperature sensors were installed at station 1 in between girder 1 to girder 2 and between girders 2 to girder 3. A third one was placed in south pier in between girder 1 to girder 2 in July 2010.

Twenty-four concrete temperature sensors are at stations 2, 6, and 10 above the girders 1, 2, 4, and 6. Additionally six concrete temperature sensors are in the bay between girder 1 and 2 at stations 2, 6, and 10. At each location one sensor is tied underside of the top rebar, and the second sensor is tied underside of the bottom rebar. Total numbers of concrete temperatures are thirty on the bridge.

The tiltmeters were placed at the center of the web on girders 1, 2, 5, and 6 at stations 3, and 9. Additional tiltmeters for girders 2 and 3 at station 0 and 12. Also 4 tiltmeters are in middle of the south & north abutments, and in the middle of the north & south pier. Total numbers of tiltmeters are sixteen on the bridge. Tiltmeters locations were chosen to determine the changes in rotation in the girder, on the face of the abutments, and on the face of the piers.

Sixteen accelerometers were installed on girders 1, 2, 3 and 6 at stations 1, 6, 7, 11 to study dynamic response of the Powder-Mill Bridge.

In addition to these sensors two pressure cells, Geokon series 3500, were installed one in each lane in the south approach. The top surface of both cells was in direct contact with the asphalt. Full instrumentation plan can be seen in Figure 3.2.3.

36

3.3   Data Acquisition System

The high speed data acquisition system (DAQ) is a set of 20 linked multichannel high speed dataloggers, iSite and 3 low speed dataloggers designed by Geocomp Corporation. In order to have remote access to each iSite box, as seen in Figure 3.3.1, they are all connected to a local hub where the data can then be transmitted wirelessly. Geocomp supports a website called iSite Central where allows researchers to monitor the bridge all the time.

The local hub was placed inside a large weather resistant enclosure between girders 3 to 4, Figure 3.3.2. The system also has an extra outlet that allows the hub and local computer to be powered. This enclosure was bolted to a steel plate in between the two girders to protect the central box from water and snow. Ethernet cables connect each iSite box with the main hub, through a flexible conduit at the south end of the each girder. The flexible conduit then connects to a junction box mounted on the abutment from at the end of the each girder. Each junction box at the end of the girders is then connected by a main line in a rigid conduit. This rigid conduit continues to the center of girder 3 and girder 4 and then connects to centralized hub enclosure. This setup allows researchers to connect DAQ remotely to stored data and check the system for any problem.

Figure 3.3.1. ISite Boxes   **Figure 3.3.2.** Local Hub

PMB has two types of loggers, low speed and high speed. The low speed data logger's maximum sampling rate is 5 Hz (5 samples per second). These boxes have 32 channels, 16 channels collect temperature data. The high speed loggers' maximum sampling rate is 1024 Hz. A sampling rate of 200 Hz was used for strain gauges, accelerometer, tiltmeter and pressure cells until October 2010. Both of these speeds can be set to lower or higher values based on the DAQ

needs. Between September 2009 and October 2010, strain reading had been recording every 5 minutes and temperature reading had been recording every 15 minutes on the iSite central. For long term monitoring of PMB there are potential data storage issues, therefore the sampling rate for the long-term data collection at PMB was reduced to 3600sec (1 point every hour) on October 18, 2010. However researchers can remotely access the central computer on the PMB to set a high sampling rate. Another issue was losing the data due to occasional power loss at the PMB. In order to prevent data loss, an uninterruptible power supply (UPS) was installed by Tattan Electric on November 22, 2011. The UPS system was mounted on the abutment inside an aluminum box. The box contains both a heat strip and a fan for temperature control. The SHM system is regularly monitored from the iSite central by researchers.

3.4 Load Tests

According to the AASHTO Manual for Bridge Evaluation (MBE) 2th Edition, load testing is the observation and measurement of the response of the bridge subjected to controlled and predetermined loading without causing changes in the elastic response of the structure (AASHTO, 2011). The goals of the load test are capturing the response of the bridge and verify the performance of the bridge or components under a known live load. The findings of this research will lead to improve the methodology for bridge condition assessment and reliability in bridge management of the future.

Based on the AASHTOMBE, there are two types of load tests: diagnostic and proof load. These tests are described below.

3.4.1. Diagnostic Test

Diagnostic test is used to understand the behavior of the bridge and to reduce the uncertainties related to deterioration, material properties and boundary conditions. Diagnostic tests can be either static or dynamic. Dynamic load test can be used to measure stress range for fatigue evaluation, frequencies of the bridge, and modes of bridge. Dynamic load test can be established with using moving loads which cause vibrations on the bridge or with time varying loads. Static load test is established using stationary loads to avoid the bridge vibrations. Position of the truck may be change during the load test (AASHTO, 2011).

3.4.2. Proof Test

Proof test is used to determine the maximum load that bridge can carry safely where the bridge behavior is within the linear-elastic range. Proof test is mostly performed as a static test (AASTHO, 2011).

The instrumentation of the PMB allows for the bridge to be an excellent test location for various types of nondestructive load tests techniques. For this study, three years diagnostic load tests were performed in 2009, 2010, and 2011 and the NDTs data were used in order to calculate rating factors of the PMB.

3.5   2009 Load Test

Two types of diagnostic load tests were performed on September 3, 2009 prior to the bridge being open to traffic. The first type of test involved the truck travelling across the bridge at a constant, low speed which is referred to as the truck crawl speed load test. The second type of test involved the truck stopping at predetermined locations on the bridge and is referred to as the stop location truck test. The crawl speed load tests had three load patterns along the length of the bridge, paths X1, X2 and X3 as seen in Figure 3.5.1. Truck paths in the diagnostic load test plan indicate the right wheel of the truck.

Figure 3.5.1 2009 Static Load Test Plan

As seen in the annotations, load path X1 was 0.61 m (2 ft) off of the northwest curb and X3 was 0.76 m (2.5 ft) off of the southwest sidewalk. Load path X2 was centered on girder 3. For the crawl speed load test, the test truck was run three times, at a speed of approximately 1.34 m/s (3 mph) in each path to ensure repeatability in the test data. For the stop location truck test, the truck was run with 14 stop locations in the truck path.

Altogether, 9 stop tests and 9 crawl speed tests were performed. In attrition, the ambient conditions in between the tests were recorded. In addition to these two tests, digital imaging was used by other researchers and Prof. Erin S. Bell from the University of New Hampshire (UNH) to collect deflection data from bridge.

Figure 3.5.2 Tri-axle Dump Truck

Tri-axle dump truck was used for 2009 truck load test, Figure 3.5.2. Truck was loaded with aggregates prior to arrival at the bridge. The weight of the truck was 72kips. Firstly the truck dimensions and wheel locations were measured three times for accuracy, Table 3.5.1. In order to have accurate axel loads, the truck wheels weights were measured three times using wheel scales, as shown in Table 3.5.2.

Table 3.5.1 2009 Test Truck Dimensions*

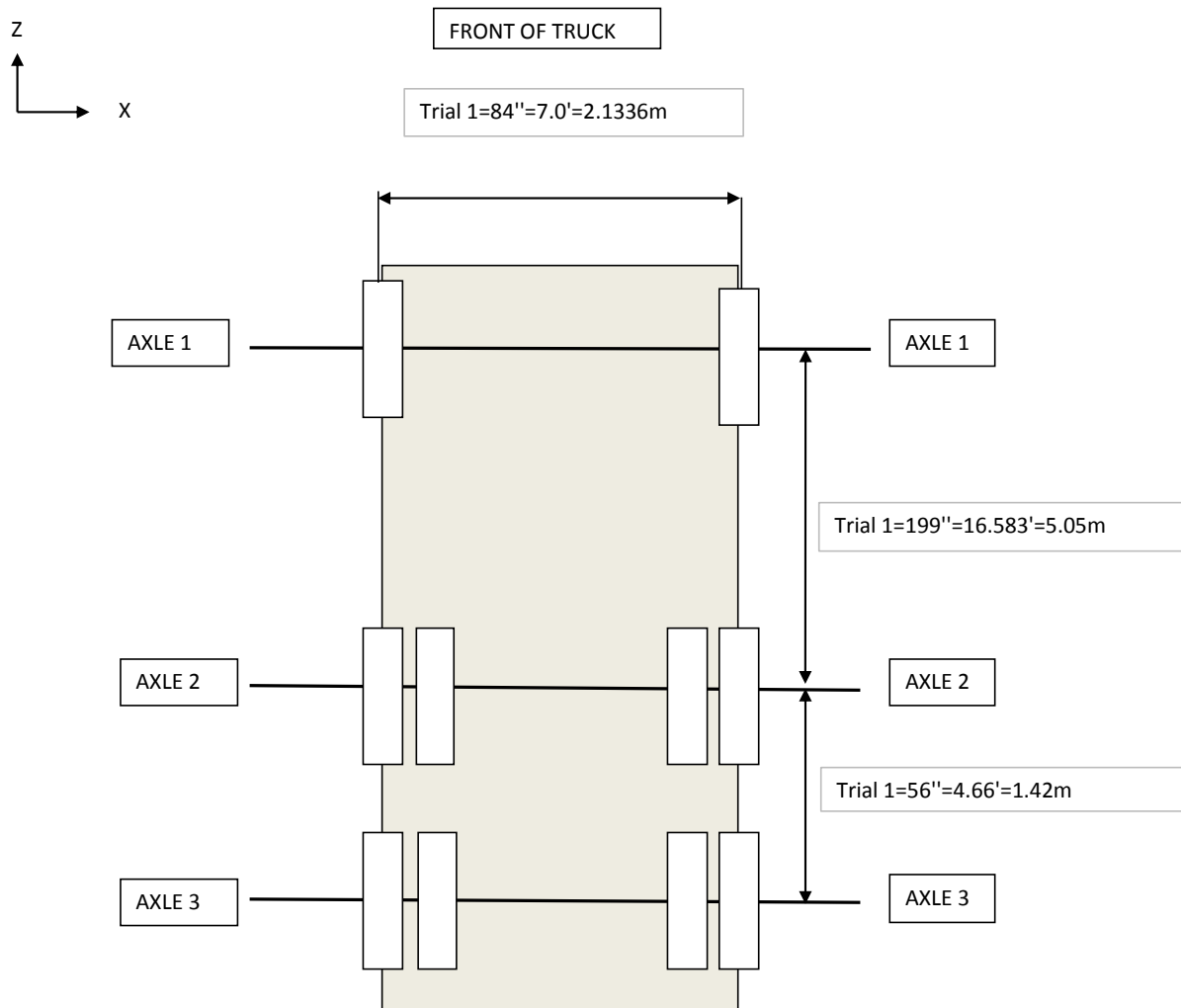| Vehicle Type:	Tri – Axle Dump Truck
Tires Width Dimension	
Front	0.203m (0.67')
Rear	0.203m (0.67')
Width – Axle 1: front (on center)	2.130m (6.98')
Spacing – Axle 1to Axle 3 (on center)	5.050m (16.57')
Spacing – Axle 1to Axle 4 (on center)	6.480m (21.26')

* For more details, check the Figure 3.5.3

42

Z

X

FRONT OF TRUCK

Trial 1=84''=7.0'=2.1336m

AXLE 1

AXLE 1

Trial 1=199''=16.583'=5.05m

AXLE 2

AXLE 2

Trial 1=56''=4.66'=1.42m

AXLE 3

AXLE 3

Table 3.5.2 2009 Test Truck Weight at Each Tire

	Prior to Test (lbs)	After Test (lbs)	Average (lbs)
Front Axle 1-1	10025	10103	10064
Front Axle 1-2	9560	9413	9487
Axle 2	N/A	N/A	N/A
Axle 3-1	6032	6340	6186
Axle 3-2	7647	7250	7448
Axle 3-3	7463	7407	7435
Axle 3-4	5493	5610	5552
Axle 4-1	6510	6710	6610
Axle4-2	7220	6957	7088
Axle 4-3	7223	7370	7297
Axle 4-4	5613	5490	5552
Total	72787	72650	72719

3.6   2010 Load Test

The 2009 load test strain measurements were used for load ratings via nondestructive test data and updating of a finite element model of the PMB as seen in Sanayei et al. (2012). Initial analysis of the 2009 load test data for use in nondestructive test data bridge load rating, showed the NDT data could only be used to evaluate load factors of girders 2, 3, and 5. Lessons learned from the 2009 load test and the now-calibrated FEM were used to design the 2010 load test plan to induce higher strain levels. The 2010 load test included two sets of testing; the dynamic load testing and the static load testing. The dynamic load test plan was prepared by PhD. Candidate Jesse Sipple from Tufts University to get overall dynamic signature of the bridge, as seen in Figure 3.6.1. In preparation of dynamic test 9 location of accelerometers were marked out on the bridge. All wires were moved from sidewalk to predetermined locations then all accelerometers were installed at predetermined locations on the bridge. Dynamic shaker were used to excite the bridge and 5 to 10 linear sine sweeps at each location were run. After setting up the dynamic shaker, 2 minutes of ambient vibration data were collected using NI DAQ.
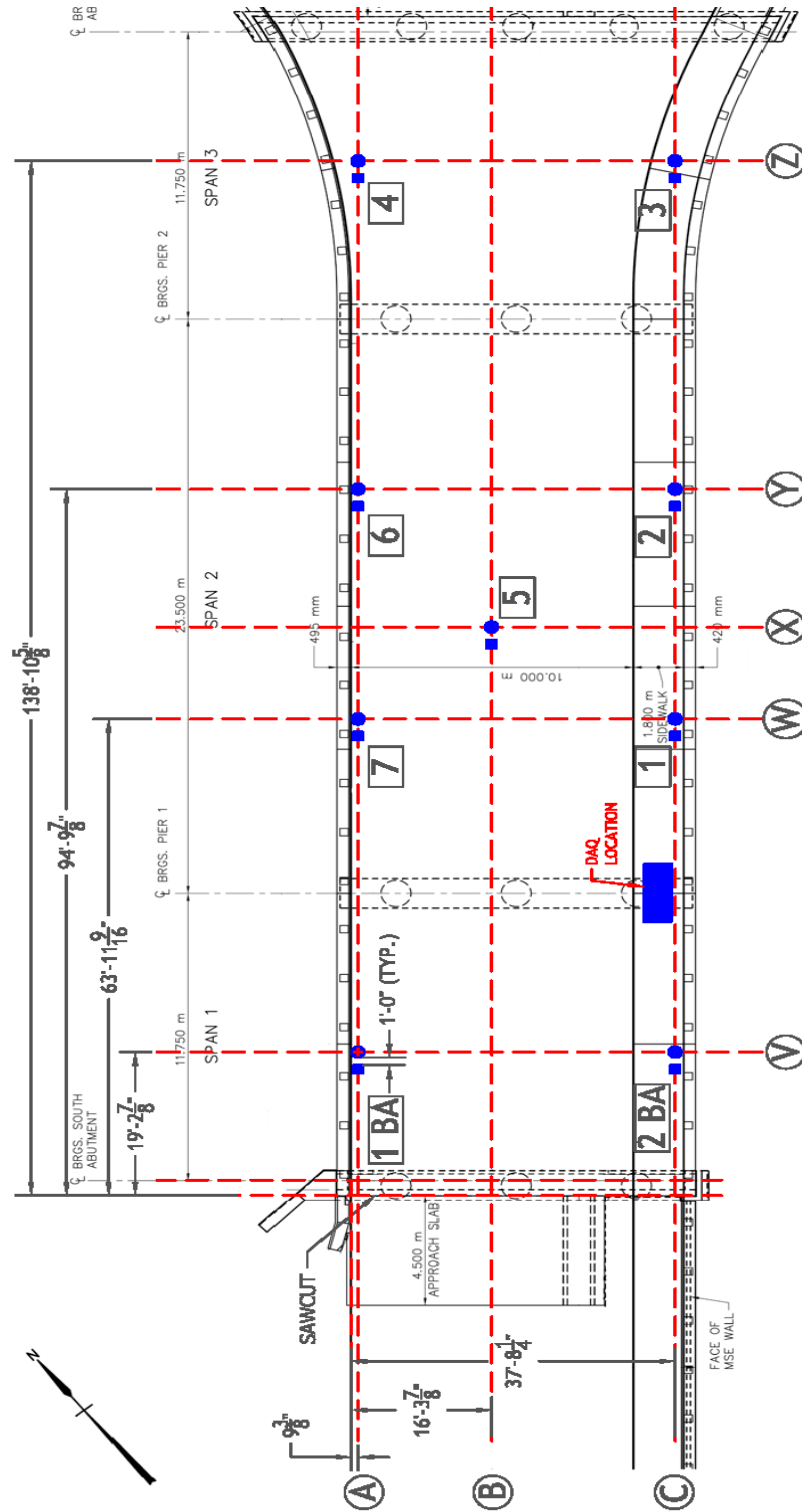
Figure 3.6.1 2010 Dynamic Load Test Plan

44

The static load test plan was prepared as part of this project. The lessons from 2009 load test showed that the truck position and truck paths did not provide the maximum strain reading for all girders. Therefore prior the 2010 load test, FEM model which was calibrated with 2009 load test was used to decide the truck location and position. Based on the results from the calibrated FEM model, 6 runs on each girder with the truck positioned in the middle of each girder were predetermined. However positioning the truck on girder 1 and on girder 6 was impossible because of safety curb and sidewalk, 4 load paths X1, X2, X3 and X4 on girder 2, 3, 4 and 5 were determined, Figure 3.6.2. The truck location was centered on the girder 2, 3 and 4 for load paths X1, X2, X3. Since centering the truck on girder 5 is not possible because of the sidewalk, truck right wheel was positioned on the girder 5 for load path X4. For the stop location load test the same 4 load paths were used with 3 stop location; the one was in the middle of the first span, the second was in the middle of middle span and the third one was in the middle span, 28.88m (94ft 9in) from the south sawcut. The 2010 load paths plan can be seen in Figure 3.6.2. Truck line in the static load test plan indicates the location of right wheel of the truck from South abutment to North abutment.
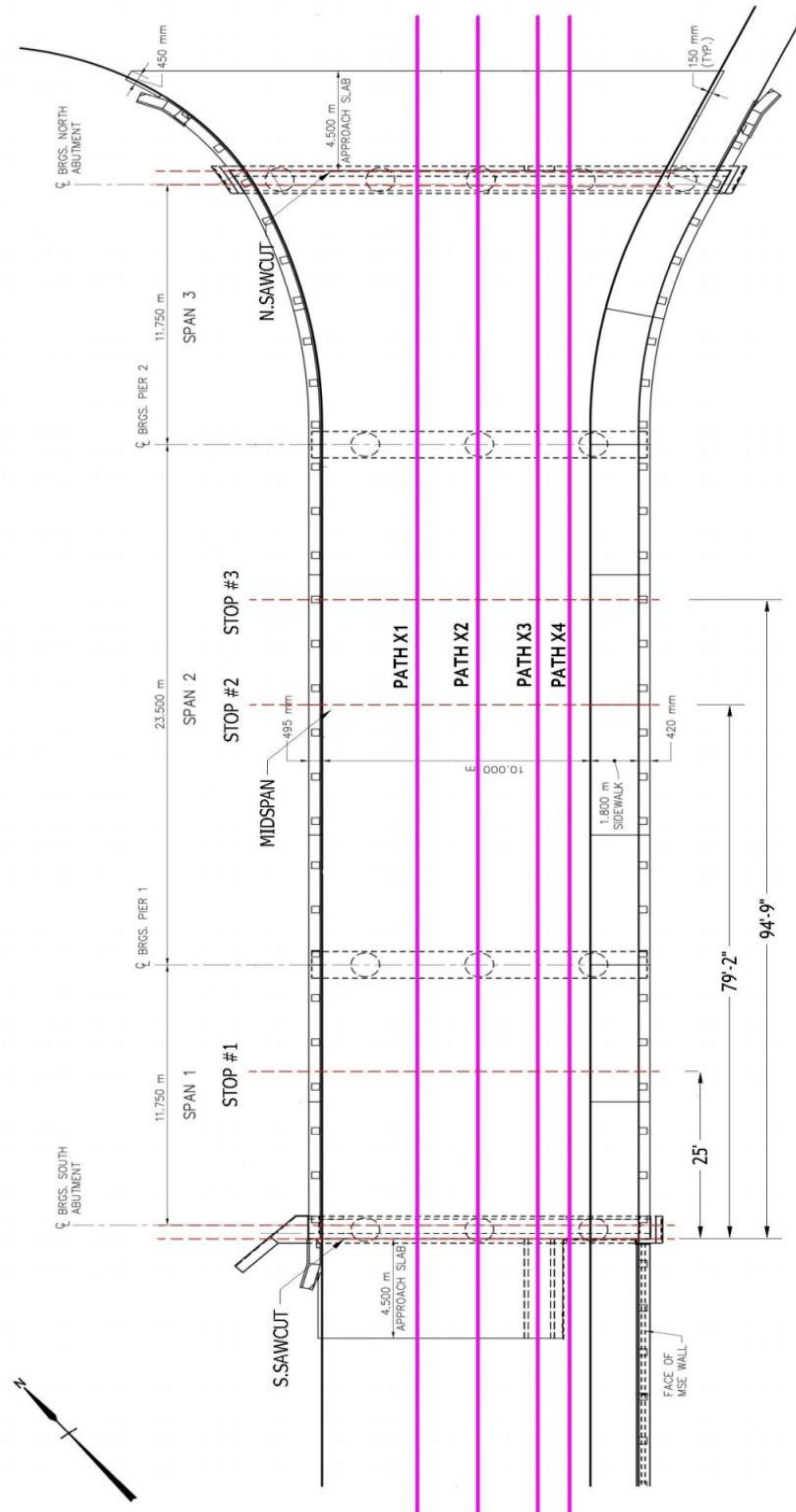
Figure 3.6.2 2010 Static Load Test Plan

46

In preparation of the static load test all locations which were needed during the test; 4 travel lanes, the middle span of the bridge, the off bridge line, and the stop locations were marked. The location of the total station at the south approach was setup. After syncing the total station with the iSite DAQ, 4 back sight points of the bridge and the traffic counter locations were shot. The truck arrived at the field loaded with aggregates and the weight of the truck was 323.38kN (72.7kips). Firstly the truck dimensions and wheel locations were measured three times for accuracy, Table 3.6.1, as in previous load tests.

Table 3.6.1 2010 Test Truck Dimensions*

Vehicle Type:	Mack Tri – Axle Dump
Tires Width Dimension	
Front	0.295m (0.97')
Rear	0.210m (0.69')
Width – Axle 1: front (on center)	2.137m (7.01')
Spacing – Axle 1to Axle 3 (on center)	5.080m (16.66')
Spacing – Axle 1to Axle 4 (on center)	6.493m (21.27')

* For more details, check the check Figure 3.6.3

In order to have accurate axel loads, the truck wheels weights were measured three times with using wheel scales, as shown in Table 3.6.2. In the first column, the weight of each tire is labeled individually. The next three columns show the weights at each tire: before the bridge test, after the bridge test, and the average value. It seems some of the weight got shifted from the front to the back of the truck.

In order to measure the exact location of the truck, a prism was placed on the backside of the truck to reference the truck. The exact location of the prism on the truck was measured. During the load test, the truck positions were recorded into the iSite DAQ system along with the time via the total station and the traffic counter, Figure 3.6.4. Data were collected via on the site laptop computer connection to the iSite boxes. Data collection was started from about 24 ft off the bridge from the bridge deck south saw cut centered at the bearing at the south abutment and continued for about 30 second after the back wheels of the truck were off the bridge. This speed was slow enough to avoid dynamic effects in the data. Between each test, dynamic test to crawl speed test and crawl speed test to stop location test, and the ambient condition of the bridge were recorded.
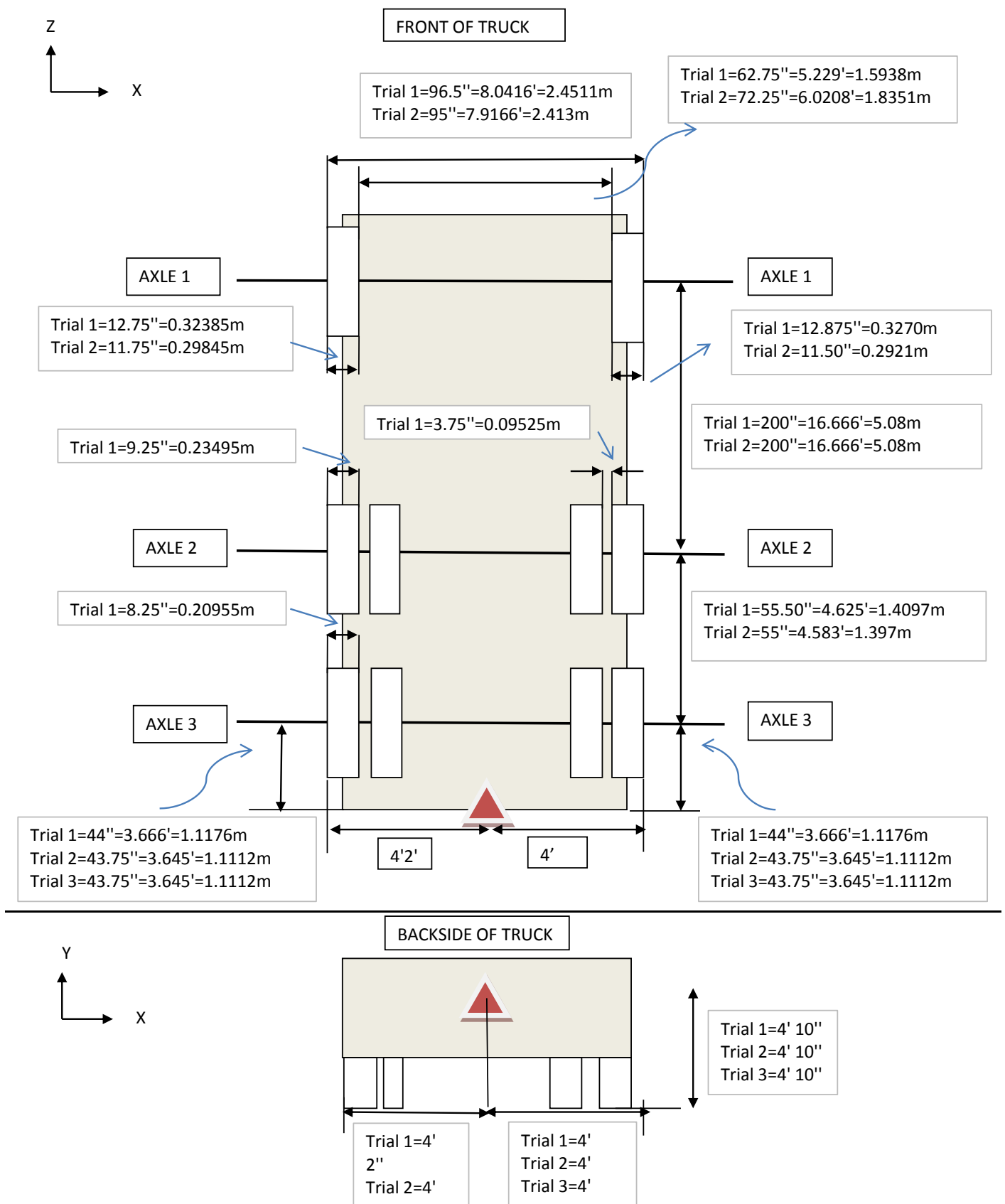
Z → X

FRONT OF TRUCK

Trial 1=96.5''=8.0416'=2.4511m
Trial 2=95''=7.9166'=2.413m

Trial 1=62.75''=5.229'=1.5938m
Trial 2=72.25''=6.0208'=1.8351m

AXLE 1

Trial 1=12.75''=0.32385m
Trial 2=11.75''=0.29845m

AXLE 1

Trial 1=12.875''=0.3270m
Trial 2=11.50''=0.2921m

Trial 1=3.75''=0.09525m

Trial 1=9.25''=0.23495m

Trial 1=200''=16.666'=5.08m
Trial 2=200''=16.666'=5.08m

AXLE 2

Trial 1=8.25''=0.20955m

AXLE 2

Trial 1=55.50''=4.625'=1.4097m
Trial 2=55''=4.583'=1.397m

AXLE 3

AXLE 3

Trial 1=44''=3.666'=1.1176m
Trial 2=43.75''=3.645'=1.1112m
Trial 3=43.75''=3.645'=1.1112m

4'2'   4'

Trial 1=44''=3.666'=1.1176m
Trial 2=43.75''=3.645'=1.1112m
Trial 3=43.75''=3.645'=1.1112m

BACKSIDE OF TRUCK

Y → X

Trial 1=4' 10''
Trial 2=4' 10''
Trial 3=4' 10''

Trial 1=4' 2''
Trial 2=4'

Trial 1=4'
Trial 2=4'
Trial 3=4'

48

Table 3.6.2 2010 Test Truck Weight at Each Tire

	Prior to Test (lbs)	**After Test (lbs)**	**Average (lbs)**
Front Axle 1-1	9662	9478	9570
Front Axle 1-2	9840	9792	9816
Axle 2	N/A	N/A	N/A
Axle 3-1	5673	5610	5642
Axle 3-2	7533	8082	7808
Axle 3-3	7613	8308	7961
Axle 3-4	6560	5343	5952
Axle 4-1	5703	5757	5730
Axle4-2	7078	7983	7531
Axle 4-3	7358	7687	7523
Axle 4-4	6905	5637	6271
Total	73927	73676	73802

During the stop location test at each stop location the truck waited about 30 seconds. The sampling rate for both crawl speed and dynamic load test were 200Hz.

Figure 3.6.4 Prism and Total Station

In addition to these tests, digital imaging and LVDTs were used by researchers and Prof. Erin S. Bell from UNH to measure the deflection during the load test.

3.7   <u>2011 Load Test</u>

In the third year of PMB health monitoring, a third load test took place on September 25, 2011. The goal of this load test was again to track the health of the bridge and use improved testing procedures on the bridge. Four sets of nondestructive tests were performed during the 2011 load

test; the dynamic load test, static load test, digital image correlation (DIC), and radar measurement. The dynamic load test plan was prepared by Doctoral Candidate, Jesse D. Sipple. In preparation of dynamic test 9 locations of accelerometers were marked out on the bridge and Wilcoxon accelerometers were placed in 9 predetermined locations on the bridge deck. In additional by Prof. Tat Fu of UNH, 6 wireless accelerometers were placed near Wilcoxon accelerometers to compare the measurement methods as seen in Figure 3.7.1. Measurements from wired and wireless measurements were close and the comparison is in progress.

Figure 3.7.1 Accelerometers

The dynamic load test plan can be seen in Figure 3.7.2. In 2011, the excitation was a step-sine wave from 2Hz to 40Hz for duration of maximum between 100 cycle or 5 seconds at 0.5 Hz increments. To determine the noise level, 2 minutes ambient measurements were recorded three times during the test.
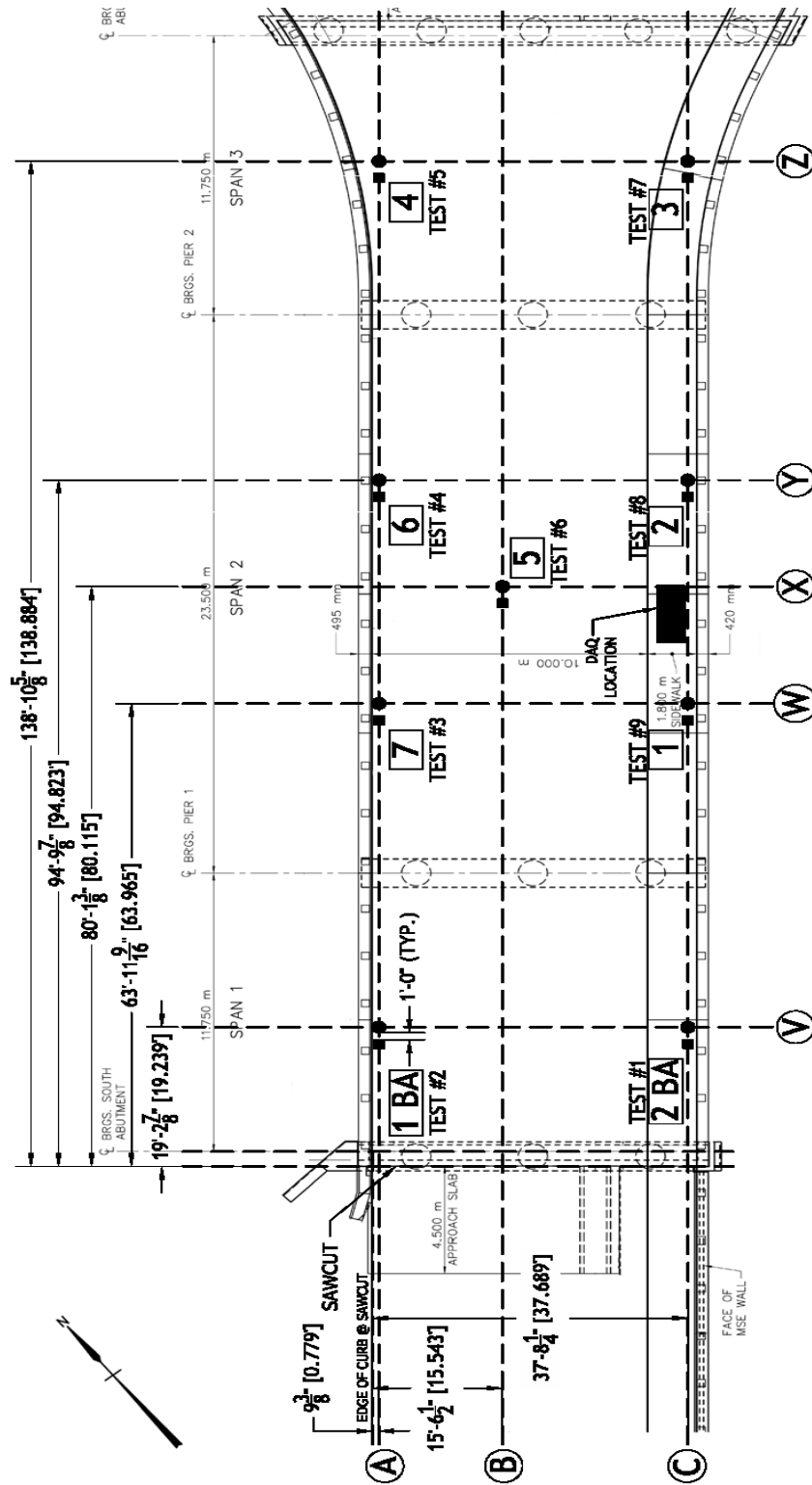
Figure 3.7.2 2011 Dynamic Load Test Plan

Before the 2011 load test, all temperature boxes sampling rates were increased to 1 reading per minute. Then the traffic counter was installed on the south saw cut and connected with the iSite DAQ. The traffic counter chip was installed on iSite box 115 channel 5.

After processing 2010 load test data, load rating factors for all girders were calculated except for girder 1 and girder 6 due to the truck position. The test truck was not positioned close enough to girder 1 and girder 6, therefore the stress level was not enough to validate these girders rating factors. Since all girders were successfully rated except for exterior girders, the same truck paths as 2010 was kept and two more load paths was added, Figure 3.7.3. Additional truck path to validate girder 1 was X0 and the right wheel of the truck was on the girder 2. This was the closest distance to the curb that the truck driver could drive safely. The other additional paths were X4 and X5 to validate girder 6. The predetermined load path was X4 and the truck right wheel was 0.6m (1.97ft) away from sidewalk. But in the field it was observed that the last load path could be improved by positioning the truck closest to girder 6. Thus, the new load path X5 was marked and the center of the truck right wheel was placed 0.10m (0.33ft) away from sidewalk.
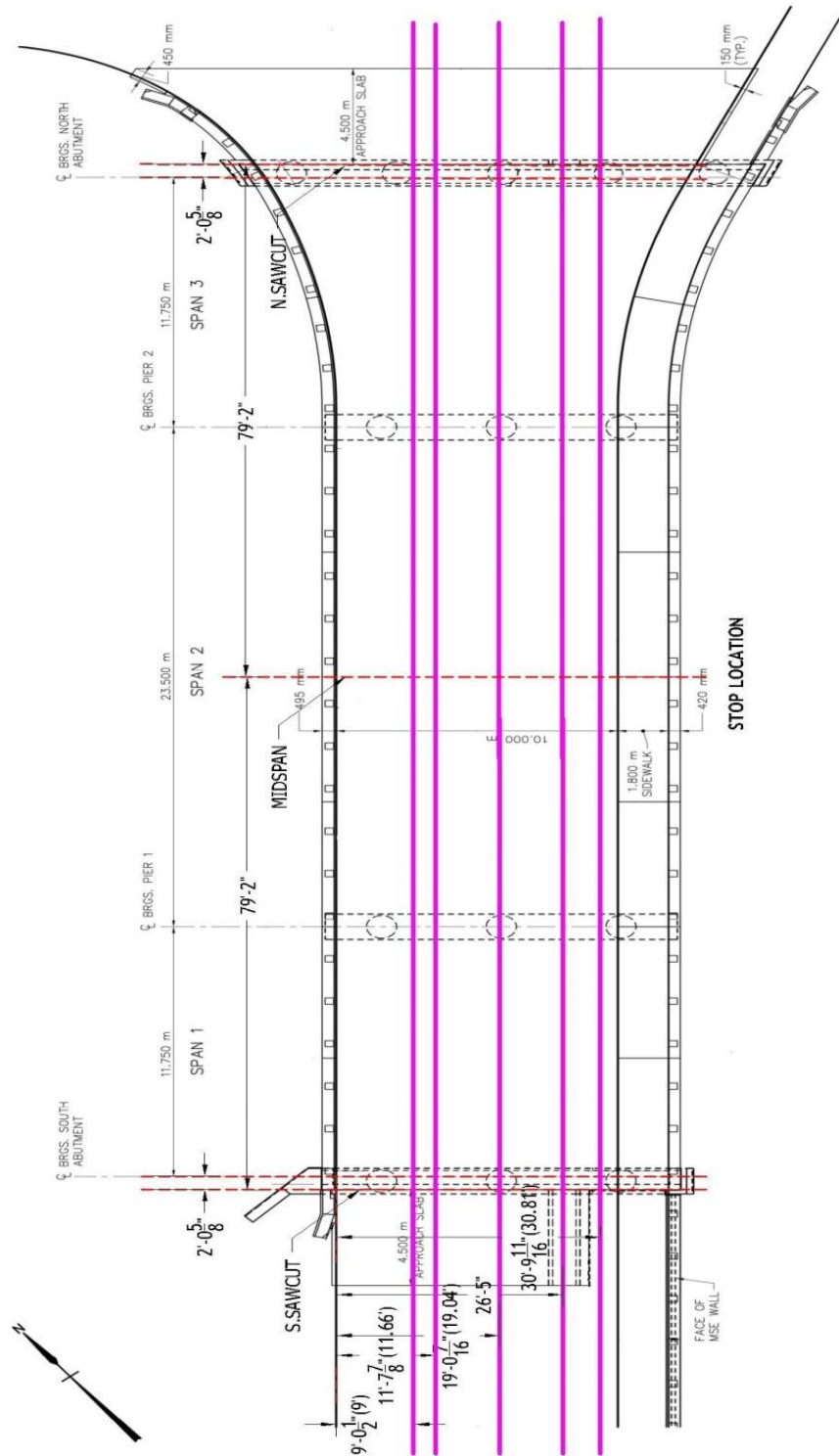
Figure 3.7.3 2011 Static Load Test Plan

Truck path in the diagnostic load test plan indicates the location of center of the right wheel of the truck from the curb.

When X4 load path was analyzed with a 320.27kN (72kips) from 2009 NDT truck using FEM model, the load path X4 it did still not create enough stress to rate girder 6. Therefore the truck weight was increased. The same Tri-axle dump truck used in 2009 and 2010 with the weight of loaded to a total 348.74kN (78.4kips) as an operational load. Firstly the truck dimensions and wheel locations were measured three times, Table 3.7.1.

Table 3.7.1 2011 Test Truck Dimensions

Vehicle Type:	Tri – Axle Dump Truck
Tires Width Dimension	
Front	0.298m (0.98')
Rear	0.216m (0.71')
Width – Axle 1: front (on center)	2.14m (7.02')
Spacing – Axle 1to Axle 3 (on center)	5.080m (16.66')
Spacing – Axle 1to Axle 4 (on center)	6.484m (21.27')

* For more details, check the check Figure 3.7.4

Similar to the previous year's test, the truck wheels weights were measured three times using the wheel scales, Table 3.7.2. It was observed that the truck wheels weight measurements before and after the test due to sifting of aggregates during the test run.

Again, a prism was placed on the backside of the truck to reference the truck and researchers measured the exact location of the prism on the truck. The test truck was run 3 times in each path. . Small changes in the truck path will cause errors in the measurements. By repeating and averaging, the measurement errors will significantly reduce.

In additional to strain data, researchers from UNH were installed 8 BDI gauges at four locations at girder 1 station 2, girder 3 station 2, girder 4 station 4, and girder 6 station 4. All BDI gauges were connected with NI DAQ system and Labview program was used for continuous data collection. For digital image correlation, researcher from UNH researchers also installed the DIC targets on each girder at station 1, 6 and 11. When the load test began, the BDI gauges, strain gauges on the bridge, and DIC started collecting data simultaneously.

School of Engineering

Tufts
UNIVERSITY

2011 Load Test Truck
Dimension and Prism Location

Merve Iplikcioglu

Z

X

FRONT OF TRUCK

Trial 1= 95.5'' (2.426m)
Trial 2= 95.75'' (2.432m)

Trial 1= 72.5'' (1.842m)
Trial 2= 72.5'' (1.842m)

AXLE 1

AXLE 1

Trial 1= 11.75'' (0.298m)
Trial 2= 11.75'' (0.298m)

Trial 1= 11.75'' (0.298m)
Trial 2= 11.75'' (0.298m)

Trial 1=5'' (0.127m)
Trial 2= 5'' (0.127m)

Trial 1= 200.25'' (5.08m)
Trial 2= 200'' (5.086m)

Trial 1= 8.5'' (0.216m)

AXLE 2

AXLE 2

Trial 1= 8.5 '' (0.216m)
Trial 2= 8.5'' (0.216m)

Trial 1= 55.5'' (1.410m)
Trial 2= 55'' (1.397m)

AXLE 3

AXLE 3

Trial 1= 44.5'' (1.13m)
Trial 2= 44.5'' (1.13m)

Trial 1= 43.5'' (1.105m)
Trial 2= 43.5'' (1.105m)

Trial 1= 21.25'' (0.540m)
Trial 2= 21.25'' 0.540m)

Trial 1= 95.5''

Trial 1= 22 '' (0.559m)
Trial 2= 22'' (0.559m)

Trial 1= 48'' (1.219m)
Trial 2= 48'' (1.219m)

Trial 1= 47.5'' (1.207m)
Trial 2= 47.5'' (1.207m)

NOTE 1: All dimension calculation need to be made using plumb bob. (*plumb bobs used for accuracy of measurement*)
NOTE 2: Check alinement of front wheel with back wheels. (*checked as shown in the figure above*)

BACKSIDE OF TRUCK

Trial 1= 58.25'' (1.480m)
Trial 2= 58.25'' (1.480m)

Y

X

Trial 1= 48'' (1.219m)
Trial 2= 48'' (1.219m)

2.5 '' (63.5mm)

Trial 1= 47.5'' (1.207m)
Trial 2=47.5'' (1.207m)
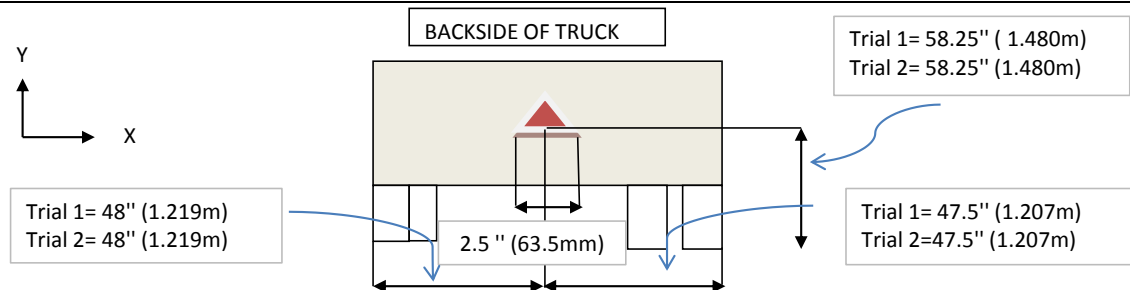
	Trial 1	Trial 2
Height of the Prism with prim poles	80'' (2.032m)	80'' (2.032m)
Height of the Prism Behind the Truck	58.25'' (1.480m)	58.25'' (1.480m)

Table 3.7.2 2011 Test Truck Weight at Each Tire

	PRIOR TO TEST (lbs)	AFTER TEST (lbs)	AVERAGE (lbs)
Front Axle 1-1	9795	9485	9640
Front Axle 1-2	9103	9740	9421
Axle 2	N/A	N/A	N/A
Axle 3-1	7175	6150	6663
Axle 3-2	8573	8825	8699
Axle 3-3	7673	8720	8196
Axle 3-4	7265	6225	6745
Axle 4-1	6754	6050	6402
Axle4-2	8272	9430	8851
Axle 4-3	8834	7355	8095
Axle 4-4	6012	7585	6799
Total	79455	79565	6799

During the load test, the truck-induced strains were recorded with the the traffic counter time via the iSite DAQ system as well as the time the total station. Data were collected from the iSite boxes via an onsite laptop computer. Data collection was started when the truck was about 24 ft of the bridge from the South sawcut and continued for 30 second after the back wheels of the truck were off the bridge. The truck speed was between 1.34m/s (3mph) to 2.24m/s (5mph), this speed was slow enough to avoid seeing any dynamic effect in the data. The sampling rate for diagnostic load test was 200Hz.

3.8   Introduction of the Past and Present AASHTO Design Trucks

The first AASHO the Standard Specifications for Highway Bridges and Incidental Structures was published in 1931 and it has been updated through 17th editions parallel to improvements in bridge design. In 1994 AASTHO introduced Load and Resistance Factor Design (LRFD) and published the first edition of AASTHO LRFD Bridge design Specifications. In 1996, the 16th edition of AASTHO Standard Specification for Highway Bridges was published. It had been adopted and included the 1993, 1994, 1995 and 1996 codes. The AASTHO Standard Specification for Highway Bridges 17th edition was published in 2002. This edition included the Allowable Stress Design (ASD) and Load Factor Design (LFD). After the 17th edition of AASTHO Standard Specification for Highway Bridges (AASHTO, 2002),

AASTHO adopted the LRFD design for entire code and has been continued to update the bridge code under LRFD Bridge Design Specifications (AASHTO, 2004). Most updated AASHTO LRFD Bridge Design Specifications is the 5th edition and has been available for use since 2010.

Four years after the first bridge design specification was published, the 2nd edition of AASTHO specifications was published in 1935. This specification included three different truck loads, H20 (40,000lb), H15 (30,000lb) and H10 (20,000lb) for three classes of highways, AA, A, and B. H20 trucks had two axles. The front axle carried 8,000lb and was 14 ft away from the rear axle that carried 32,000lb as shown in Figure 3.8.1.
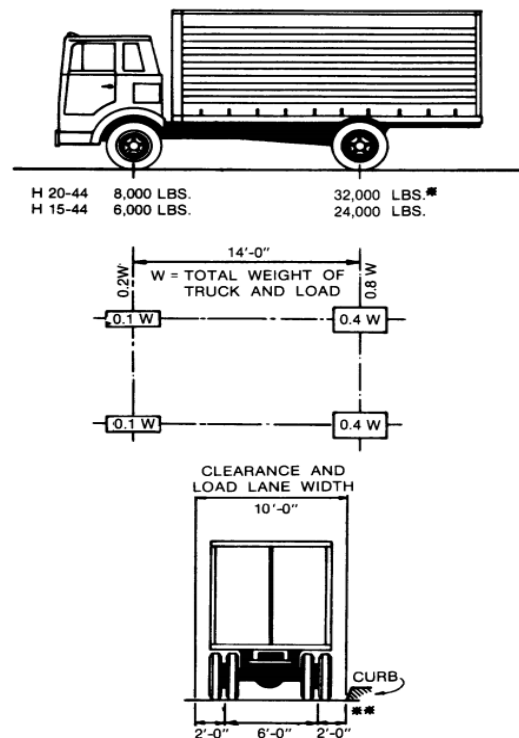
Figure 3.8.1 AASHTO H20 Design Truck

(*Source: Standard Specification for Highway Bridges, 17th Edition, Figure 3.7.6A*)

In 1941, the 3rd edition of ASSTHO specification was published. HS type truck load was introduced for the first time. In 1944, the 4th, edition of Bridge Design specifications was published.   The HS20-44 truck weight is 72,000 pounds and H symbolizes highway, S symbolizes semitrailer, 20 is the weight of the truck in tons and 44 is the designed year of adoption. The front axle load is 8,000 lbs and the rear axles are 32,000 lbs each. The distance between rear axles of the HS truck was allowed to vary from 14 to 30 ft. Figure 3.8.2 describes the HS20 design truck characteristics.
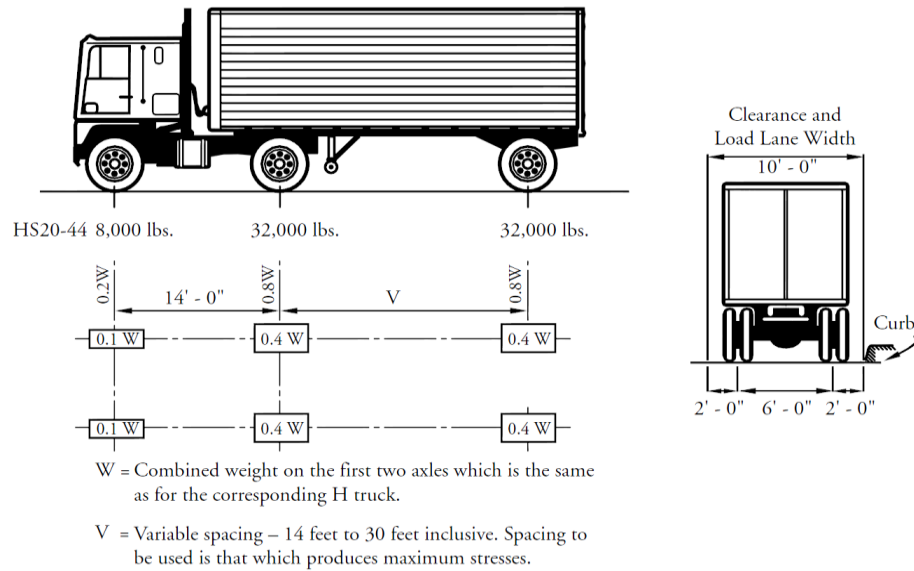
Figure 3.8.2 AASHTO HS20 Design Truck

(Source: PCI Bridge Design Manual, July 2003, Figure 7.2.2.1.3-1)

Some states officials and bridge engineers were concerned that the HS20 truck did not provide actual truck load conditions. At the end of the 1990s states such as Texas and California required the use of the HS25 truck due to heavy truck loads caused by NAFTA agreement. The HS25 (90,000lb) truck weight is 25 percent higher than HS20 (72,000lb). The HS25 front axle increased to 10,000lb and the rear axle loads became 40,000lb in each axle. Again, the distance between rear axles of HS truck was allowed to vary from 14 to 30 ft. Figure 3.8.3 shows the HS25 design truck axle loads.
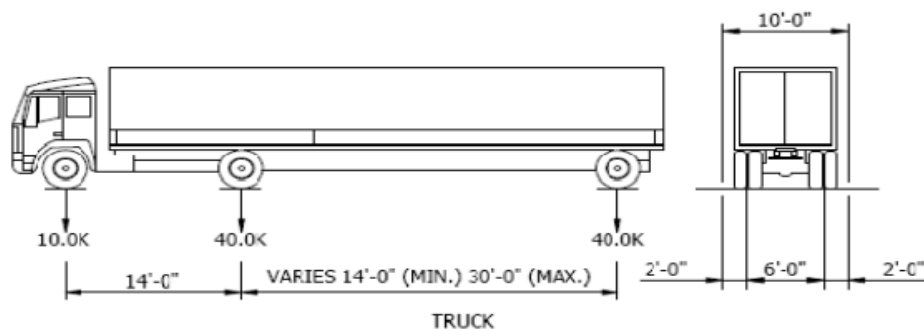
Figure 3.8.3 AASHTO HS25 Design Truck

(Source: Indiana Department of Transportation, Bridge Inspection Manual, June 2010, Figure 3:7-2)

The new design load HL93 was established in 2004 by AASTHO LRFD Bridge Design Specification as shown in Figure 3.8.4. HL symbolizes highway load and 93 designates the year of development (the original year of introduction) in the AASTHO LRFD Bridge Design Specification. The HL93 truck loads include "design truck plus design lane" or "design tandem plus design lane" or "dual design truck plus design lane". Bridge design engineers compare all three to see which produces the worst case and the bridge is built based on the worst truck load case (Baker and Puckett, 2007). AASTHO HL93 truck design loads are shown in Figure 3.8.5. The HL93 (72,000lb) "design truck" is identical to HS20 (72,000lb) but HL93 "design tandem" is 25,000lb rather than 24,000lb in HS20, as shown in Figure 3.8.4. However, HS25 (90,000lb) "design truck" axle load of 40,000lb was larger than HL93 (72,000lb) axle load of 32,000lb.
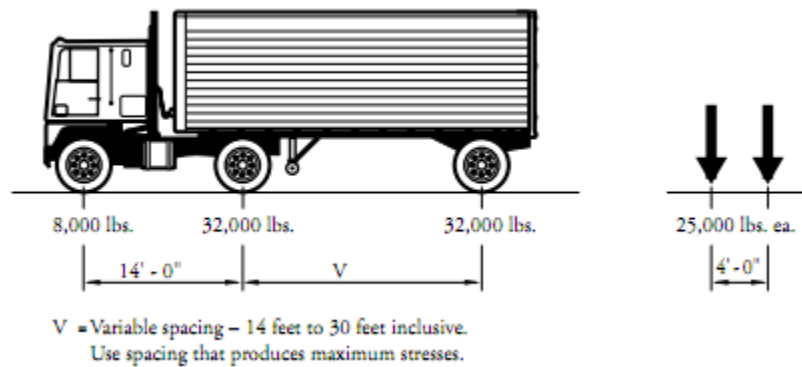
Figure 3.8.4 AASHTO HL93 Design Truck

(Source: PCI Bridge Design Manual, July 2003, Figure 7.2.2.1.4-1)
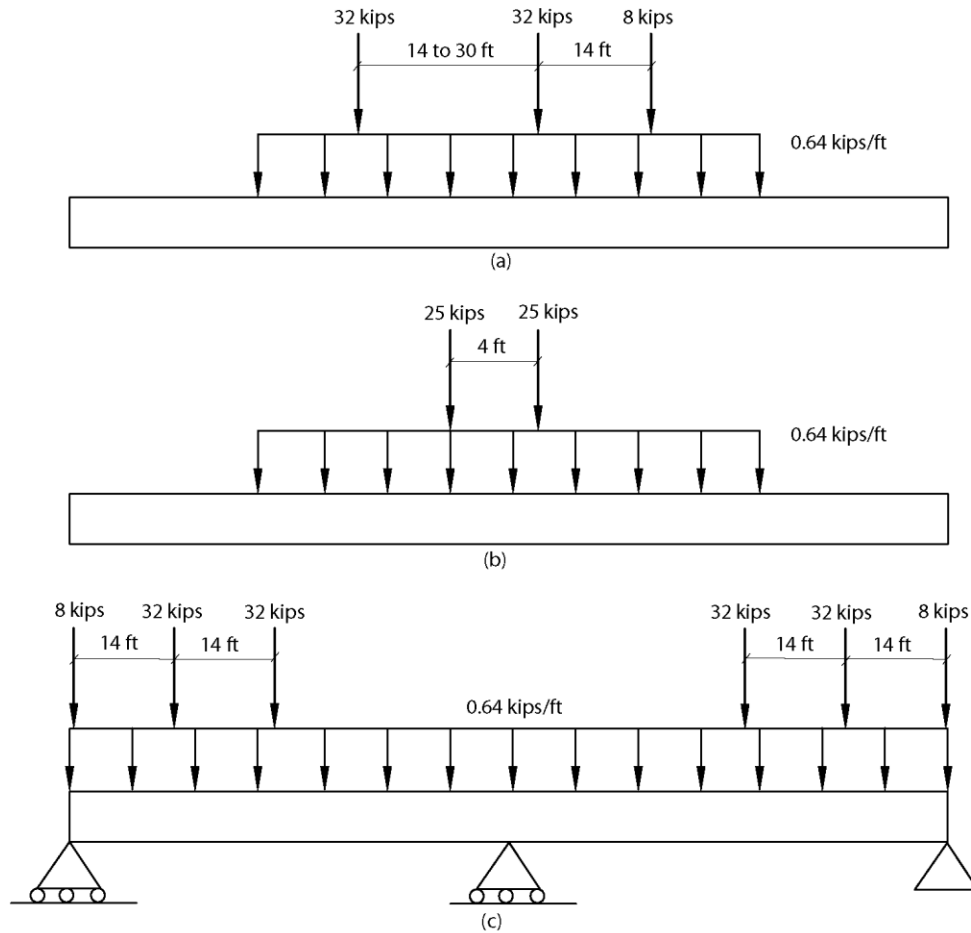
Figure 3.8.5 AASTHO HL93 Design Loads. (a) Design truck plus design lane, (b) Design tandem plus design lane, (c) Dual design

After October 1, 2007, Federal Highway Administration required to adoption of new LRFD method for all new bridge design (FHWA 2006).

3.9   Powder-Mill Bridge Design Truck

Powder-Mill Bridge (PMB) was designed by Fay, Spofford, and Thorndike (FST) in 2004 and was constructed by ET&L Corporation in 2009. FST used Allowable Stress Design (ASD) method for design. Annual average daily traffic (ADT) of PMB counted 2,000 vehicle per day (VPD), and the bridge is expected to experience about 2,500 VPD by 2015 (FST 2007). FST used a higher design truck load of HS25 than the recommended HS20 by AASTHO for the bridge design. The higher load was used based on the recommendation of the MassHighway Bridge Manual (MHD 2005), the detail information is given in chapter 2, section 2.4.1.

Table 3.9.1 Information about Design Truck of PMB

Requirements	Design Truck
AASTHO Standard Specification for Highway Bridge, 17th Edition 2002	HS20
Mass Highway Bridge Manual, 2005	HS25
Fay, Spofford and Thorndike (FST) design truck for PMB, 2004 (used for PMB design & load rating)	HS25

CHAPTER 4

Evaluation of Powder-Mill Bridge Rating Factors by Hand Calculation and Virtis 6.3

Powder-Mill Bridge girders were load rated at two levels, inventory and operating levels using ASD and LFD methods for both positive and negative moment region. The inventory rating level corresponds to the routine live load capacity for bridge traffic for an indefinite period of time. The operating rating level describes the live load capacity for the less frequent vehicles. The operating rating is commonly used to decide the maximum permissible live load, which the bridge could be safely carried. Based on the current design methods, the load and resistance factor design (LRFD) capacity of the bridge member are evaluated in three levels of load rating; design load rating, legal load rating, and permit load rating. Inventory and operating level ratings are determined under the design load rating using LRFD method.

Based on FHWA October 30, 2006 policy, for bridges designed by either ASD or LFD specifications, the rating factors of the members shall be based on LRFD method or LFD method (FHWA, 2006). However, Powder Mill Bridge falls under the guidelines of the Massachusetts Department of Transportation (MassDOT) Bridge Manual and according to the latest MassDOT Bridge Manual, if a bridge was designed using a method other than the LRFD specifications, it should be rated using the June 2007 Chapter 7 Bridge Load Rating Guidelines (MassDOT, 2005) and both ASR and LFR methods should be included. In order to include all methods which are

defined in The Manual for Bridge Evaluation (MBE) (2011a); ASR, LFR, and LRFR methods were used to calculate the load rating factors of PMB.

4.1 <u>Evaluation of Rating Factors by Hand Calculation</u>

Powder-Mill Bridge (PMB) rating factors were calculated using Standard Specification for Highway Bridges (AASHTO, 2002) and MBE (AASHTO, 2011). All superimposed dead loads were distributed using 60/40 distribution to all girders. CSI bridge program was used to create a simple three span frame models was created for both interior and exterior girders in order to calculate critical moments for both negative and positive moment regions. After finding these moment values, impact factors, distribution factors and multiple presence factor were applied to critical moment, Equation 1 and 2. It should be noted that the distribution factors in AASHTO (2002) are applied to wheel loads which are half axle loads of design truck.

$$\text{Impact} = \frac{15.24}{L + 38} \qquad \text{(AASHTO, 2002 Section 3.8.2 in S.I. Units)} \qquad (1)$$

$$Distribution\ Factor = \frac{S}{5.5} \qquad \text{(AASHTO, 2002 Section 3.23.2.3.1.5)} \qquad (2)$$

The general expression of the ASR and LFR equation which is used to determine rating factors is:

$$RF = \frac{C - A_1 D}{A_2 L (1 + I)} \qquad \text{(AASHTO, 2011 Section 6B.4.1)} \qquad (3)$$

'RF' is the rating factor for the live load carrying capacity, 'C' is the capacity of the member, 'D' is the dead load effect on the member, 'L' is the live load effect on the member and 'I' is the impact factor. A_1 and A_2 are the dead and live load factors, respectively.

The ASD method considers the service condition only and uses the linear elastic methods of analysis. The dead load factor (A_1) and live load factor (A_2) are both equal to 1.0 for inventory and operating level. For inventory level the capacity of the bridge is equal to $0.55 F_y$ where the 'F_y' is the yield stress of the steel.

The LFD method is based on the ultimate member capacity. The dead load factor (A_1) and live load factor (A_2) are equal to 1.3 and 2.17 for inventory level and 1.3 and 1.3 for operating level, respectively. The capacity of bridge members were calculated at the plastic moment.

The general expression to determine LRFR load rating factor is:

$$RF = \frac{C - \gamma_{DC} \times DC - \gamma_{DW} \times DW - \gamma_P \times P}{\gamma_{LL} \times (LL + IM)}$$ (ASSHTO, 2011a Equation 6A.4.2.1-1)   (4)

The load factors for load rating calculation changes based on the type of the bridge and also limit state which is defined in AASHTO 2010. According the MBE, strength is the primary limit state for load rating (AASHTO, 2011a). The dead load factor γ_{DC} equal to 1.25, superimposed dead load factor γ_{DW} equal to 1.50 and live load factor γ_{LL} equal to 1.75 for inventory level and 1.25, 1.50, and 1.35 for operating level respectively.

Haunch distance was considered in vertical position of the deck but it was not included in calculating the strength of the section. Sample calculation for girder 3 using both ASD and LFD methods can be seen in following page.

Table 4.1.1 Rating Factors by Hand Calculation for Positive Moment Region

(b) ASD Method			**(b)** LFD Method		
Girder #	Inventory RF	Operating RF	Girder #	Inventory RF	Operating RF
1	3.13	4.62	1	3.63	6.06
2	1.95	2.98	2	2.65	4.43
3	1.95	2.98	3	2.65	4.43
4	1.95	2.98	4	2.65	4.43
5	1.95	2.98	5	2.65	4.43
6	2.88	4.37	6	3.30	5.51

Table 4.1.2 Rating Factors by Hand Calculation for Negative Moment Region

(b) ASD Method

Girder #	Inventory RF	Operating RF
1	2.67	4.07
2	1.57	2.55
3	1.57	2.55
4	1.57	2.55
5	1.57	2.55
6	2.32	3.72

(b) LFD Method

Girder #	Inventory RF	Operating RF
1	3.00	5.01
2	2.17	3.62
3	2.17	3.62
4	2.17	3.62
5	2.17	3.62
6	2.76	4.61

Table 4.1.3 Rating Factors by Hand Calculation for Negative Moment Region
LRFR Method

Girder #	Inventory RF	Operating RF
1	3.56	4.62
2	2.53	3.28
3	2.53	3.28
4	2.53	3.28
5	2.53	3.28
6	3.30	4.29

4.2 Example Calculation for Negative and Positive Moment Region using ASD Method for Interior Girder in MatCAD

CALCULATION FOR POSITIVE MOMENT REGION

1. Calculation of Rating Factors using ASD Method for Interior Girders

1.1 Allowable stress design rating formulation, equation 1 :

$$(1) \quad RF_{I\_ASD} = \frac{\left[M_{RI} - M_{DL} \cdot \left(\dfrac{S_L}{S_{DL}} \right) - M_{SDL} \cdot \left(\dfrac{S_L}{S_{SDL}} \right) \right]}{\left(M_{LL} \right)}$$

(AASHTO, 2011 page A43, adapted from Eq. 6B.4.1-1)

1.2 Rating Factors for Inventory Level:

(2) The resisting capacity $\quad M_{RI} = f_I \cdot S^L$

(AASHTO, 2011 Table 6B.5.2.1-1)

1.3 Calculated Section Modulus:

$$S_{L\_pos} := 1.34 \cdot 10^7 \, mm^3$$

$$S_{DL\_pos} := 0.887 \cdot 10^7 \, mm^3$$

$$S_{SDL\_pos} := 1.216 \cdot 10^7 \, mm^3$$

1.4 Calculation of resisting capacity:

$$F_y := 50 \cdot ksi$$

$$f_I := 0.55 \cdot F_y$$

$$f_I = 0.19 \cdot GPa$$

$$M_{RI\_pos} := f_I \cdot S_{L\_pos}$$

$$M_{RI\_pos} = 2.54 \times 10^3 \cdot kN \cdot m$$

1.5 Calculated Moments Values By Hand:

$$M_{DL\_pos} := 404.31 \, kN \cdot m$$

$$M_{SDL\_pos} := 165.70 \, kN \cdot m$$

$$M_{LL\_pos} := 896.64 \, kN \cdot m$$

1.6 Calculation of Rating Factors for Girder 3 and Girder 5 in Inventory Level:

$$RF_{I\_ASD\_pos} := \frac{\left[M_{RI\_pos} - M_{DL\_pos} \cdot \left(\dfrac{S_{L\_pos}}{S_{DL\_pos}} \right) - M_{SDL\_pos} \cdot \left(\dfrac{S_{L\_pos}}{S_{SDL\_pos}} \right) \right]}{\left(M_{LL\_pos} \right)}$$

$$RF_{I\_ASD\_pos} = 1.95$$

1.7 Rating Factors for Operating Level:

(3) The resisting capacity $\quad M_{RO} = f_O \cdot S^L$

1.8 Calculation of resisting capacity:

$$f_O := 0.75 \cdot F_y$$

$$f_O = 0.26 \cdot GPa$$

$$M_{RO\_pos} := f_O \cdot S_{L\_pos}$$

$$M_{RO\_pos} = 3.46 \times 10^3 \cdot kN \cdot m$$

1.9 Calculation of Rating Factors for Girder 3 and Girder 5 in Operating Level:

$$RF_{O\_ASD\_pos} := \frac{\left[M_{RO\_pos} - M_{DL\_pos} \cdot \left(\dfrac{S_{L\_pos}}{S_{DL\_pos}} \right) - M_{SDL\_pos} \cdot \left(\dfrac{S_{L\_pos}}{S_{SDL\_pos}} \right) \right]}{\left(M_{LL\_pos} \right)}$$

$$RF_{O\_ASD\_pos} = 2.98$$

67

CALCULATION FOR NEGATIVE MOMENT REGION

2. Calculation of Rating Factors using ASD Method for Interior Girders

2.1 Allowable stress design rating formulation, equation 1 :

$$(1) \quad RF_{I\_ASD} = \frac{\left[M_{RI} - M_{DL} \cdot \left(\frac{S_L}{S_{DL}} \right) - M_{SDL} \cdot \left(\frac{S_L}{S_{SDL}} \right) \right]}{\left(M_{LL} \right)}$$

(AASHTO, 2011 page A43, adapted from Eq. 6B.4.1-1)

2.2 Rating Factors for Inventory Level:

$$(2) \quad \text{The resisting capacity} \qquad M_{RI} = f_I \cdot S_L$$

(AASHTO, 2011 Table 6B.5.2.1-1)

2.3 Calculated Section Modulus:

$$S_{L\_neg} := 1.04 \cdot 10^7 \, mm^3$$

$$S_{DL\_neg} := 0.887 \cdot 10^7 \, mm^3$$

$$S_{SDL\_neg} := 1.04 \cdot 10^7 \, mm^3$$

2.4 Calculation of resisting capacity:

$$F_y := 50 \cdot ksi$$

$$f_I := 0.55 \cdot F_y$$

$$f_I = 0.19 \cdot GPa$$

$$M_{RI\_neg} := f_I \cdot S_{L\_neg}$$

$$M_{RI\_neg} = 1.97 \times 10^3 \cdot kN \cdot m$$

2.5 Calculated Moments Values By Hand:

$$M_{DL\_neg} := 515.35 \, kN \cdot m$$

$$M_{SDL\_neg} := 211.21 \, kN \cdot m$$

$$M_{LL\_neg} := 735.27 \, kN \cdot m$$

2.6 Calculation of Rating Factors for Girder 3 and Girder 5 in Inventory Level:

$$RF_{I\_ASD\_neg} := \frac{\left[M_{RI\_neg} - M_{DL\_neg} \cdot \left(\frac{S_{L\_neg}}{S_{DL\_neg}} \right) - M_{SDL\_neg} \cdot \left(\frac{S_{L\_neg}}{S_{SDL\_neg}} \right) \right]}{\left(M_{LL\_neg} \right)}$$

$$RF_{I\_ASD\_neg} = 1.57$$

2.7 Rating Factors for Operating Level:

(3) The resisting capacity $\qquad M_{RO} = f_O \cdot S^L \qquad$ (AASHTO, 2011 Table 6B.5.2.1-1)

2.8 Calculation of resisting capacity:

$$f_O := 0.75 \cdot F_y$$

$$f_O = 0.26 \cdot GPa$$

$$M_{RO\_neg} := f_O \cdot S_{L\_neg}$$

$$M_{RO\_neg} = 2.69 \times 10^3 \cdot kN \cdot m$$

2.9 Calculation of Rating Factors for Girder 3 and Girder 5 in Operating Level:

$$RF_{O\_ASD\_neg} := \frac{\left[M_{RO\_neg} - M_{DL\_neg} \cdot \left(\frac{S_{L\_neg}}{S_{DL\_neg}} \right) - M_{SDL\_neg} \cdot \left(\frac{S_{L\_neg}}{S_{SDL\_neg}} \right) \right]}{\left(M_{LL\_neg} \right)}$$

$$RF_{O\_ASD\_neg} = 2.55$$

4.3 Calculation of Negative Moment Region Rating Factors using LRFD Method

For Interior Girders:

General expression of LRFR:

$$RF = \frac{C - (\gamma_{DC}) \cdot (DC) - (\gamma_{DW}) \cdot (DW) - (\gamma_P) \cdot (P)}{(\gamma_{LL}) \cdot (LL + IM)}$$

(AASHTO Manual 6A.4.2.1-1)

For the Strength Limit States:

(AASHTO Manual 6A.4.2.1-2)

$$C = \phi_c \cdot \phi_s \cdot \phi \cdot R_n$$

Resistance Factors:

ϕ = Resistance factor for Strength Limit State for Flexure

$\phi := 1.0$

(AASHTO Manual, C6A.4.2.1)

ϕ_C = Condition factor for uncertainties increasing with age of bridge

(AASHTO Manual, Table 6A.4.2.3-1)

$\phi_c := 1.0$

ϕ_S = System factor for level of redundancy in the bridge

(AASHTO Manual, Table 6A.4.2.4-1)

$\phi_s := 1.0$

Load Factors:

For Inventory and Operating Level only the Live Live Load factors changes:

$\gamma_{DC} := 1.25$ $\qquad$ $\gamma_{DW} := 1.50$ $\qquad$ $\gamma_{LLin} := 1.75$ $\qquad$ $\gamma_{LLop} := 1.35$

(AASHTO Manual, Table 6A.4.2.2-1)

Dynamic Load Allowance (IM):

(AASHTO Manual, C6A.4.4.3)

$IM := 0.33$

Composite Section Properties For Interior Girder:

*Girder Section Properties are taken from PMB Drawings sheet 14 of 20 sheets

$t_{deck} := 200\,mm$ $t_{f\_int} := 26\,mm$ $d_{int} := 915\,mm$

$f_c := 0.03\,GPa$

$t_{w\_int} := 17\,mm$ $b_{f\_int} := 305\,mm$

$f_y := 0.34474\,GPa$

$d_{w\_int} := d_{int} - \left(2 \cdot t_{f\_int}\right) = 0.863\,m$

$f_{yreinf} := 0.420\,GPa$

$Spacing_{int} := 2250\,mm$

$t_{haunch\_int} := 41\,mm$

Calculation of Nominal Member Resistance for Negative Moment Section:

!! Condition needs to be checked if the PNA is in the web or in the top flange. Based on the condition Mp can be calculated from table D6.1-2

Condition check:

!! Ps not calculated because looking at negative moment

$P_c := f_y \cdot t_{f\_int} \cdot b_{f\_int}$

$P_c = 2.734 \times 10^6\,N$

$P_w := f_y \cdot t_{w\_int} \cdot d_{w\_int}$

$P_w = 5.058 \times 10^6\,N$

$P_t := P_c$

$P_t = 2.734 \times 10^6\,N$

$P_{rb} + P_{rt} = P_{totalreinf}$

$P_{totalreinf} := 2127\,kN$

$P_c + P_w \geq P_t + P_{totalreinf}$ PNA lies in the web

$P_c + P_w = 7.791 \times 10^6\,N$ $P_t + P_{totalreinf} = 4.861 \times 10^6\,N$

71

Calculation of PNA:

$$Y := \left(\frac{d_{w\_int}}{2} \right) \cdot \left[\left[\left(\frac{P_c - P_t - P_{totalreinf}}{P_w} \right) \right] + 1 \right]$$

Y =0.25 m

$Y = 0.25 \text{ m}$ from bottom of the top flange
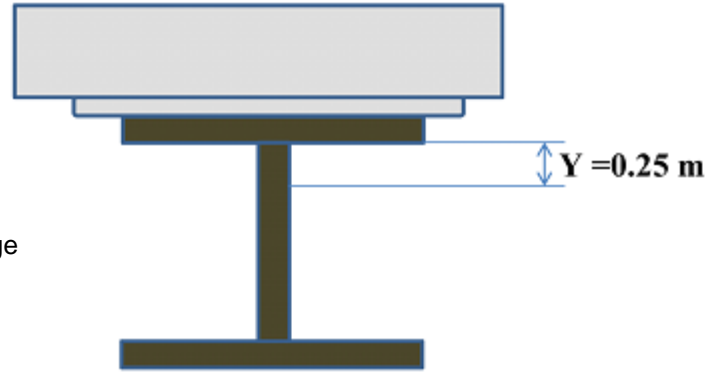
Calculation of Plastic Moment   (Mp):

$$M_p := \frac{P_w}{2 \cdot d_{w\_int}} \cdot \left[Y^2 + \left(d_{w\_int} - Y \right)^2 \right] + \left[\left(\frac{t_{deck}}{2} + 41 \text{ mm} + t_{f\_int} + Y \right) \cdot P_{totalreinf} \right] + \left[P_t \cdot \left(Y + \frac{t_{f\_int}}{2} \right) \right] + P_c \cdot \left[\left(d_{w\_int} - Y \right) + \frac{t_{f\_int}}{2} \right]$$

$M_p = 4.602 \times 10^3 \cdot \text{kN} \cdot \text{m}$

$C := M_p$

$C = 4.602 \times 10^3 \cdot \text{kN} \cdot \text{m}$

Calculation of Live Load Distribution:

Two or more design lanes loaded:

$$DF = 0.075 + \left(\frac{S}{9.5} \right)^{0.6} \cdot \left(\frac{S}{L} \right)^{0.2} \cdot \left[\frac{K_g}{12 \cdot L \cdot \left(t_s \right)^3} \right]^{0.1}$$

(AASHTO Specification, Table4.6.2.2.2b-1 US Units)

$$K_g = n \cdot \left(I_{in} + A \cdot e_g^{2} \right)$$

$E_b := 199.948 \text{ GPa}$

$E_d := 25.924 \text{ GPa}$

$n := \dfrac{E_b}{E_d} = 7.713$

$I_{in} := 9754.189 \text{ in}^4$

$$e_{g\_in} := \left[t_{haunch\_int} + \frac{1}{2} \cdot \left(t_{deck} + d_{int} \right) \right] = 23.563 \cdot \text{in}$$

Interior, W920x238

$A_{int} := 30400 \text{ mm}^2$

$A_{int\_in} := A_{int}$

$A_{int\_in} = 47.12 \cdot in^2$

$K_{g\_in} := n \cdot \left(I_{in} + A_{int\_in} \cdot e_{g\_in}^2 \right) = 2.77 \times 10^5 \cdot in^4$

$t_{deckin} := 7.874$

$L := 77.1$

$S := 7.382$

$K := 277000$

$$DF_{int\_2\_lanes} := \left[0.075 + \left(\frac{S}{9.5} \right)^{0.6} \cdot \left(\frac{S}{L} \right)^{0.2} \cdot \left[\frac{K}{12 \cdot L \cdot \left(t_{deckin} \right)^3} \right]^{0.1} \right] = 0.587$$

Calculation of Rating Factors for Interior Girders:

$DC_{int} := 515.350 \ kN \cdot m$

$DW_{int} := 211.210 \ kN \cdot m$

$m := 1.2$

$LL_{interior} := 877.98 \ kN \cdot m \cdot (1 + IM) \cdot DF_{int\_2\_lanes} \cdot m$

$$RF_{in\_inv} := \frac{C - \left(\gamma_{DC} \right) \cdot \left(DC_{int} \right) - \left(\gamma_{DW} \right) \cdot \left(DW_{int} \right)}{\left(\gamma_{LLin} \right) \cdot \left(LL_{interior} \right)}$$

$RF_{in\_inv} = 2.529$

$$RF_{in\_opr} := \frac{C - \left(\gamma_{DC} \right) \cdot \left(DC_{int} \right) - \left(\gamma_{DW} \right) \cdot \left(DW_{int} \right)}{\left(\gamma_{LLop} \right) \cdot \left(LL_{interior} \right)}$$

$RF_{in\_opr} = 3.279$

For Exterior Girders:

General expression of LRFR:

$$RF = \frac{C - \left(\gamma_{DC}\right) \cdot (DC) - \left(\gamma_{DW}\right) \cdot (DW) - \left(\gamma_{P}\right) \cdot (P)}{\left(\gamma_{LL}\right) \cdot (LL + IM)}$$

(AASHTO Manual 6A.4.2.1-1)

For the Strength Limit State:

$$C = \phi_c \cdot \phi_s \cdot \phi \cdot R_n$$

(AASHTO Manual 6A.4.2.1-2)

Resistance Factors:

ϕ = Resistance factor for Strength Limit State for Flexure

$\phi := 1.0$

(AASHTO Manual, C6A.4.2.1)

ϕ_C = Condition factor for uncertainties increasing with age of bridge

(AASHTO Manual, Table 6A.4.2.3-1)

$\phi_c := 1.0$

ϕ_S = System factor for level of redundancy in the bridge

(AASHTO Manual, Table 6A.4.2.4-1)

$\phi_s := 1.0$

Load Factors:

For Inventory and Operating Level only the Live Live Load factors changes:

$\gamma_{DC} := 1.25$ $\qquad$ $\gamma_{DW} := 1.50$ $\qquad$ $\gamma_{LLin} := 1.75$ $\qquad$ $\gamma_{LLop} := 1.35$

(AASHTO Manual, Table 6A.4.2.2-1)

Dynamic Load Allowance (IM):

(AASHTO Manual, C6A.4.4.3)

$IM := 0.33$

Composite Section Properties For Interior Girder:

*Girder Section Properties are taken from PMB Drawings sheet 14 of 20 sheets

$t_{deck} := 200\ mm$ $t_{f\_int} := 40\ mm$ $d_{int} := 943\ mm$

$f_c := 0.03\ GPa$ $t_{w\_int} := 22\ mm$ $b_{f\_int} := 308\ mm$

$f_y := 0.34474\ GPa$

$d_{w\_int} := d_{int} - 2 \cdot t_{f\_int} = 0.863\ m$

$f_{yreinf} := 0.420\ mm$

$Spacing_{int} := 2250\ mm$

$t_{haunch\_int} := 41\ mm$

Calculation of Nominal Member Resistance for Negative Moment Section:

!! Condition need to be check if the PNA is in the web or in the top flange? Based on the condition Mp can be calculated from table D6.1-2

Condition check:

$P_c := f_y \cdot t_{f\_int} \cdot b_{f\_int}$

$P_c = 4.247 \times 10^6\ N$

$P_w := f_y \cdot t_{w\_int} \cdot d_{w\_int}$

$P_w = 6.545 \times 10^6\ N$

$P_t := P_c$

$P_t = 4.247 \times 10^6\ N$

$P_{rb} + P_{rt} = P_{totalreinf}$

$P_{totalreinf} := 2127\ kN$

$P_c + P_w \ge P_t + P_{totalreinf}$ PNA lies in the web

75

Calculation of PNA:

$$Y := \left(\frac{d_{w\_int}}{2} \right) \cdot \left[\left(\frac{P_c - P_t - P_{totalreinf}}{P_w} \right) + 1 \right]$$

$$Y = 0.291 \ m$$

Calculation of Plastic Moment (Mp):

$$M_p := \frac{P_w}{2 \cdot d_{w\_int}} \cdot \left[Y^2 + \left(d_{w\_int} - Y \right)^2 \right] + \left[\left(\frac{t_{deck}}{2} + 40 \, mm + t_{f\_int} + Y \right) \cdot P_{totalreinf} \right] + \left[P_t \cdot \left(Y + \frac{t_{f\_int}}{2} \right) \right] + P_c \cdot \left[\left(d_{w\_int} - Y \right) + \frac{t_{f\_int}}{2} \right]$$

$$M_p = 6.399 \times 10^3 \cdot kN \cdot m$$

$$C := M_p$$

$$C = 6.399 \times 10^3 \cdot kN \cdot m$$

Calculation of Live Load Distribution:

Two or more design lanes loaded:

$$DF = 0.075 + \left(\frac{S}{9.5} \right)^{0.6} \cdot \left(\frac{S}{L} \right)^{0.2} \cdot \left[\frac{K_g}{12 \cdot L \cdot \left(t_s \right)^3} \right]^{0.1}$$

(AASHTO Specification, Table4.6.2.2.2b-1 US Units)

$$K_g = n \cdot \left(I_{in} + A \cdot e_g^2 \right)$$

$$E_b := 199.948 \ GPa$$

$$E_d := 25.924 \ GPa$$

$$n := \frac{E_b}{E_d} = 7.713$$

$$I_{in} := 15039.71 \ in^4$$

$$e_{g\_in} := \left[t_{haunch\_int} + \frac{1}{2} \cdot \left(t_{deck} + d_{int} \right) \right] = 24.114 \cdot in$$

Exterior, W920x345

$$A_{ext} := 44000 \ mm^2$$

$$A_{ext\_in} := A_{ext}$$

$$A_{ext\_in} = 68.2 \cdot in^2$$

$$I_{ex} := 15039.71 \ in^4$$

$$K_{g\_ex} := n \cdot \left(I_{ex} + A_{ext\_in} \cdot e_{g\_in}^{\ 2} \right) = 4.219 \times 10^5 \cdot in^4$$

$$in_{deckin} := 7.874$$

$$\underset{\sim}{t}_L := 77.1$$

$$\underset{\sim}{S} := 7.382$$

$$\underset{\sim}{K} := 421900$$

$$DF_{ext\_2\_lanes} := 0.075 + \left(\frac{S}{9.5} \right)^{0.6} \cdot \left(\frac{S}{L} \right)^{0.2} \cdot \left[\frac{K}{12 \cdot L \cdot \left(t_{deckin} \right)^3} \right]^{0.1} = 0.609$$

Calculation of Rating Factirs for Exterior Girders:

$$DC_{ext} := 555.710 \ kN \cdot m$$

$$DW_{ext\_gr1} := 255.580 \ kN \cdot m$$

$$DW_{ext\_gr6} := 513.490 \ kN \cdot m$$

$$\underset{\sim}{m} := 1.2$$

$$LL_{extrior} := 877.420 \ kN \cdot m \cdot (1 + IM) \cdot DF_{ext\_2\_lanes} \cdot m = 852.806 \cdot kN \cdot m$$

$$RF_{exgr1\_inv} := \frac{C - \left(\gamma_{DC}\right)\cdot\left(DC_{ext}\right) - \left(\gamma_{DW}\right)\cdot\left(DW_{ext\_gr1}\right)}{\left(\gamma_{LLin}\right)\cdot\left(LL_{extrior}\right)}$$

$$RF_{exgr1\_inv} = 3.565$$

$$RF_{exgr1\_opr} := \frac{C - \left(\gamma_{DC}\right)\cdot\left(DC_{ext}\right) - \left(\gamma_{DW}\right)\cdot\left(DW_{ext\_gr1}\right)}{\left(\gamma_{LLop}\right)\cdot\left(LL_{extrior}\right)}$$

$$RF_{exgr1\_opr} = 4.622$$

$$RF_{exgr6\_inv} := \frac{C - \left(\gamma_{DC}\right)\cdot\left(DC_{ext}\right) - \left(\gamma_{DW}\right)\cdot\left(DW_{ext\_gr6}\right)}{\left(\gamma_{LLin}\right)\cdot\left(LL_{extrior}\right)}$$

$$RF_{exgr6\_inv} = 3.306$$

$$RF_{exgr6\_opr} := \frac{C - \left(\gamma_{DC}\right)\cdot\left(DC_{ext}\right) - \left(\gamma_{DW}\right)\cdot\left(DW_{ext\_gr6}\right)}{\left(\gamma_{LLop}\right)\cdot\left(LL_{extrior}\right)}$$

$$RF_{exgr6\_opr} = 4.286$$

4.4   <u>Load Rating Program, Virtis 6.3 by AASHTOWare</u>

In 1990s the AASHTO started to work on a new software package for load rating, called Virtis. Before Virtis, Bridge Rating and Analysis of Structural Systems (BRASS) had been used by bridge owners. BRASS was developed by the Wyoming Department of Transportation. AASHTO improved the new load rating program Virtis using BRASS (Thompson, 1999).

The old load rating program were written using FOTRAN computer language program. AASHTO developed Virtis, since the old load rating program was not user-friendly because of those following reasons.

- Updating the software with the current bridge design specification was really difficult
- Formatting of the old software was text file, it was not supported graphically
- It did not have database bridge management capability

The goal was creating a user-friendly program and increases the productivity of Engineers in data entry and analysis according to new load rating requirements. In Virtis, bridge materials and structural components such as beams, and parapets can easily be selected from Virtis library and a bridge can quickly modeled for load rating calculations. In order to standardize the calculation of rating factors nationwide, AASHTOWare has been developing enhancements to create a finite element analysis engine for Virtis (AASHTO Task Froce Meeting, 2011).

At the end of 2006, 112 licensees of Virtis had been purchased, 37 of them that was purchased by state DOTs (BRIDGEWare, 2006). The available latest version of Virtis is 6.3 built on July 12, 2011. This version of Virtis includes (AASHTOWare):

- Additional cross sectional types for floor truss
- Selection of the LRFD specification edition beginning with the 4th Edition 2008 Interim
- Support for the LRFD 4th Edition 2009 Interim
- Support for the LRFD 5th Edition
- Support for the LRFD 5th Edition 2010 Interim
- Support for the Manual for Bridge Evaluation First Edition (2008)

- Support for the Manual for Bridge Evaluation First Edition (2010 Interim)
- Support for the Manual for Bridge Evaluation Second Edition (2011)
- Support for Windows 7 operating system
- LRFR permit vehicle with lane load

In this chapter, the design office rating factors of PMB was calculated using AASHTO BRIDGEWare program. Access to Virtis 6.3 was provided by FST (Fay, Spofford & Thorndike). PMB was designed based on AASHTO Standard Specifications for Highway Bridges, 17th edition 2002 and this specification was used by Virtis 6.3 to calculate rating factors. Since HS25 design truck was used for PMB design based on MassDOT requirement in 2005, PMB rating factors were calculated using this design truck with two different methods, ASD and LFD.

4.5   Evaluation of Rating Factors by Virtis 6.3

Before starting the load rating calculation, new bridge name and information was defined inside the Virtis 6.3. For this purpose, from the Bridge Explorer toolbar new bridge button was clicked and the Bridge ID, name, and description of the bridge were filled. After defining the Powder-Mill Bridge, the bridge was saved on the system with other bridge inside the library.

Structural steel was used for PMB is AASHTO M 270M, Grade 345W and Material type of PMB reinforcement steel is ASTM A615M, Grade 420. Concrete material properties are 30 MPa for all concrete elements except sidewalk and safety curb, 35Mpa for sidewalk and safety curb. Since Virtis has AASHTO library in the program, all these information copied from the library.

Two load cases were defined; non composite dead load case and superimposed dead load case. All calculation for these load cases made by hand. Noncomposite dead load case which included haunch, diaphragms and SIP form and superimposed dead load case which included safety curb, sidewalk, railing and wearing surface.

After completing Frame Plan Details, framing plan of the PMB was available to check. After saving frame plan detail information, "view schematic" button was appeared in the bridge workspace tool; by clicking this button bridge framing plan was checked as seen in Figure 4.4.1.
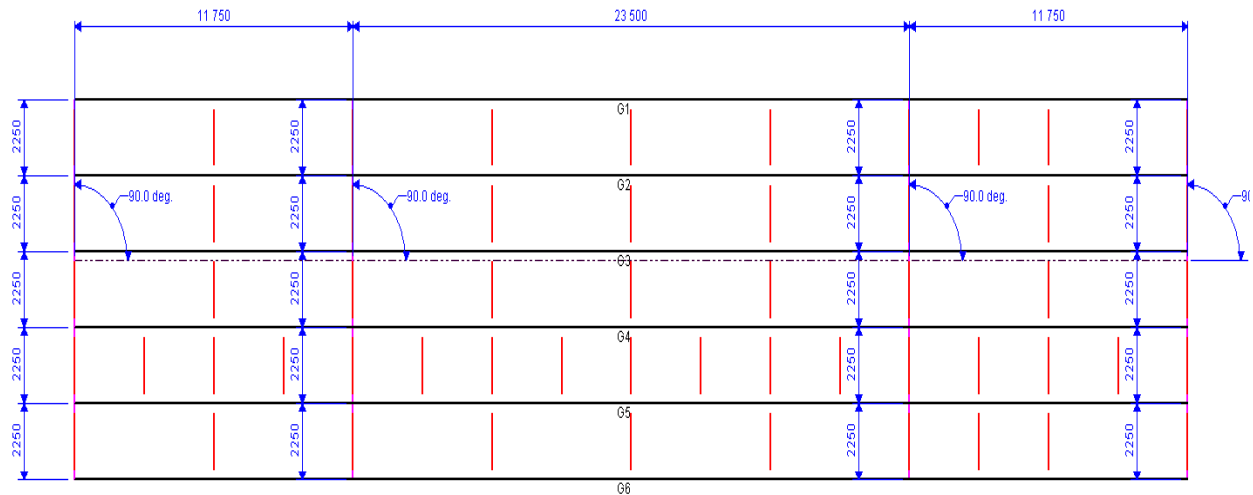
Figure 4.4.1 Framing Plan

Member loads were defined for both non-composite dead load and superimposed dead loads. For superimposed dead load 60/40 distribution was used based on MassDOT Bridge Manual. MassDOT requirement Part I, Paragraph 7.2.4.9 (MassDOT, 2005):

"For stringer bridges with deck slabs, the sidewalk, safety curb, railings and median superimposed dead loads can be distributed to beams using either a 60/40 distribution, as specified in Paragraph 3.5.3.3 of this Bridge Manual, or to be distributed equally to all beams. If the use of both these methods creates a disparity in the rating between the interior and exterior beams, that distribution method which produces the highest overall bridge rating shall be utilized to rate the affected components. The wearing surface superimposed dead loads shall always be distributed uniformly between all beams. The use of superimposed dead load distribution factors which lie in between those specified above shall not be used."

Exterior girder, G1 and G6 have fascia girder at the north end of the span 3 in order to support the varying deck width at this location. These side girders were not seen in the framing plan in the program but uniform loading of these fascia girders loads were added as a distributed load between point 2.937m and 11.75 m in third span and as a concentrated load at point 2.937m.

81

Under the section of "Defining Structural Typical Section" deck, parapet, median, railing, generic, sidewalk, lane position and wearing surface was defined. The typical deck section plan was checked by clicking "view schematic", as seen in Figure 4.4.2.
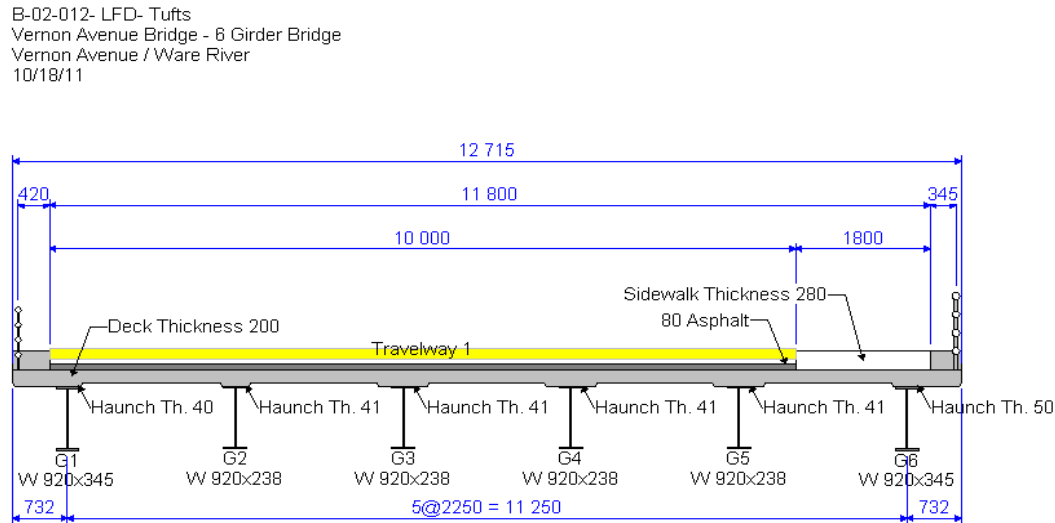
Figure 4.4.2 Typical Deck Section

Two separate programs were created to evaluate load rating of PMBB with two different methods, ASD and LFD. The capacity of the members are evaluated as an inventory level and operating level for the ASD and LFD methods. The result of ASD and LFD methods load rating calculation can be seen the Table 4.4.1.

Table 4.4.1 Rating Factor by Virtis 6.3* for Negative Moment Region

(a) ASD Method

Girder #	Inventory RF	Inventory Tons	Operating RF	Operating Tons
1	2.84	127.89	4.19	188.48
2	1.76	78.97	2.65	119.36
3	1.76	78.97	2.65	119.36
4	1.76	78.97	2.65	119.36
5	1.76	78.97	2.65	119.36
6	2.45	110.11	3.79	170.70

(b) LFD Method

Girder #	Inventory RF	Inventory Tons	Operating RF	Operating Tons
1	4.68	210.58	7.80	350.97
2	2.70	121.95	4.52	203.25
3	2.70	121.36	4.49	202.27
4	3.19	143.35	5.31	238.92
5	3.19	143.47	5.31	239.12
6	4.43	199.91	7.40	333.19

*PMB design truck is HS25, the weight of this truck is 90kips (45 UStons)

4.6 Scanned Documents for Hand Calculation and Virtis

Evaluation of Rating Factors by Hand Calculation with ASD Method;

Evaluation of Interior Girders:

I Beam W 920×238 (from VAB drawing sheet 14 of 20 sheets)

Beam Designation	Top Flange	Web	Bottom Flange
Beam No 2,3,4 & 5	26 × 305	17 × 863	26×305

Properties of W920×238 AISC, 2005 Third Edition

$A = 30400 mm^2$

$I_x = 4.06 \times 10^9 mm^4$ (AISC – Table 5-2)

— Non Composite Section —
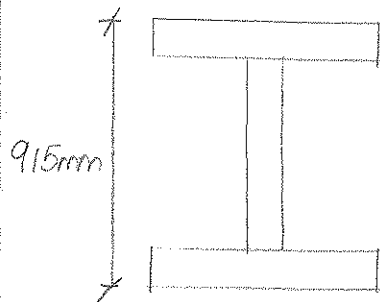
$\bar{y} = 915/2 = 457.5mm$

$S_t = \dfrac{4.06 \times 10^9}{457.5} = 8.874 \times 10^6 mm^3 = S_t^{DL}$

$S_b = \dfrac{4.06 \times 10^9}{457.5} = \{8.874 \times 10^6 mm^3 = S_b^{DL}\}$

915mm

— Effective Flange Width —

(1) 1/4 (L) ⇒ $1/4 \times 11.75 = 2.938m$
$\qquad\qquad\qquad 1/4 \times 23.5 = 5.875m$

(2) $12 \cdot t_s$ ⇒ $12 \times 0.2m = 2.4m$

(3) S ⇒ 2.25 ✓

AASHTO Standart Specifications for Highway Bridges 17th, 2002
10.38.3 Effective Flange Width

For composite section, the concrete is transformed into an equivalent area of steel by dividing the area of the slab by the modular ratio. Live load plus impact stresses are carried by the composite section using a modular ratio of n.

$E_s = 199948 MPa$

Calculation of E_C (AASHTO, 2002 section 8.7.1)

$E_C = 57,000 \sqrt{f_c'}$ (US units)

$E_C = 57,000 \sqrt{4351 psi} = 3.76 \times 10^6 psi = 25,924 MPa$ $n = E_S/E_C = 7.7$

Structural steel AASHTO M270M Grade 345W (50ksi)

Concrete High Performance Cement Concrete 30MPa (4.35ksi)

Short term composite section properties, $n=7.7$ (positive flexure)
_____

Interior girders;

$A (mm^2)$	$y (mm)$	$A \cdot y$	$\lvert y-\bar{y}\rvert$	$A(y-\bar{y})^2$	I_o
CONC. $=\dfrac{(A_{slab}+A_{haunch})/7.7}{(4.5\times10^5 + 15580)/7.7}$ $= 6.046\times10^4$	$915+41+200/2$ $= 1056$	$=6.38\times10^7$	$=201$	$=2.44\times10^9$	$\left(\dfrac{2250}{7.7}\right)\times 200^3/12$ +haunch $= 1.95\times10^8$
STEEL $=30400$ $+$ $\overline{9.086\times10^4}$	$=457.5$	$=1.39\times10^7$ $+$ $\overline{7.77\times10^7}$	$=397.5$	$=4.80\times10^9$ $+$ $\overline{7.24\times10^9}$	$=4.06\times10^9$ $+$ $\overline{4.25\times10^9}$

$\bar{y} = \dfrac{\Sigma(A\cdot y)}{\Sigma(A)} = \dfrac{7.77\times10^7}{9.086\times10^4} = 855mm$

$I_x = 7.24\times10^9 + 4.25\times10^9 = 11.49\times10^9 mm^4$

$S_t = \dfrac{11.49\times10^9}{301} = 3.81\times10^7 mm^3$ $S_b = \dfrac{11.49\times10^9}{855} = 1.34\times10^7 mm^3 = S_b^L$ ✓ (M^+)

Long term composite section properties, $3n = 23.1$ (positive flexure)
interior girders;
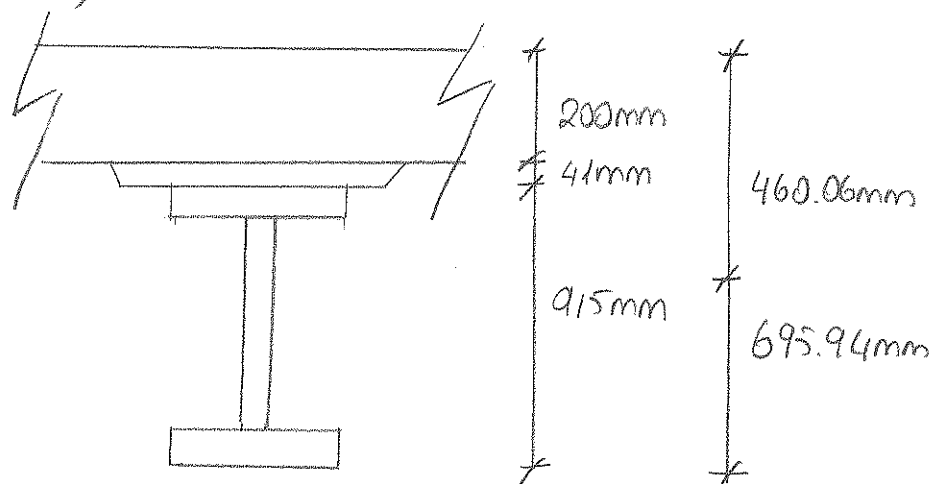
	$A(mm^2)$	$y(mm)$	$A.y$	$|y-\bar{y}|$	$A.(y-\bar{y})^2$	I_0
Conc.	2.015×10^4	$= 1056$	$= 2.127 \times 10^7$	$= 360.06$	2.61×10^9	6.503×10^7
Steel	$+ \dfrac{30400}{5.055 \times 10^4}$	$= 4575$	$+ \dfrac{1.391 \times 10^7}{3.518 \times 10^7}$	$= 238.44$	$+ \dfrac{1.728 \times 10^9}{4.338 \times 10^9}$	$+ \dfrac{4.06 \times 10^9}{4.125 \times 10^9}$

$$\bar{y} = \frac{\sum(A \cdot y)}{\sum(A)} = \frac{3.518 \times 10^7}{5.055 \times 10^4} = 695.94\,mm$$

$$I_x = 4.338 \times 10^9 + 4.125 \times 10^9 = 8.463 \times 10^9\,mm^4$$

$$S_t = \frac{8.463 \times 10^9}{460.06} = 1.839 \times 10^7\,mm^3$$

$$S_b = \frac{8.463 \times 10^9}{695.94} = \left\{ 1.216 \times 10^7\,mm^3 = S_b^{SDL} \right\}\ (M^+)$$

VAB Dead and Superimposed Dead Load Calculations.

Deck slab = $0.2m \times 2.250m \times 23.576 \ kN/m^3 = 10.61 \ kN/m$

Haunch $= [0.305 + (2 \times 0.025)] \times 0.041 + (0.025 \times 0.041) \times 23.576 \ kN/m^3 = 0.367 kN/m$

Diaphram $= (68.56 kg/m \times 9.81 \ N/kg \times 2.25m)/47m = 0.298 kN/m /2 = 0.149 \ kN/m$

Beam $= 238 kg/m \times 9.81 \ N/kg = 2334.78 \ N/m = 2.33 \ kN/m$

Dead Load $=$ Deck slab + haunch + Beam + diaphram

$$DL = 10.61 \ kN/m + 0.367 kN/m + 2.33 kN/m + 0.149 \ kN/m$$

$$DL = \{13.50 \ kN/m\}$$

Railing $\Rightarrow$ @ sidewalk $= 1.81 \ kN/m$

@ safety curb $= 1.26 \ kN/m$.

Sidewalk $= \left(\dfrac{0.3022 + 0.28}{2} \right) \times 2.22m \times 23.576 \ kN/m^3 = 15.24 \ kN/m$

Safety curb $= 0.495m \times 0.28m \times 23.576 \ kN/m^3 = 3.27 \ kN/m$.

Wearing Surface $= 0.08m \times 25.150 \ kN/m^3 \times 10m = 20.12 \ kN/m /6 = 3.35 \ kN/m$

⚐ Mass Highway Bridge Manual - Part I June 2007 section 7.2.4.9;

For stringer bridges the sidewalk, safety curbs and railings superimposed dead loads can be distributed to beams using 60/40 distribution.

Therefore;

$$SDL_{GR1} = (3.27 \ kN/m + 1.26 \ kN/m) \times 0.6 + 3.35 \ kN/m = \{6.61 \ kN/m\}$$

$$SDL_{GR6} = (15.24 kN/m + 1.81 kN/m) \times 0.6 + 3.35 kN/m = \{13.28 kN/m\}$$

$$SDL_{inter.} = (1.31 + 1.26 + 15.24 + 3.27)/4 \times 0.4 + 3.35 = \{5.46 \ kN/m\}.$$

→ Moment values from beam model was created in CSiBridge.

	Positive Max. Moments (kNm)	Negative Max. Moments (kNm)
$DL_{(interior)}$	404.31 kNm	515.35 kNm
$SDL_{(interior)}$	165.70 kNm	211.21 kNm
$LL_{(interior)}$	535.31 kNm	438.97 kNm

Impact Factor;

$$I = \frac{15.24}{L+38} \quad \text{(SI unit)} \quad \text{(AASHTO, 2002 \ 3.8.2)}$$

$$I = \frac{15.24}{23.5+38} = 24.78 \sim \%25$$

Distribution Factor;

$$DF = S/5.5 \quad \text{(U.S unit)} \quad \text{(AASHTO, 2002 \ 3.23.2.3.1.5)}$$

$$DF = 7.38ft /5.5 = 1.34$$

Rating Factors Calculation using ASD Method
For Positive Moment Region

$$RF = \frac{M_{RI} - M_{DL}\frac{f_b^L}{f_b^{DL}} - M_{SDL}\frac{f_b^L}{f_b^{SDL}}}{M_{LL+I}} \quad \begin{array}{l}\text{(AASHTO, 2011 Page A-43}\\ \text{adopted from Eq. 6B.4.1-1)}\end{array}$$

VAB design truck   HS-25

| 177.9 kN
(40 kips) | 177.9 kN
(40 kips) | 44.5 kN
(10 kips) |
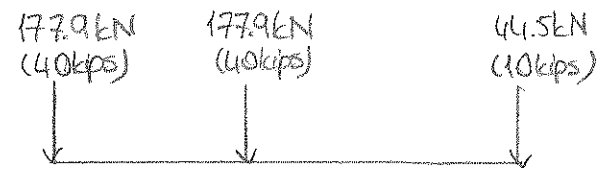
The distribution factors in AASHTO, 2002 applies to wheel loads which are half the axle loads. Therefore axle 1, 2, and 3 22.25 kN, 88.95 kN and 88.95 kN respectively.

The beam model were created using CSiBridge; three span continuous beam fixed – rolled – rolled.

<u>Loadings</u>

Descriptions	Type
DL → Girder + concrete deck + haunch	UDL
SDL → Wearing surface + curbs + sidewalk + railings	UDL
LL → HS-25 truck	Moving load

Invalley Level resisting capacity (AASHTO, 2011 Table 6B.5.2.1-1);

$F_y = 50ksi \qquad Me_I = f_I \cdot Sb^L$

$f_I = 0.55 F_y = 0.55 \times 50ksi = 27.5 ksi = 189.61 MPa$.

$Me_I = 0.18961 Pa \times 1.34 \times 10^7 mm^3 = 2541 kNm$.

$M_{LL+I} = (1+25) \times 1.34 \times 535.3 kNm = 896.64 kNm$

$$RF^+_{6R2inv} = \frac{2541 - 404.31 \left(\frac{1.34 \times 10^7}{8.874 \times 10^6} \right) - 165.70 \left(\frac{1.34 \times 10^7}{1.216 \times 10^7} \right)}{896.64}$$

$RF^+_{6R2inv} = 1.95$

All loads were equally distributed to all 6 girders and all interior girders sections are save therefore the rating factors for all interior girders are save;

$RF^+_{6R3inv} = 1.95$

$RF^+_{6R4inv} = 1.95$

$RF^+_{6R5inv} = 1.95$

Operating Level resisting capacity (AASHTO, 2011 Table 6B.5.2.1-2)

$F_y = 50ksi \qquad Me_o = f_o \cdot Sb^L$

$f_o = 0.75 \cdot F_y = 0.75 \times 50ksi = 37.5 ksi = 258.55 MPa$.

$Me_o = 0.25855 \times 1.34 \times 10^7 mm^3 = 3465 kNm$

$$RF^+_{6R2opr} = \frac{3465 - 404.31 \left(\frac{1.34 \times 10^7}{8.874 \times 10^6} \right) - 165.70 \left(\frac{1.34 \times 10^7}{1.216 \times 10^7} \right)}{896.64}$$

$RF^+_{6R2opr} = 2.98 = RF^+_{6R3opr} = RF^+_{6R4opr} = RF^+_{6R5opr}$

Evaluation of Exterior Girders:

I Beam W920×345 (from VAB drawing sheet 14 of 20 sheets)

Beam Designation	Top Flange	Web	Bottom Flange
Beam No 1 & 6	40×308	22×863	40×308

Properties of W920×845   AISC, 2005 Third Edition.

$A = 44000 \text{mm}^2$

$I_x = 6.26 \times 10^9 \text{mm}^4$
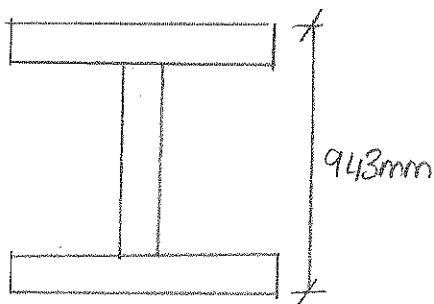
__ Non-Composite Section __

$\bar{y} = 943/2 = 471.5 \text{mm}$

$S_t = \dfrac{6.26 \times 10^9}{471.5} = 1.328 \times 10^7 \text{mm}^3 = S_t^{DL}$

$S_b = \dfrac{6.26 \times 10^9}{471.5} = \{1.328 \times 10^7 \text{mm}^3 = S_b^{DL}\}$

Short term composite section properties, n=7.7 (positive flexure) exterior girders;

2250mm

200mm
41mm
943mm

358.33
825.67mm
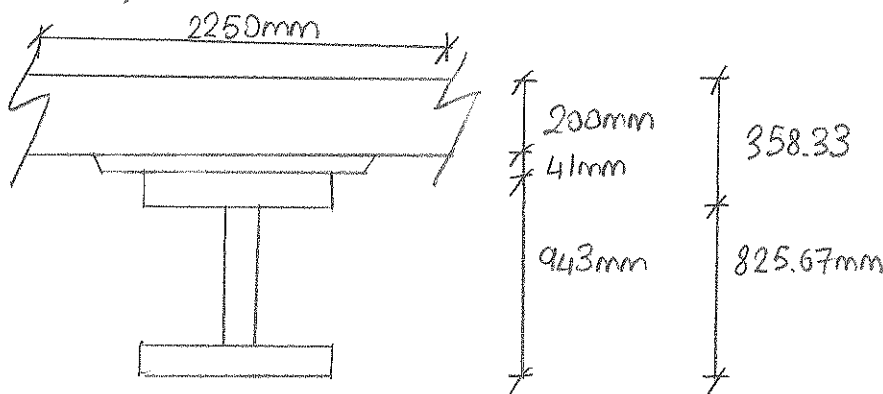
	$A(\text{mm}^2)$	$y(\text{mm})$	$A \cdot y$	$|y-\bar{y}|$	$A \cdot (y-\bar{y})^2$	I_o
Conc.	6.046×10^4	1084	6.55×10^7	258.33	4.034×10^9	1.951×10^8
Steel	$+\ 44000$	471.5	$+\ 2.075 \times 10^7$	354.17	$+\ 5.519 \times 10^9$	$+\ 6.26 \times 10^9$
	1.0446×10^5		8.625×10^7		9.55×10^9	6.455×10^9

$$\bar{y} = \frac{\sum(A \cdot y)}{\sum(A)} = \frac{8.625 \times 10^7}{1.0446 \times 10^5} = 825.67\,mm$$

$$I_x = 9.55 \times 10^9 + 6.455 \times 10^9 = 1.600 \times 10^{10}\,mm^4$$

$$S_t = \frac{1.600 \times 10^{10}}{358.33} = 4.466 \times 10^7\,mm^3$$

$$S_b = \frac{1.600 \times 10^{10}}{825.67} = \boxed{1.937 \times 10^7\,mm^3 = S_b^L}$$

Long term composite section properties, $3n = 23.1$ (positive flexure) about girders;
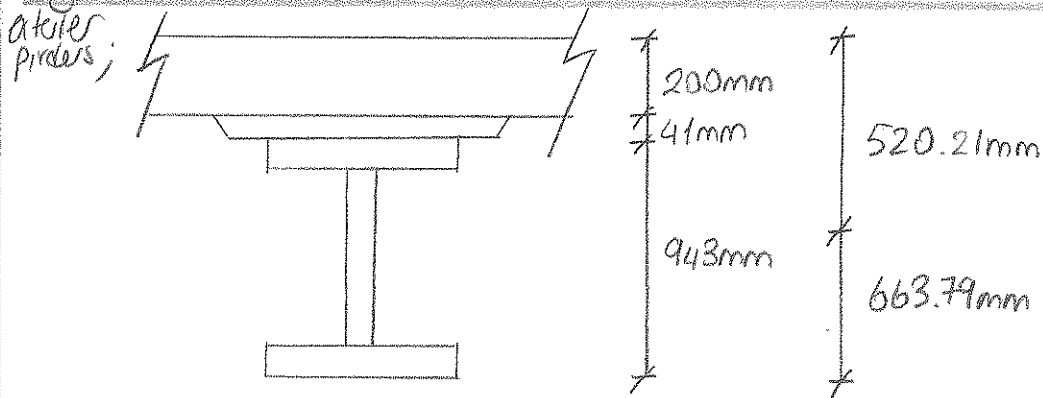
	A (mm²)	y (mm)	A·y	$|y-\bar{y}|$	$A|y-\bar{y}|^2$	I_o
conc	2.015×10^4	1084	2.184×10^7	420.21	3.558×10^9	6.503×10^7
Steel	$+\ 44000$	471.5	$+\ 2.074 \times 10^7$	192.29	$+\ 1.626 \times 10^9$	$+\ 6.26 \times 10^9$
	6.415×10^4		4.258×10^7		5.184×10^9	6.32×10^9

$$\bar{y} = \frac{\sum(A \cdot y)}{\sum(A)} = \frac{4.258 \times 10^7}{6.415 \times 10^4} = 663.79$$

$$I_x = 5.184 \times 10^9 + 6.32 \times 10^9 = 1.150 \times 10^{10}\,mm^4$$

$$S_t = \frac{1.150 \times 10^{10}}{520.21} = 2.21 \times 10^7\,mm^3$$

$$S_b = \frac{1.150 \times 10^{10}}{663.79} = \boxed{1.732 \times 10^7\,mm^3 = S_b^{SDL}}$$

Inventory Level resisting capacity (AASHTO 2011, Table 6B.5.2.1-1)

$F_Y = 50ksi$ $M_{eI} = f_I \cdot S_b^L$

$f_I = 0.55 F_Y = 0.55 \times 50ksi = 27.5 ksi = 189.61 MPa.$

$M_{eI} = 0.18961 \times 1.937 \times 10^7 mm^3 = 3673 kNm$

	Positive Max. Moments (kNm)	Negative Max. Moments (kNm)
DL (exterior)	436.40 (61 and 66)	555.71 (61 and 66)
SDL (exterior)	200.71 (61), 403.25 (66)	255.58 (61), 513.49 (66)
LL (exterior)	535.48 (61 and 66)	438.71 (61 and 66)

$M_{LL+I} = (1+0.25) \times 1.34 \times 535.48 = 896.93 kNm$

$$RF^+_{6R1inv} = \frac{3673 - 436.40 \left(\frac{1.937 \times 10^7}{1.328 \times 10^7}\right) - 200.71 \left(\frac{1.937 \times 10^7}{1.732 \times 10^7}\right)}{896.93 kNm}$$

$RF^+_{6R1inv} = 3.13$

$RF^+_{6R1inv} = 2.88$

Operating Level resisting capacity (AASHTO 2011, Table 6B.5.2.1-2)

$F_Y = 50ksi$ $M_{eO} = f_O \cdot S_b^L$

$M_{eO} = 0.25855 \times 1.937 \times 10^7 = 5008 kNm.$

$$RF^+_{6R1opr} = \frac{5008 - 436.40 \left(\frac{1.937 \times 10^7}{1.328 \times 10^7}\right) - 200.71 \left(\frac{1.937 \times 10^7}{1.732 \times 10^7}\right)}{896.64}$$

$RF^+_{6R1opr} = 4.62$

$RF^+_{6R6opr} = 4.37$

Positive Moment RFs by Hand Calculation with ASD.

Girder #	Inventory RFs.	Operating RFs
1	3.13	4.62
2	1.95	2.98
3	1.95	2.98
4	1.95	2.98
5	1.95	2.98
6	2.88	4.37

Composite section properties (negative flexure)

Interior girders;

#16 TYP at piers.

#13 TYP (Top & Bot.)

50mm

50mm

200mm

41mm

915mm

4 @ 120mm   3 @ 195mm   3 @ 195mm   4 @ 120mm

	ASTM	
	D	A
#13	12.7	129
#16	15.9	199
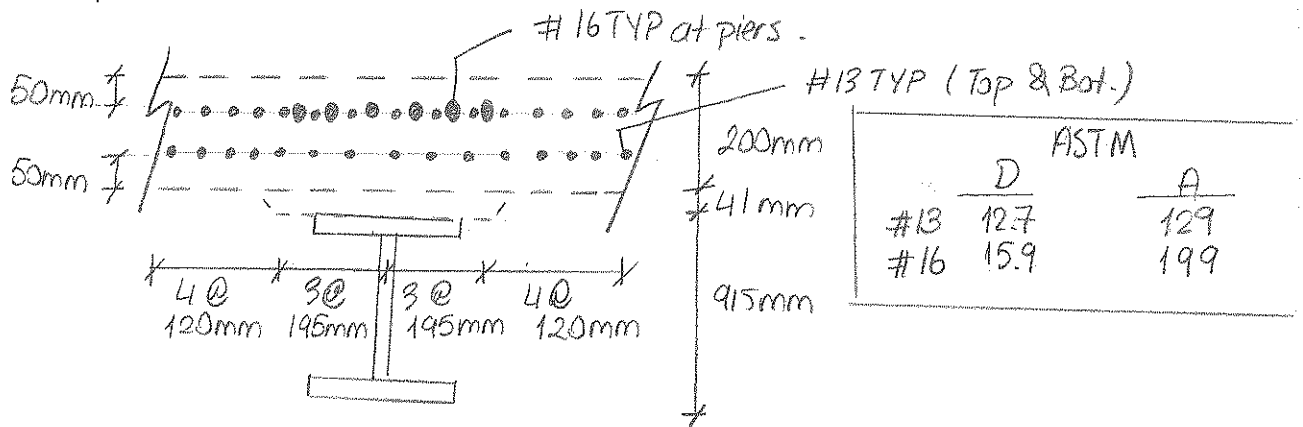
	$A(mm^2)$	$y(mm)$	$A \cdot y$	$|y-\bar{y}|$	$A \cdot (y-\bar{y})^2$	I_o
STEEL	=30400	=457.5	$=1.39\times10^7$	=86.78	$=2.29\times10^8$	$=4.06\times10^9$
TOP REINF. (15#13, 6#16)	$=(15\times129)+(6\times199)$ $=3129$	$=915+41+142$ $=1098$	$=3.44\times10^6$	=553.72	$=9.59\cdot10^8$	—
BOTTOM REINF. (15#13)	$=(15\times129)$ $=1935$	$=915+41+50+12.7/2$ $=1012.35$	$=1.96\times10^6$	=468.07	$=4.24\times10^8$	—
	3.546×10^4		1.930×10^7		1.61×10^9	4.06×10^9

$$\bar{y} = \frac{\Sigma(A\cdot y)}{\Sigma(A)} = \frac{1.930\times10^7}{3.546\times10^4} = 544.28mm$$

$$I_x = 1.61\times10^9 + 4.06\times10^9 = 5.672\times10^9 mm^4$$

$$St = \frac{5.672 \times 10^9}{611.72} = 9.272 \times 10^6 \, mm^3 \quad Sb = \frac{5.672 \times 10^9}{544.28} = 1.04 \times 10^7 \, mm^3 = S_b^L = S_b^{SDL}$$

Rating Factors Calculation using ASD Method
For Negative Moment Region

Inventory Level Resisting Capacity (AASHTO, 2011 Table 6B.5.2.1-1):

$$M_{RI} = f_I \cdot Sb^L$$

$$f_I = 0.55 \times Fy = 0.55 \times 50 ksi = 27.5 ksi = 189.61 MPa.$$

$$M_{RI} = 0.18961 \times 1.04 \times 10^7 = 1972 \, kNm.$$

$$M_{LL+I} = (1+25) \times 1 \times 1.34 \times 438.97 \, kNm = 735.27 \, kNm$$

$$RF_{6R2inv}^- = \frac{1972 - 515.35 \left(\frac{1.04 \times 10^7}{8.874 \times 10^6}\right) - 211.21 \left(\frac{1.04 \times 10^7}{1.04 \times 10^7}\right)}{735.27}$$

$$RF_{6R2inv}^- = 1.57 \quad \text{for all interior girders.}$$

Operating Level Resisting Capacity (AASHTO, 2011 Table 6B.5.2.1-2)

$$M_{RO} = f_O \cdot Sb^L$$

$$f_O = 0.75 \times Fy = 0.75 \times 50 ksi = 37.5 ksi = 258.55 MPa.$$

$$M_{RO} = 0.25855 \times 1.04 \times 10^7 = 2690 \, kNm$$

$$RF_{6R2opr}^- = \frac{2690 - 515.35 \left(\frac{1.04 \times 10^7}{8.874 \times 10^6}\right) - 211.21 \left(\frac{1.04 \times 10^7}{1.04 \times 10^7}\right)}{735.27}$$

$$RF_{6R2opr}^- = 2.55$$

composite section properties (negative flexure)

exterior girders;
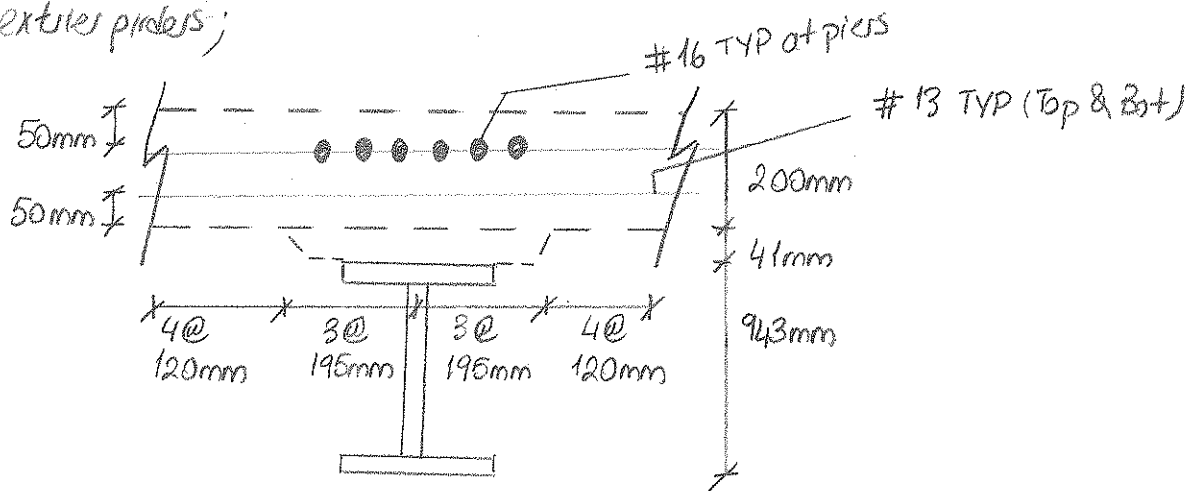
	A(mm²)	y(mm)	A.y	|y-ȳ|	A.(y-ȳ)²	I₀
STEEL	44000	471.5	2.075×10^7	64.58	1.84×10^8	6.26×10^9
TOP REINF.	3129	1126	3.52×10^6	589.92	1.09×10^9	—
(16#13, 6#16)	+ 1935	1040.35	+ 2.01×10^6	504.27	+ 4.92×10^8	+ —
	4.906×10^4		2.63×10^7		1.77×10^9	6.26×10^9

$$\bar{y} = \frac{\Sigma(A \cdot y)}{\Sigma(A)} = \frac{2.63 \times 10^7}{4.906 \times 10^4} = 536.08 \text{ mm}$$

$$I_x = 1.77 \times 10^9 + 6.26 \times 10^9 = 8.03 \times 10^9$$

$$S_t = \frac{8.03 \times 10^9}{647.92} = 1.24 \times 10^7 \text{ mm}^3$$

$$S_b = \frac{8.03 \times 10^9}{536.08} = 1.50 \times 10^7 \text{ mm}^3 = S_b^L = S_b^{SDL}$$

Inverky Louel Resisting Capacity (AASHTO ,2011 Table 6B.5.2.1-1);

$M_{RI} = f_I \cdot S_b^L$

$f_I = 0.55 \times F_y = 0.55 \times 50 ksi = 27.5 ksi = 189.61 MPa$

$M_{RI} = 0.18961 \times 1.50 \times 10^7 = 2844\ kNm$

$M_{LL+I} = (1+25) \times 1.34 \times 438.71 = 734.84\ kNm$

$$RF^-_{GR1inv} = \frac{2844 - 555.71 \cdot \left(\frac{1.50 \times 10^7}{1.328 \times 10^7}\right) - 255.58 \left(\frac{1.50 \times 10^7}{1.50 \times 10^7}\right)}{734.84\ kNm}$$

$RF^-_{GR1inv} = 2.67$

$RF^-_{GR6inv} = 2.32$

Opearing Level Resisting Capacity (AASHTO ,2011 Table 6B.5.2.1-2)

$M_{RO} = f_O \cdot S_b^L$

$f_I = 0.75 \times F_y = 0.75 \times 50 ksi = 375 ksi = 258.55 MPa$

$M_{RO} = 0.25855 \times 1.50 \times 10^7 = 3878 kNm$

$$RF^-_{GR1opr} = \frac{3878 - 555.71 \left(\frac{1.50 \times 10^7}{1.328 \times 10^7}\right) - 255.58 \left(\frac{1.50 \times 10^7}{1.50 \times 10^7}\right)}{734.84}$$

$RF^-_{GR1opr} = 4.07$ $RF^-_{GR6opr} = 3.72$

Negative Mouent RFs by Hand Calculation with ASD.

Girder #	Inverky RFs	Operating RFs
1	2.67	4.07
2	1.57	2.55
3	1.57	2.55
4	1.57	2.55
5	1.57	2.55
6	2.32	3.72

Evaluation of Rating Factors by Hand Calculation with LFD Methods;

Interior Girders;

Positive Moment Section; $C = 0.85 \cdot f_c' \cdot b \cdot t_s$ (AASHTO, 2002 10-123)

$C = 0.85 \times 30 \, MPa \times 2250 \, mm \times 200 \, mm = 11475 \times 10^7 \, N = 11475 \, kN$

b = effective width of slab
t_s = slab thickness

$C = (AF_y)_{bf} + (AF_y)_{tf} + (AF_y)_W$ (AASHTO, 2002 10-124)

$(AF_y)_{bf} = 344.74 \, MPa \times 26 \, mm \times 305 \, mm = 2733.79 \, kN$

$(AF_y)_{bf} = (AF)_{tf} = 2733.79 \, kN$ $\Big\}$ $C = 10,525 \, kN$

$(AF_y)_W = 344.74 \, MPa \times 17 \, mm \times 863 \, mm = 5057.68 \, kN$

When the compressive force in the slab is less than the value given by Equation 10-124, the top portion of the steel section will be subjected to the compressive force 'C';

$11475 \, kN > 10.525 \, kN$ PNA is in the slab

$\bar{y} = \dfrac{C - (AF_y)_c}{0.85 \cdot f_c' \cdot b}$ (AASHTO, 2002 10-125)

$(AF_y)_c$ is the product of the area and yield point of that part of reinforcement which lies in the compression zone of the slab. But for calculation the force in longitudinal reinforcement may be conservatively neglected $(AF_y)_c = 0$

$\bar{y} = \dfrac{10,525 \, kN}{0.85 \times 30 \times 2250} = 183.44$ from the top of the concrete deck slab.

The distance from the top of the slab to neutral axis at the plastic moment Dp, shall satisfy;

$\left(\dfrac{Dp}{D'}\right) \le 5$ (AASHTO, 2002 10-129a)

98

$$D' = \beta \frac{(d + t_s + t_h)}{7.5}$$ (AASHTO, 2002   10-129a)

$\beta = 0.7$ for $F_y = 50,000$ and $70,000 psi$

$$D' = 0.7 \frac{915mm + 200mm + 41mm}{7.5} = 107.89$$

D_p = distance from the top of the slab to the plastic neutral axis.

$D_p = 183.44m$

$$\frac{D_p}{D'} = \frac{183.44}{107.89} = 1.70 \le 5 \checkmark$$

for $D' < D_p \le 5D'$

$107.89 < 183.44 \le 539.45 mm \checkmark$

$$M_u = \frac{5M_p - 0.85M_y}{4} + \frac{0.85M_y - M_p}{4}\left(\frac{D_p}{D'}\right)$$ (AASHTO, 2002 10-129c)

M_y = Moment capacity at first yield of composite positive moment section, calculated as F_y times the section modulus with respect to the tension flange. The modular ratio, n shall be used to compute the transformed section properties.

$$M_y = F_y \cdot S_b^L = 344.74 MPa \times 1.344 \times 10^7 mm^3 = 4.63 \times 10^9 \ N mm$$
$$= 4.63 \times 10^6 \ kNmm$$

Calculation of M_p;

Moment arms about PNA

Compression Flange: $d_c = (t_s - \bar{y}) + h + \frac{t_f}{2} \Rightarrow (200mm - 183.44mm) + \frac{26}{2} + 41 = 70.56mm$

$d_w = (t_s - \bar{y}) + h + t_f + \frac{D}{2} \Rightarrow (200 - 183.44) + 41 + 26mm + \frac{863mm}{2} = 515.06mm$

Tension Flange: $d_t = (t_s - \bar{y}) + h + t_f + D + \frac{t_{bf}}{2}$

$d_t = (200 - 183.44) + 41 + 26mm + 863 + \frac{26mm}{2} = 959.56mm$

$$M_P = \left(\frac{\bar{y}^2 \cdot P_s}{245} \right) + (AF_y)_{tf} \times dc + (AF_y)_W \times dW + (AF_y)_{bf} \times dt$$

$$P_s = 0.85 \times 80 MPa \times 2250 \times 183.44mm = 10.524 \times 10^6 N = 10520 kN$$

$$M_P = \left(\frac{183.44^2 \cdot 10520}{2.200} \right) + (2733.79 \times 70.56 + 5057.68 \times 515.06 + 2733.79 \times 959.56)$$

$$M_P = 8.85 \times 10^5 + 1.928 \times 10^5 + 2.605 \times 10^6 + 2.623 \times 10^6$$

$$M_P = 6.305 \times 10^6 \, kNmm$$

$$M_u = \frac{5 \cdot (6.305 \times 10^6) - 0.85(4.63 \times 10^6)}{4} + \frac{0.85(4.63 \times 10^6) - 6.305 \times 10^6}{4} \cdot 1.70$$

$$M_u = 6.897 \times 10^6 + (-1.007 \times 10^6) = 5.89 \times 10^6 \, kNmm = 5890 \, kNm.$$

Load Factor Rating Formulation (AASHTO, Manual 2011 page A-46 adapted from Eq. 6B.4.1-1)

$$RF = \frac{M_R - A_1 \cdot M_D}{A_2 \cdot M_{L+I}}$$

Moment Results From CSI Bridge.

	Positive Max Moment	Negative Max Moment
DL (int)	404.81 kNm	515.35 kNm
SDL (int)	165.70 kNm	211.21 kNm
LL (int)	535.81 kNm	438.97 kNm
DL (ext)	436.40 kNm (all ext.)	555.71 kNm (all ext.)
SDL (ext)	200.71 (for 61), 403.25 (for 66)	255.58 (for 61), 513.49 (for 66)
LL (ext)	535.48 kNm (all ext.)	438.71 kNm (all ext.)

Inventory level ; $A_1 = 1.3$ and $A_2 = 2.17$ (AASHTO Manual, 2011 6B.4.3)

$M_{LL+I} = (1+25) \times 1.34 \times 535.31 = 896.64$ kNm

$$RFGR_{2inv} = \frac{5890 - 1.3(404.31 + 165.70)}{2.17 \times 896.64} = 2.65$$

All interior probes RFs are same since the dead loads were equally distributed.

$RFGR_{2inv} = RFGR_{3inv} = RFGR_{4inv} = RFGR_{5inv} = 2.65$

Operating level ; $A_1 = 1.3$ and $A_2 = 1.3$

$2.17 / 1.3 = 1.67$

$RFGR_{2opr} = 2.65 \times 1.67 = 4.43 = RFGR_{3opr} = RFGR_{4opr} = RFGR_{5opr}$.

<u>Exterior Girders</u>.

(a)　$C = 0.85 . fc' . b . ts$　(AASHTO, 2002　10-123)

$C = 0.85 \times 30\,MPa \times 2250mm \times 200mm = 11.475 \times 10^6 N = 11475$ kN

$C = (AF_y)bf + (AF_y)tf + (AF_y)w$　(AASHTO, 2002　10-124)

$(AF_y)bf = 344.74\,MPa \times 40mm \times 308mm = 4.247 \times 10^6 N$

$(AF_y)w = 344.74\,MPa \times 22mm \times 863 = 6.545 \times 10^6 N$ } $C = 15.039 \times 10^6 N$

$(AF_y)bf = (AF_y)tf = 4.247 \times 10^6 N$

$C_{conc} = 11475$ kN $< C_{steel} = 15039$ kN　PNA is in the steel beam.

Thus　use ;　$C' = \dfrac{\Sigma(AF_y) - C}{2}$　(AASHTO, 2002　10-126)

$$C' = \frac{15039 - 11475}{2} = 1782 \text{ kN}$$

$(AF_y)tf = 344.74\,MPa \times 40mm \times 308mm = 4247 > 1782$ kN　N.A in top flange.

for　$C' < (AF_y)tf$　$\Rightarrow$　$\bar{y} = \dfrac{C'}{(AF_y)tf} . tf$　(AASHTO, 2002　10-127)

$$\bar{y} = \frac{C'}{(AF_y)t_f} \cdot t_f = \frac{1782\,KN}{4247\,KN} \times 40mm = 16.78\,mm$$

$$\left(\frac{Dp}{D'}\right) \leq 5 \qquad (AASHTO, 2002 \quad 10-129a)$$

$$D' = \beta\,\frac{(d+t_s+t+h)}{7.5} \qquad \beta=0.7 \quad for \; F_y = 50,0000 \; and \; 70,000\,psi$$

$$D' = 0.7\,\frac{(943+200+40)}{7.5} = 110.41$$

$$D_p = t_s + \bar{y} = 200mm + 16.78mm = 216.78mm$$

$$\frac{D_p}{D'} = \frac{216.78}{110.41} = 1.96 \leq 5 \checkmark$$

for $\quad D' < D_p \leq 5D'$

$$110.41 < 216.78 \leq 552.05 \checkmark$$

$$Mu = \frac{5Mp-0.85My}{4} + \frac{0.85My-Mp}{4}\left(\frac{Dp}{D'}\right) \qquad (AASHTO, 2002 \; 10-129c)$$

$$My = F_y \cdot S_b^L = 344.74\,MPa \times 1.937\times10^7 mm^3 = 6.677\times10^9\,N\,mm$$
$$= 6.677\times 10^6 \; KN\,mm$$

Calculation of Mp;

$$d_s = \frac{t_s}{2} + \bar{y} + h = \frac{200}{2} + 40mm + 16.78 = 156.78mm$$

$$d_w = \frac{D}{2} + (t-\bar{y}) = \frac{863}{2} + (40-16.78) = 454.72mm$$

$$d_t = (t-\bar{y}) + D + \frac{t}{2} = 906.22mm$$

$$Mp = \frac{Pc}{2tc}\left[(\bar{Y})^2 + (tc-Y)^2\right] + Ps.ds + Pwdw + Pfdf$$

$$Mp = \frac{344.74 \times 40 \times 308}{2 \times 40}\left[16.78^2 + (40-16.78)^2\right] + \quad 11475 \times 156.78 +$$

$$6545 KN \times 454.72 + 4247 KN \times 906.22$$

$$Mp = (53.08\,KNmm)\cdot(2576 \times 10^2) + 1.81 \times 10^6 + 2.97 \times 10^6 + 3.84 \times 10^6$$

$$Mp = \quad 8.609 \times 10^6\,KNmm$$

$$Mu = \frac{5\cdot(8.609 \times 10^6) - (0.85 \times 6.677 \times 10^6)}{4} + \frac{0.85(6.677 \times 10^6) - 8.609 \times 10^6}{4} \times 1.96$$

$$Mu = \quad 9.342 \times 10^6 - 1.437 \times 10^6 = 7.90 \times 10^6 = 7900\,KNm$$

Inventry Level; $A_1 = 1.3$ and $A_2 = 2.17$ (AASHTO Manual 2011, 6B-4.3)

$$RF6R_{1inv} = \frac{7900 - 1.3(200.71 + 436.40)}{2.17 \times 896.93} = 3.63$$

$RF6R_{1inv} = 3.63$ $\qquad$ $RF6R_{6inv} = 3.30$

Operating Level ; $A_1 = 1.3$ and $A_2 = 1.3$

$2.17/1.3 = 1.67$

$RF6_{1opr} = 3.63 \times 1.67 = 6.06$ $\qquad$ $RF66_{opr} = 5.51$

Rating Factors By Hand Calculation with LFD M^+

Girder #	Inventry RF	Operating RF
1	3.63	6.06
2	2.65	4.43
3	2.65	4.43
4	2.65	4.43
5	2.65	4.43
6	3.30	5.51

Negative Moment section for Interior Girders;

For reinforcing bars;

$A_{rb} \cdot f_y = [(30 \times 129) + (6 \times 199)] \times 420 MPa = 2.127 \times 10^6 N = 2127 kN$

For steel section;

$C = (Af_y)bf + (Af_y)tf + (Af_y)w$

$(Af_y)bf = 2733.79 kN = (Af_y)tf$ $\Big\}$ $10525 kN$

$(Af_y)w = 5057.68 kN$

$10525 > 2127 kN$ PNA is within the steel.

$C' = \dfrac{10525 - 2127}{2} = 4199 kN$

$(Af_y)tf = 2733.79 < C' = 4199 kN$

Therefore;

$\bar{y} = tf + \dfrac{C' - (Af_y)tf}{(Af_y)w} \cdot D = 26 + \dfrac{4199 - 2733.79}{5057.68} \cdot 863 = 276.01 mm$

$D' = \beta \dfrac{(d + ts + th)}{7.5} = \dfrac{915 + 200 + 41}{7.5} \times 0.7 = 107.89$

$Dp = 200 + 276.01 = 476.01 mm$ $Dp/D' = \dfrac{476.01}{107.89} = 4.41 \leq 5 \checkmark$

for $D' < Dp \leq 5D'$ $\Rightarrow$ $107.89 < 476.01 < 539.45 mm$

Calculation of Mp;

$$M_{steel} = [(915+41) - (276.01)]/2 \times 10525 = 3.578 \times 10^6 \text{ kNm}$$

$$m_{reinforce} = (915 - 678.99 + 200 - 50) \times 2127 = 8.21 \times 10^5 \text{ kNm}$$

$$\overline{4.399 \times 10^6 \text{ kNm}}$$

Inventory level; $A_1 = 1.3$ $A_2 = 2.17$

$$M_{L+I} = 438.97 \times (1.25) \times (1.34) = 735.27$$

$$RF_{6e2inv} = \frac{4399 - 1.3(515.35 + 211.21)}{(735.27) \cdot 2.17} = 2.17$$

RF_{6e2inv} = all interior girders inventory rating factors = 2.17

Operating level; $A_1 = 1.3$ $A_2 = 1.3$

$$2.17/1.3 = 1.67 \qquad RF_{6all int opr} = 2.17 \times 1.67 = 3.62.$$

Exterior Girders;

Fes reinforcing bars; $A_b \cdot F_y = 2126.8 \text{ kN}$

Fes steel section; $C = 15039 \text{ kNm}$.

$$C' = \frac{15039 - 2126.8}{2} = 6456.1 \text{ kN}$$

$$(AF_y)_{tf} = 4247 \leq C'$$

Therefore;

$$\bar{y} = 40 + \frac{6456.1 - 4247}{6545} \cdot 863 = 831.28 \text{ mm}$$

$$D_p = 200 + 831.28 = 531.28 \text{ mm}.$$

$$D' = \frac{943+200+40}{7.5} \times 0.7 = 110.41$$

$$D_P/D' = \frac{531.28}{110.41} = 4.81 \leq 5$$

Calculation of Mu

$$m_{steel} = [(943+41)-(331.28)]/2 \times 15039 = 4.908 \times 10^6$$

$$m_{renfor} = (943-651.72+200-50) \times 2127 = 9.386 \times 10^5$$

$$\underline{5.846 \times 10^6}$$

Inventory level; $A_1 = 1.3$ $A_2 = 2.17$

$$RF_{6R1inv} = \frac{5846 - 1.3(555.71+255.58)}{2.17 \times 734.84} = 3.00$$

$$RF_{6R6inv} = 2.76$$

Operating level; $A_1 = 1.3$ $A_2 = 1.3$

$$2.17/1.3 = 1.67$$

$$RF_{6R1opr} = 5.28 \qquad RF_{6R6opr} = 4.61$$

Rating Factors By Hand Calculation with LFD M

Girder #	Inventory RF	Operating RF
1	3.00	5.01
2	2.17	3.62
3	2.17	3.62
4	2.17	3.62
5	2.17	3.62
6	2.76	4.61

*

10.88.1.3 The ratio of the moduli of elasticity of steel (29,000,000psi) to those of normal weight concrete (W = 145pcf) of various design strengths shall be as follows:

f_c' = unit ultimate compressive strength of concrete as determined by clinder tests at the age of 28 days in pounds per square inch.

n = ratio of modulus of elasticity of steel to that of concrete. The value of n, as a function of the ultimate cylinder strength of concrete, shall be assumed as follows:

f_c' =   2,000 - 2,300   n = 11
           2,400 - 2,800   = 10
           2,400 - 3,500   = 9
           3,600 - 4,500   = 8
           4,600 - 5,900   = 7
           6,000 - more   = 6

In VA8 80Mpa concrete used and f_c' = 4.351 ksi.
So I used n = 7.6

Hand Calculation:

ES = 199948 MPa $n = \dfrac{ES}{Ec} = \dfrac{199948}{25742} = 7.76$ (used in Virtis)

Ec = 25742 MPa.

$EC = 4700 \sqrt{f_c'}$ ⟹ f_c' = 4.351 ksi = 29.999 MPa (N/mm²)
(SI units)
          ⟹ $EC = 4700\sqrt{29.999} = 25742$ MPa //

*
Ref, AASHTO Standart Specifications for Highway Bridges 17th, 2002.

Evaluation of Rating
Factors by Virtis 6.3

1

* 10.38.3   Effective Flange Width, (Page 304)

* 10.38.3.1   In composite girder construction the assumed effective width of the slab as a T-beam flange shall not exceed the following:

(1) One-fourth of the span length of the girder

(2) The distance center to center of girders.

(3) Twelve times the least thickness of the slab.

* 10.38.3.2   For girders having a flange on one side only, the effective flange width shall not exceed 1/12 of the span length of the girder, or six times the thickness of the slab, or one-half the distance center to center of the next girder.

INTERIOR GIRDERS:

(1) 1/4 × (11.75) = 2.9375m

    1/4 × (23.5) = 5.875m   EFW = 2.25m

(2) ☐ 2.25m. ☐

(3) 12 × 0.2m = 2.4m

EXTERIOR GIRDERS:

(1) 1/12 × (11.75) = ☐ 0.979m ☐   EFW = 0.979 + 0.732 = 1.711m

    1/12 × (23.5) = 1.958m

(2) 6 × 0.2 = 1.2m

(3) 2.25/2 = 1.125m

Overhang = 732.5m = 0.732m

* Ref, AASHTO Standart Specification for Highway Bridges 17th, 2002

Live Load Distribution Factors

S = Average stringer spacing, $S = 2.26m = 7.382 ft$.

* 3.23.2.3.1.5 where S is more than 6ft and less than 14ft.

$$\frac{S}{4.0 + 0.26S} \quad (ft. \, U.S) \quad = \quad \frac{S}{1220 + 0.25S} \quad (in \, S.I) \, (mm) \qquad *$$

* Formula from standart Specifications for Highway Bridges 17th, 2002 page 13

$$\frac{S}{1220 + 0.25S} = \boxed{1.26227} \quad (for \, exterior)$$

For interior, Table 3.23.1, page 83

$S/7$ (if S exceeds 6' use footnote f) (Designed for one traffic lane)

$7.382/7 = \boxed{1.0545}$ (1 lane) (interior)

$S/5$ (if S exceeds 10' use footnote f) (Designed for two or more traffic lane)

$7.382/5.5 = \boxed{1.34218}$ (2 lane) (interior)

* 3.24.2, Page 35 or Figure 3.7.7A standart HS trucks in the figure, the center line of wheel seen 2' but it required that, the center line of wheels shall be assumed to be 1' from face of curb.

$1 ft = 304.8 mm$.

* Ref, AASHTO Standart Specifications for Highway Bridges, 17th, 2002.

CURB
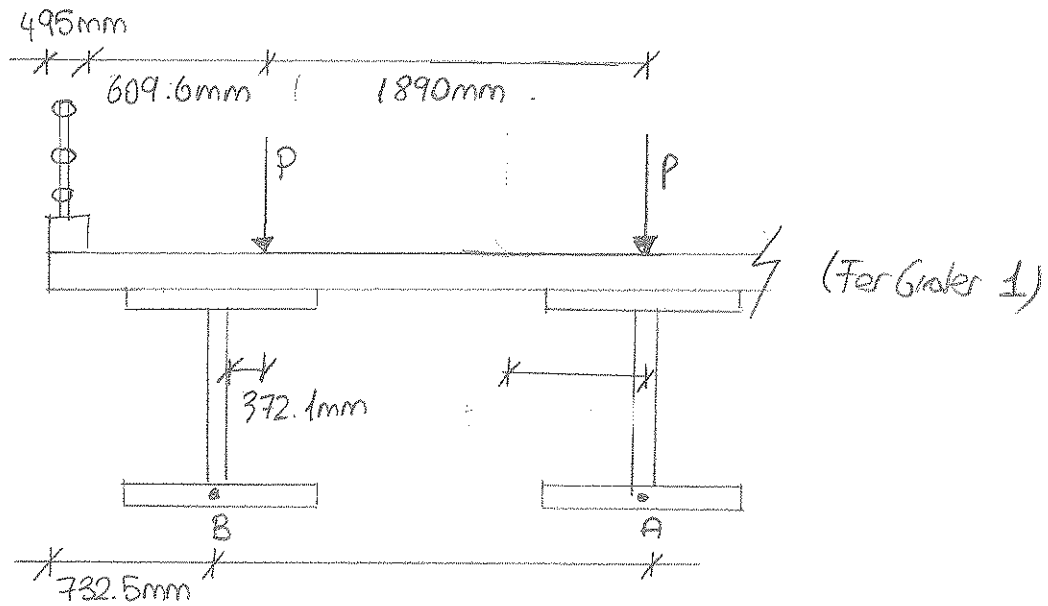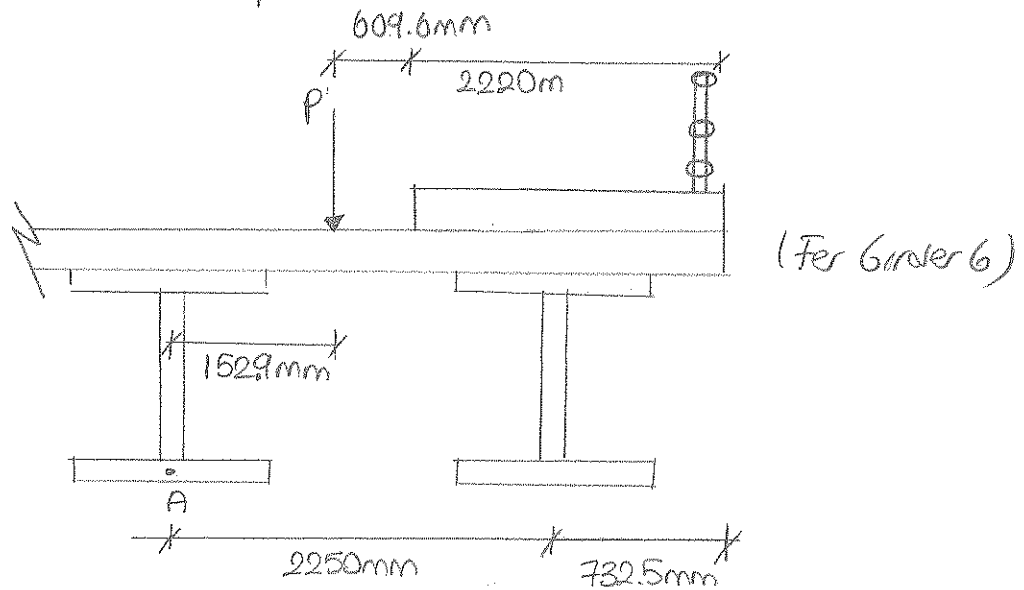
495mm

609.6mm   1890mm

P   P

(For Girder 1)

372.1mm

B   A

732.5mm

$$\circlearrowleft^+ \Sigma M_A = -P \times 1890mm + DF \times 2250.$$

$$DF = 0.84$$

SIDEWALK

609.6mm

P'   2220m

1529mm

A

2250mm   732.5mm

(For Girder 6)

$$\circlearrowleft^+ \Sigma M_A = P(1529) - F(2250) = 0$$

$$DF = 0.068$$

Dead Load Calculation - Haunch

Interior Girders;

(From South Abutment to Field Splice)

305mm

$\updownarrow$ 41mm

W920×238

25mm 25mm *

* (Sheet 18 of 20
Stay-in-place form details / Haunch Detail)
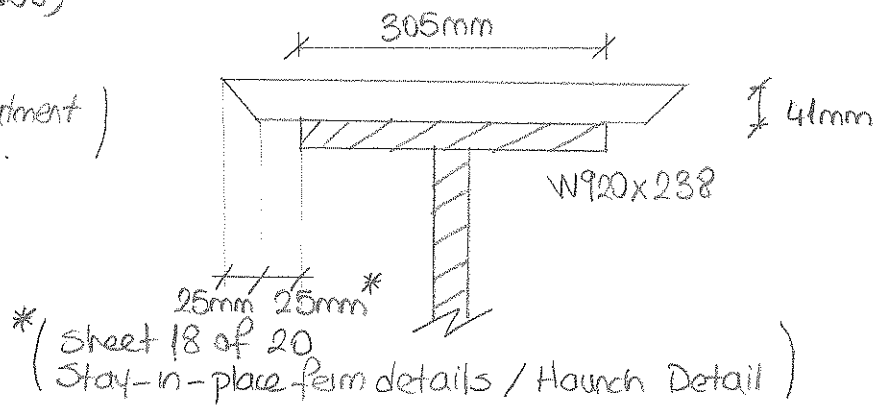
$$A_{Haunch} = \left[305 + (2 \times 25)\right] \times 41 + (25 \times 41) = 15580\, mm^2 = 0.01558\, m^2$$

$$W_{Haunch} = 0.01558\, m^2 \times 23.576\, KN/m^3$$

$$= 0.3673\, KN/m \quad (25.168\, plf)$$

(From Field Splice to North Abutment)

305mm

$\updownarrow$ 40mm

W920×238

25mm 25mm
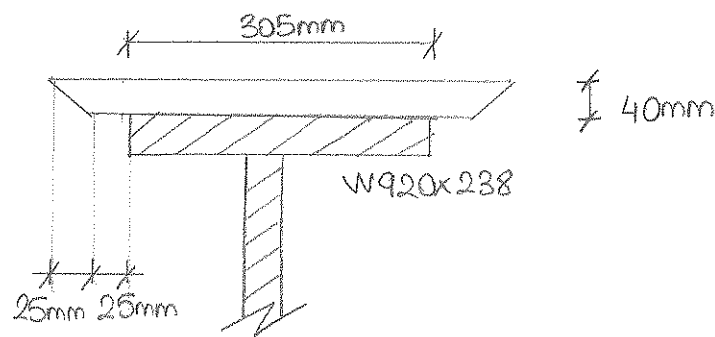
$$A_{Haunch} = \left[305 + (2 \times 25)\right] \times 40 + (25 \times 40) = 15200\, mm^2 = 0.01520\, m^2$$

$$W_{Haunch} = 0.01520\, m^2 \times 23.576\, KN/m^3$$

$$= 0.3584\, KN/m \quad (24.558\, plf)$$
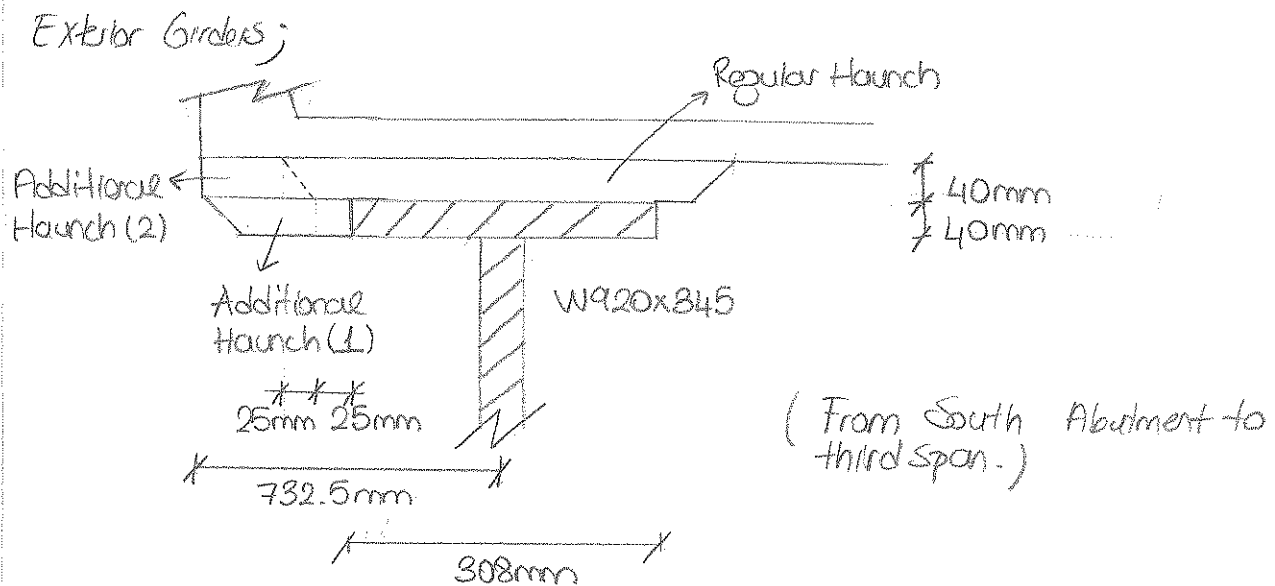
Exterior Girders;

Additional haunch (1)

$$A_{haunch} = (732.5 - 308/2) \times 40 = 23140 mm^2 = \underline{0.02314 m^2}$$

Additional haunch (2)

$$A_{haunch} = (732.5 - 308/2 - 50) \times 40 = 21140 mm^2 = \underline{0.02114 m^2}$$

Regular Haunch   Area from interior girder calculations;

$$A_{haunch} = (15580 + 15200)/2 = 15390 mm^2 = \underline{0.01539 m^2}$$

Total $A_{haunch} = 0.02314 + 0.02114 + 0.01539 = 0.05967 m^2$

$$W_{haunch} = 0.05967 m^2 \times 23.576 kN/m = 1.4067 kN/m \ (96.395 pcf)$$

Fascia Girders;
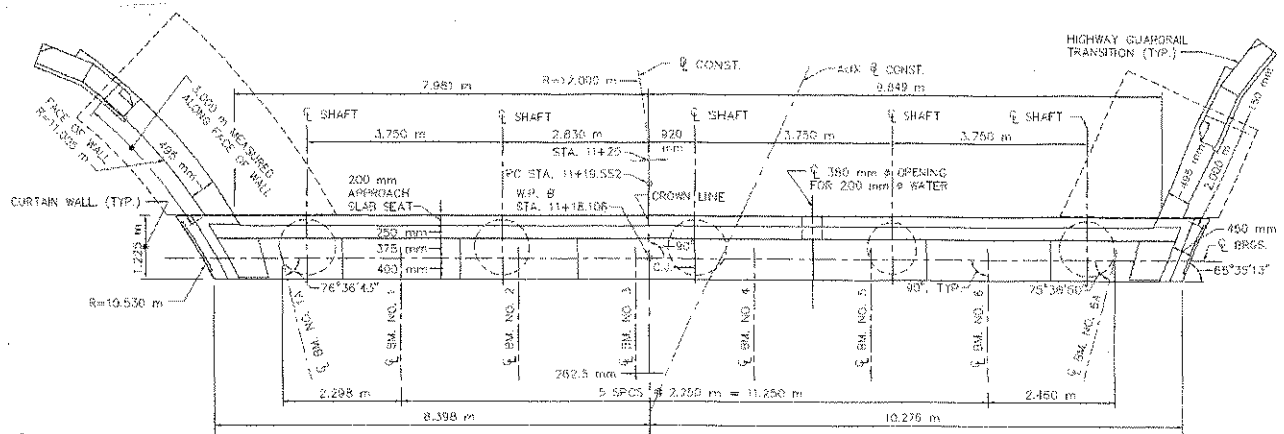
West overhang;

$$8.398 - (2.25 \times 2) - 2.298 - 0.2625 = 1.3375m$$

Additional Haunch (1)

$$A_{haunch} = \left[1337.5 - (305/2)\right] \times 20.1 = 23818mm^2 = \underline{0.023818m^2}$$

Additional Haunch (2)

$$A_{haunch} = \left[1337.5 - (305/2) - 50\right] \times 20.1 = 22813.5mm^2 = \underline{0.022813m^2}$$

Regular Haunch

$$A_{haunch} = \left[305 + (2 \times 25)\right] \times 39 + (25 \times 39) = 14820mm^2 = \underline{0.01482m^2}$$

Total Haunch $= 0.023818 + 0.022813 + 0.01482 = 0.06145m^2$

$W_{haunch} = 0.06145m^2 \times 23.576 \, kN/m = 1.4487 \, kN/m \; (99.270plf)$

East overhang;

$10.276 - (2 \times 2.25) - 2.460 - (2.250 - 0.2625) = 1.3285m$

Additional Haunch (1)

$A_{haunch} = \left[1328.5 - (305/2)\right] \times 20.1 = 23637.6mm^2 = 0.023637m^2$

Additional Haunch (2)

$A_{haunch} = \left[1328.5 - (305/2) - 50\right] \times 20.1 = 22632.6mm^2 = 0.02263m^2$

Regular Haunch from west calculation;

$A_{haunch} = 0.01482m^2$

Total $A_{haunch} = 0.023637 + 0.02263 + 0.01482 = 0.061087m^2$

$W_{haunch} = 0.061087m^2 \times 23.576 kN/m = 1.44018 kN/m \quad (98.684 plf)$

Diaphragms;

D1 → MC460 × 63.5

$W_{diaphragm} = 63.5 \, kg/m \times 9.81 \, N/kg \times 2.25m = 1401.60 \, N$

Additional weight for BOHS (%30 of $W_{diaphragm}$) = 420.48 N

Total $W_{diaphragm} = 1401.60 + 420.48 = 1822.08 \, N$

9 Diaphragms between two girders = 9 × 1822.08 = 16398.72 N

As a uniform load

⟹ 16398.72 N / 47m = 348.908 N/m

For interior girder = 348.908 N/m = 0.3489 KN/m

For exterior girder = 348.908 × 1/2 = 174.454 N/m = 0.17445 KN/m

9 Diaphragms between two girders = 16398.72 N

Since two girders share this load 16398.72/2 = 8199.36 N

As a Uniform load → 8199.36N / 47m = 174.45

For interior 174.45 N/m = 0.1744 KN/m

For exterior 174.45/2 = 87.22 = 0.08722 KN/m

S.I.P Form (Stay-in-place Forms);   1pa = 0.001 KN/m²

Mass Highway Bridge Manual drawing 7.2.3

Girder spacing 2.25m from drawing → 214 Pa = 0.214 KN/m²

2.25m × 0.214 KN/m² = 0.4815 KN/m (interior)

0.4815/2 = 0.2475 (exterior)

Superimposed Dead Load Calculation

Railing

MHD Bridge Manual Drawing No 9.1.1

Unit weight of type 53-TL4 bridge rail

@ sidewalk = 1.31 kN/m

@ safety curb = 1.26 kN/m

Wearing Surface

HMA Wearing Surface = 80mm (sheet 18 of 20 / Detail E)

W_{HMA} = 0.08m × 25.16 kN/m³ × 10m (roadway width)

W_{HMA} = 20.12 kN/m / 6 girder = 3.35 kN/m

Sidewalk

Sidewalk depth = 200 + 80 = 280mm (sheet 18 of 20 / Detail E)

length = 1.8 + 0.42 = 2.22m

$S \rightarrow$ 0.01 $S \leftarrow$ 0.02

x = 0.022
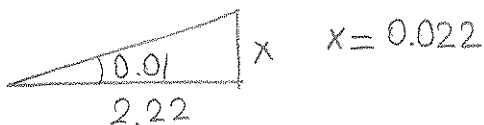
Depth = 0.022 + 0.28 = 0.3022 m

$W_{sidewalk}$ = $\left(\dfrac{0.3022 + 0.28}{2} \right)$ × 2.22m × 23.576 kN/m³ = 15.235 kN/m

$W_{safetycurb}$ = 0.495m × 0.28m × 23.576 kN/m³ = 3.267 kN/m

Evaluation of Rating
Factors by Virtis 6.3

Deck Reinforcement

Exterior Girders;

1711mm (Effective width of slab)

#16 (TYP.)

#13 (TYP)
(TOP & BOT.)

3 space @ 120mm   3 space @ 195mm   3 space @ 195mm

$d\#16 = 15.8mm$

978.5mm   732.5mm
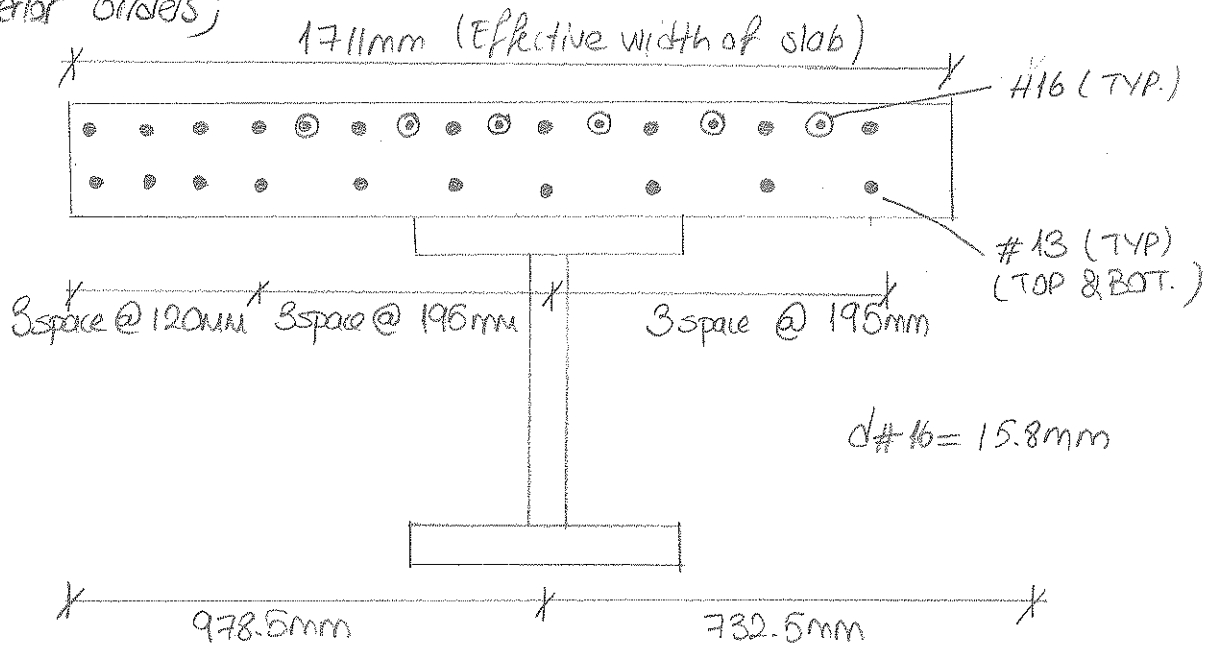
Average Spacing : $(3 \times 120) + (6 \times 195)/9 = 170mm$. (For #13)

Distance from top rebar : $25mm + 15.8 + 15.8/2 = 48.7mm$

Distance from bottom rebar : $50mm + 15.8 + 15.8/2 = 73.7mm$

M. I.

Interior Girders;
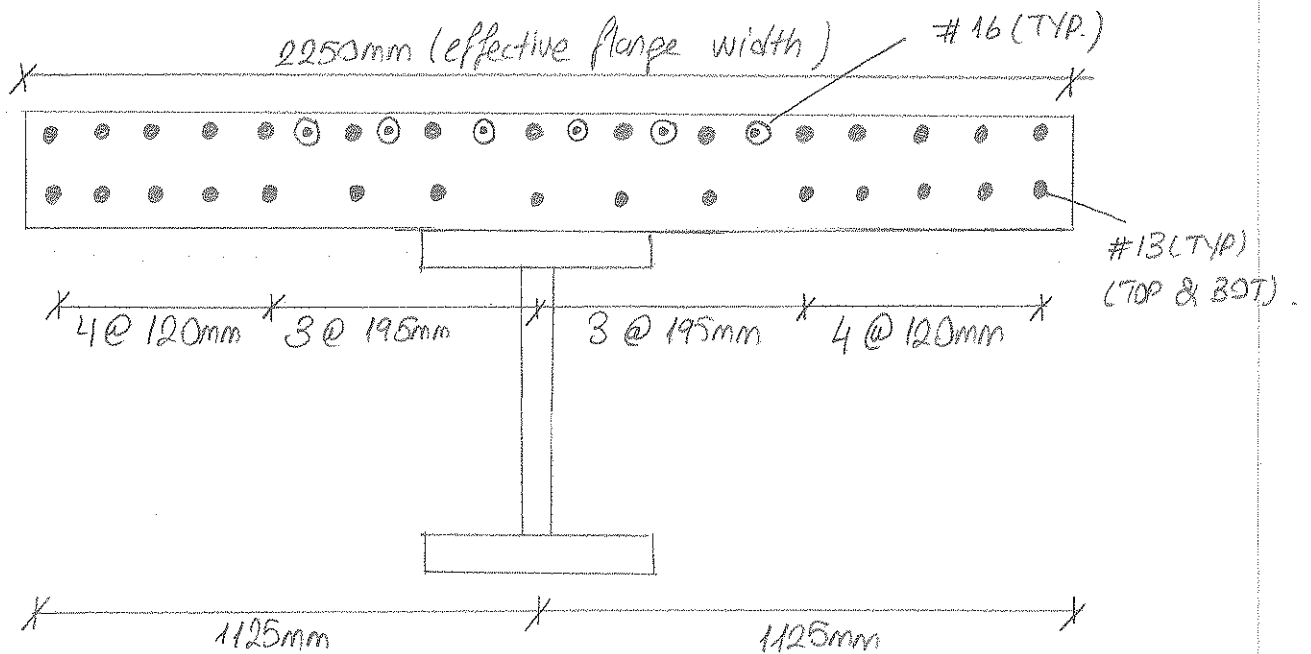
Average Spacing $= (8 \times 120) + (6 \times 195)/14 = 152.14 \sim 152mm$ (for #13)

Distance from top $= 48.7mm$.

Distance from bottom $= 73.7mm$.

Superimposed dead loads = safety curb, sidewalk, railing, wearing surface.

Non-composite dead loads = utilities, haunch, diaphgram, SIP forms.

MASSDOT Highway : Interior %40 of (sidewalk, safety curbs, barriers/railings)

$\qquad$ exterior %60 of (" " " " ") as

well as vehicular and pedestrian live load on sidewalk.

MEMBERS

Girders west to east;

GIRDER 1

* Uniform loading

Non-composite loading :

Span1 : $1.407 + 0.24075 + 0.08722 = 1.73497$ kN/m

Span2 : 1.73497 kN/m

Superimposed Dead loading :

Span 1 : $(3.267 + 1.26) \times 0.6 + 3.35 = 6.0662$ kN/m

Span2 : 6.0662 kN/m

* Distributed loading

Since third span has connection at point of 2.937m with fascia girder 1A;

Non-composite loading :

Haunch : $(1.4487 + 1.4067)/2 = 1.4277$ kN/m for span 3

Span 3 : $1.4277 + 0.4815 + 0.08722 = 1.996$ kN/m
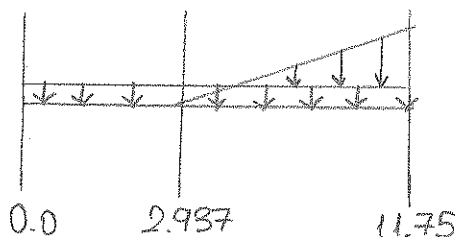
0.0   2.937   11.75
(1.996kN/m) (1kN/m)   Non-composite dead load.
(6.06 kN/m) (4.43kN/m) Superimposed dead load.

119

Superimposed Dead loading :

Wearing Surface : $20.12 \, kN/m \, / \, 8 \, girder = 2.515 \, kN/m$.

Span 3 : $(3.267 + 1.26) \times 0.4 + 2.515 = 4.325 \, kN/m$.

* Concentrated Load

$0.3102 \, kN$

(non-composite load/2) + (fascia girder) = $2.962 \, kN/m$

$2.298m$ $D_1 = 0.767m$

A ———— B

$2.938m$ $5.875m$
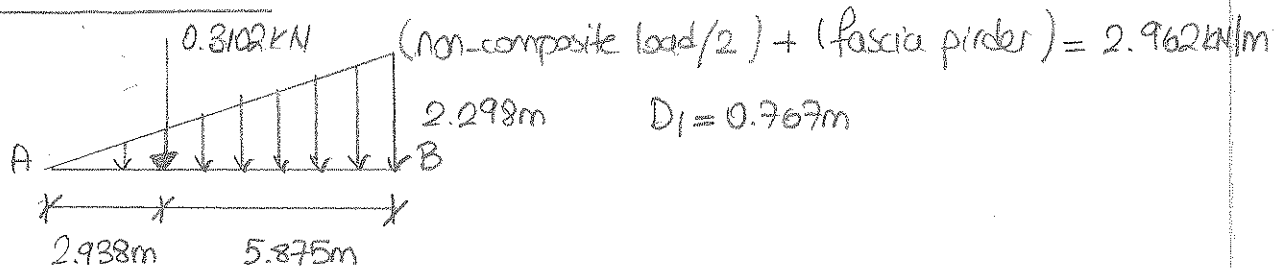
Weight of diaphragm : $63.5 \, kg/m \times 9.81 \, N/kg \times 0.767m = 477.22 \, N$

Additional weight for bolts : $143.167 \, N$

Total $= 477.22 + 143.167 = 620.386 \, N/1000 = 0.6203/2 = 0.3102 \, kN$

$$\stackrel{C+}{\Sigma} M_B = -5.875m \times 0.3102 + R_A \times 8.813 - \frac{(2.962 \times 8.813)}{2} \times \frac{8.813}{3}$$

$$= R_A = 4.5574 \, kN //$$

GIRDER 2

Non composite loading :

Span 1 : $0.3673 + 0.4815 + 0.1744 + 0.08722 = 1.110 \, kN/m$
Span 2 : $1.110 \, kN/m$
Span 3 : $0.3584 + 0.4815 + 0.1744 + 0.08722 = 1.1015 \, kN/m$

Superimposed loading :

Span 1 : $(1.31 + 1.26 + 15.235 + 3.267)/4 \times 0.4 + 3.35 = 5.457 \, kN/m$
Span 2 : $5.457 \, kN/m$
Span 3 : $(1.31 + 1.26 + 15.235 + 3.267)/4 \times 0.4 + 2.515 = 4.622 \, kN/m$

* Everything uniformly added no distributed load.

* No concentrated load.

GIRDER 3

Non-Composite Loading:

Span 1 : $0.3673 + 0.4815 + 0.3488 = 1.197$ kN/m

Span 2 : 1.197 kN/m

Span 3 : $0.3584 + 0.4815 + 0.3488 = 1.1887$ kN/m

Superimposed Dead Loading:

Span 1 : 5.457 kN/m

Span 2 : 5.457 kN/m

Span 3 : 4.622 kN/m

* Everything uniformly added, no distributed load.
* No concentrated load.

GIRDER 4

Only difference from other interior girders is, girder 4 shares utilities loading with girder 5.

Non-Composite Loading:

Span 1 : $0.3673 + 0.4815 + 0.3488 + 0.896/2 = 1.6459$ kN/m

Span 2 : 1.6459 kN/m

Span 3 : $0.3584 + 0.4815 + 0.3488 + 0.896/2 = 1.6331$ kN/m

Superimposed Dead Loading:

Span 1 : 5.457 kN/m

Span 2 : 5.457 kN/m

Span 3 : 4.622 kN/m

* Everything uniformly added, no distributed load.
* No concentrated load.

GIRDER 5

Non Composite Loading :

Span 1 : $0.3673 + 0.4815 + 0.1744 + 0.08722 + 0.896/2 = 1.558 \, kN/m$

Span 2 : $1.558 \, kN/m$

Span 3 : $0.3584 + 0.4815 + 0.1744 + 0.08722 + 0.896/2 = 1.549 \, kN/m$

Superimposed Loading :

Span 1 : $5.457 \, kN/m$

Span 2 : $5.457 \, kN/m$

Span 3 : $4.622 \, kN/m$.

* Everything uniformly added, no distributed load .
* No concentrated load .

GIRDER 6

Non-composite loading :

Span 1 : $1.407 + 0.24075 + 0.08722 = 1.73497 \, kN/m$

Span 2 : $1.73497 \, kN/m$

Superimposed loading :

Span 1 : $(15.285 + 1.31) \times 0.6 + 3.35 = 13.277 \, kN/m$

Span 2 : $13.277 \, kN/m$

* Distributed Loading

Since girder 6 has connection at third span with fascia girder;

Non-Composite Loading:

Haunch: 1.4254 for span 3

Span 3 : $1.4254 + 0.4815 + 0.08722 = 1.9941$ kN/m

between 0m – 2.937m $\longrightarrow$ 1.9941 kN/m

between 2.937 – 11.75m $\longrightarrow$ 1 kN/m

Superimposed Dead Loading:

Span 3 : $(15.235 + 1.31) \times 0.4 + 2.515 = 9.133$ kN/m

between 0m – 2.937m $\longrightarrow$ 13.277 kN/m

between 2.937m – 11.75 $\longrightarrow$ 9.133 kN/m

* Concentrated load
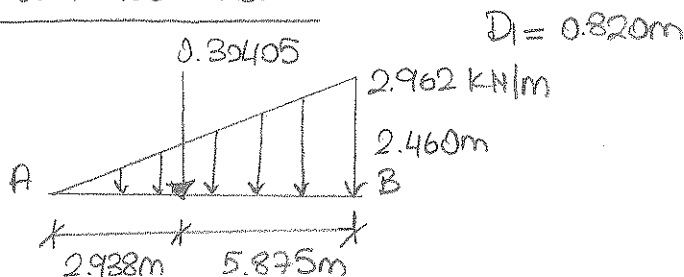
Weight of diaphragm : $63.5 kg/m \times 9.81 N/kg \times 0.820m = 510.896 N$

Additional weight for bolts : 170.268 N

Total = $510.896 + 170.268 = 681.074 N / 1000 = 0.68107 / 2 = 0.3405$ kN

Weight of fascia girder = $201 kg/m \times 9.81 N/kg = 1971.81 N/m = 1.972$ kN/m

$\sum M_B \overset{\curvearrowright +}{=} (-5.875 \times 0.80405) + (R_A \times 8.813) - \dfrac{(2.962 \times 8.813)}{2} \times \dfrac{8.813}{3}$

$= R_A = 4.5533$ kN //

CHAPTER 5

Evaluation of Powder-Mill Bridge Rating Factors Using Nondestructive Load Test Data

Bridge performance parameters like serviceability, safety, maintenance etc. should be better understood by using non-destructive testing results. AASHTO, The Manual for Bridge Evaluation offers information to engineers about bridge non-destructive testing and evaluation. The procedure in this manual is the research findings from NCHRP Project 12-28 (13)A, "Bridge Rating Through Non Destructive Load Testing" conducted by A.G. Lichtenstein in 1998.

The definition of nondestructive load test was described in NCHRP Project report as follows (NCHRP, 1998):

"Nondestructive load testing is the observation and measurement of the response of a bridge subjective to controlled and predetermined loadings without causing change in the elastic response of the structure. The principle of load testing is simply the comparison of the field response of the bridge under the test loads with its theoretical performance as predicted by analysis."

The diagnostic test plan should be prepared carefully and all details should be explained in the plan. The test truck position and the weight should stress all critical members on the bridge, therefore deciding the magnitude of the load and load patterns are critical. Analytical calculation might be helpful to decide which location of the truck provides the maximum moment on the bridge. The test truck weight cannot be more than state legal load without permit. Test truck axle loads and spacing has to be known and the truck speed has to be 5mph or less to prevent any vibration.

If the bridge has severe deterioration, inspection and analytical calculations may assist in determining if a nondestructive load test is required. In some situations bridge is unsuitable for NDT testing (NCHRP, 1998):

- If the cost of testing is the same or more than the cost of bridge rehabilitation
- If the bridge, according to calculations, cannot sustain even the lowest level of load
- If there is possibility of sudden failure
- If the load test is impractical because of inadequate access to the span

If the bridge exhibits linear behavior during the diagnostic load test, the result can be used for load rating. The result from diagnostic load is used to adjust the analytical load rating or update the analytical model. Non destructive load testing mostly improve the load rating of the bridge (AASHTOb, 2011). It should be noted that usually exterior girders rating factors are less reliable than interior girders because of participation of parapets, curbs and sidewalk in theoretical calculation. Therefore, load testing may develop the accuracy of the behavior of exterior girders (AASHTOb, 2011). Bridge owner use load testing to capture the bridge true behavior more accurately.

Procedure of the diagnostic load test can be as followed based on (NCHRP, 1998):

- Preliminary inspection and theoretical rating
- Development of load test program
- Planning and preparation for load test
- Execution of load test
- Evaluation of load test results

- Determination of final load rating
- Reporting

5.1   <u>Procedure for Using Diagnostic Load Test Data</u>

The diagnostic test result can be used to validate the actual behavior of the bridge by guidance of the AASHTO, The Manual for Bridge Evaluation, 2011. The following equation provides the load rating based on load test results with updating the analytical results.

(1) $$RF_T = RF_c * K$$ (AASHTO, 2011 – 8.8.2.3-1)

$RF_T =$ load rating factors for the live-load capacity based on the load test result

$RF_C =$ rating factor based on calculation prior to incorporating test results

$K \quad =$ adjustment factor resulting from the comparison of measurement test behavior with the analytical model

The benefit of the diagnostic test results is obtained by K. The K factor is estimated under the following formulation:

(2) $$K = 1 + K_a * K_b$$ (AASHTO, 2011 – 8.8.2.3.1-1)

$K_a =$ accounts for both the benefit derived from the load test with consideration of section factor resisting the applied test load

$K_b =$ accounts for the understanding of the load test results when compared with those predicted by theory

If the K factor equal to 1, it means that the test results is agree with analytical calculated rating factors. If K factor greater than 1, the bridge capacity is higher than the analytical calculated rating factors. If K factor is smaller than 1, it means that the bridge behavior is worse than analyticaly calculated rating factors.

The K_a factor is determined by suing the following equations.

(3) $$K_a = \frac{\varepsilon_C}{\varepsilon_T} - 1$$ (AASHTO, 2011 – 8.8.2.3.1-2)

ε_T = maximum member strain measurement during the load test

ε_C = corresponding calculated strain due to the test vehicle, at its position on the bridge which produced ε_T

(4) $$\varepsilon_C = \frac{L_T}{(SF)*E}$$ (AASHTO, 2011 − 8.8.2.3.1-3)

L_T = calculated theoretical load effect in member corresponding to the measurement strain ε_T

SF = member appropriate section factor

E = member modulus of elasticity

The factor of K_b should be between 0 and 1 to show the level of benefit at the rating level. The K_b factor is obtained from the level of relationship between T and W. T is the unfactored test vehicle and W is the unfactored gross rating load effect. If the K_b equal to 0, the test result cannot be validate. After calculation of T and W the K_b values can be found using the table 8.8.2.3.1-1 in the AASHTO The Manual for Bridge evaluation.

Diagnostic testing is beneficial to evaluate the actual behavior of the bridge. It should be noted that the participation of nonstructural members and secondary members' effect on the bridge can be observed more accurately by using diagnostic test results. After diagnostic test the capacity of the bridge might be calculated less than the design capacity, this also help the bridge owner to decide whether to post or maintenance the bridge. Non-destructive testing has an essential role in long term bridge monitoring and bridge management.

5.2 Scanned Documents for Three Years Nondestructive Load Rating

Evaluation of Rating Factors using 2009 NDT Data
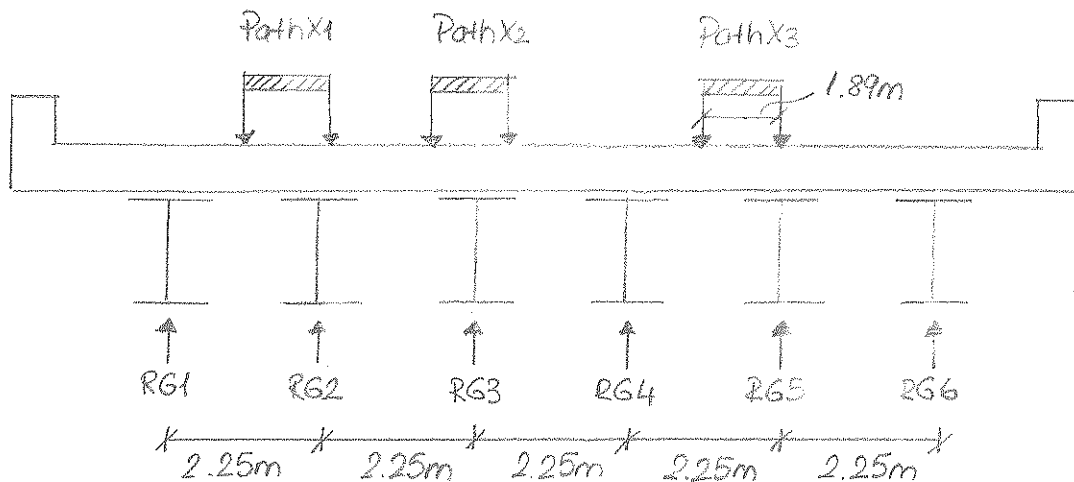
Path X1   Path X2   Path X3

1.89m

R_{G1} R_{G2} R_{G3} R_{G4} R_{G5} R_{G6}

2.25m   2.25m   2.25m   2.25m   2.25m

Lever Rule

to Compute Live Load Distribution Factors.

Exterior Girders;

Girder 1 ; $R_{G1} = 0.5P (1.89m / 2.25m)$ $\Rightarrow$ $DF_{GR1} = 0.42$

Girder 6 ;   Cannot Validate $DF_{GR6} = N/A$

Interior Girders;

Girder 2 ; $R_{G2} = 0.5P (2.25m/2.25m) + 0.5P(0.36/2.25)$ $\Rightarrow$ $DF_{GR2} = 0.58$

Girder 3 ; $R_{G3} = 0.5P (1.805m/2.25m) + 0.5P(1.805/2.25m)$ $\Rightarrow$ $DF_{GR3} = 0.58$

Girder 4 ; $R_{G4} = 0.5P (1.89m/2.25m)$ $\Rightarrow$ $DF_{GR4} = 0.42$

Girder 5 ; $R_{G5} = 0.5P (2.25m/2.25m) + 0.5P (0.36/2.25)$ $\Rightarrow$ $DF_{GR5} = 0.58$

Girder #	DFS	Truck Path
1	0.42	X1
2	0.58	X1
3	0.58	X2
4	0.42	X3
5	0.58	X3
6	N/A	— (Because of the truck position DF for G6 could not be calculated)

Maximum Strain Recorded During 2009 load Test.

Girder #	Strain Gauge #	Location of SGs	Max. Reading (µE)	Truck Path
1	SG6	Bottom Flange	92.91	X1
2	SG22	" "	96.94	X1
3	SG42	" "	93.09	X2
4	SG61	" "	81.56	X3
5	SG82	" "	88.43	X3
6	SG96	" "	60.63	X3

2009 Test Truck Axle Loads;

$\qquad$ 118.07 kN $\quad$ 118.42 kN $\qquad$ 87.31N
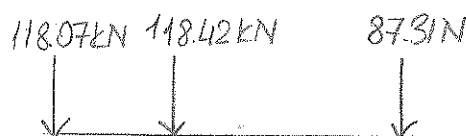
Note; test truck axles were weighed before the test and after test then averaged.

Test truck axles weight was multiplied by DFs was found in previous page.
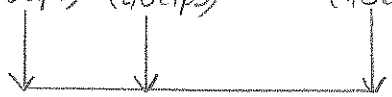
Girder 1   49.59 kN   49.74 kN   36.67 kN

Girder 2   68.49 kN   68.68 kN   50.65 kN

Girder 3   68.49 kN   68.68 kN   50.65 kN

Girder 4   49.59 kN   49.74 kN   36.67 kN

Girder 5   68.49 kN   68.68 kN   50.65 kN

Girder 6   DFs. N/A

Those load applied to simple frame model in SAP2000, from the moment values the strain data (E_c) calculated.

Since strain gauges were not located, the maximum moment location, the modification factor (MF) was used.

To calculate the MF the VAB design truck HS-25 truck was used.

AASHTO HS-25 Truck Axle loads;   177.9kN   177.9kN   44.5kN
                                  (40kips)   (40kips)   (10kips)

Maximum moment caused by HS-25 ; M_{Max} = 1062 kN_m

Maximum moment at gauges locations by HS-25 ; M_{Max56} = 940 kN_m

$$MF_{for\,all} = \frac{M_{Max}}{M_{Max56}} = \frac{531.53}{470.30} = 1.13$$

Girder #	Strain Gauge #	Max Strain Reading (µE)	MF	ε_T (µE)
1	S66	92.91	1.13	104.99
2	S622	96.94	1.13	109.54
3	S642	93.09	1.13	105.19
4	S661	81.56	1.13	92.16
5	S682	88.43	1.13	99.98
6	S696	60.63	1.13	68.52

Calculation of Ec

$$Ec = \frac{LT}{(SF)\cdot E} \qquad (\text{AASHTO Manual, 2011 Eq. } 8.8.2.3.1-3)$$

$E = 200$ kN/mm^2 $SF_{tot} = 1.34 \times 10^7$ mm^3 $ST_{ex} = 1.937 \times 10^7$ mm^3

Girder 1 ; $\varepsilon_{G1} = \dfrac{341.79 \times 1000}{1.937 \times 10^7 \times 200} \times 10^6 = 88.23\,\mu E$

Girder 2 ; $\varepsilon_{G2} = \dfrac{471.51 \times 1000}{1.34 \times 10^7 \times 200} \times 10^6 = 175.94\,\mu E$

Girder 3 ; $\varepsilon_{G3} = 175.94\,\mu E$

Girder 4; $\varepsilon_{Gr4} = \dfrac{341.79 \times 1000}{1.34 \times 10^7 \times 200} \times 10^6 = 127.53 \,\mu\varepsilon$

Girder 5; $\varepsilon_{Gr5} = 175.94 \,\mu\varepsilon$

Girder #	$\varepsilon_T (\mu\varepsilon)$	$\varepsilon_L (\mu\varepsilon)$	$Ka = (\varepsilon_L/\varepsilon_T) - 1$
1	104.99	88.23	−0.16
2	109.54	175.94	0.61
3	105.19	175.94	0.67
4	92.16	127.53	0.38
5	99.98	175.94	0.76
6	68.52	N/A	N/A

$Ka = \dfrac{\varepsilon_L}{\varepsilon_T} - 1$ 　　(AASHTO Manual, 2011 Eg. 8.8.2.3.1-2)

T = result from SAP using the test truck weight

W = result from SAP using HS25 truck weight

Calculation of Kb for 2009

Girder #	T(kNm)	W(kNm)	T/W	Kb	$K = 1 + Ka \cdot Kb$
1	341.79	896.64	0.38	0	1
2	471.51	896.64	0.53	0.8	1.49
3	471.51	896.64	0.53	0.8	1.54
4	341.79	896.64	0.38	0	1
5	471.51	896.64	0.53	0.8	1.61
6	N/A	N/A	N/A	N/A	N/A

AASHTO Manual, 2011 Table 8.8.2.3.1-1 used to find value of Kb.

Evaluation of Rating Factors using 2010 NDT Data

Lever Rule
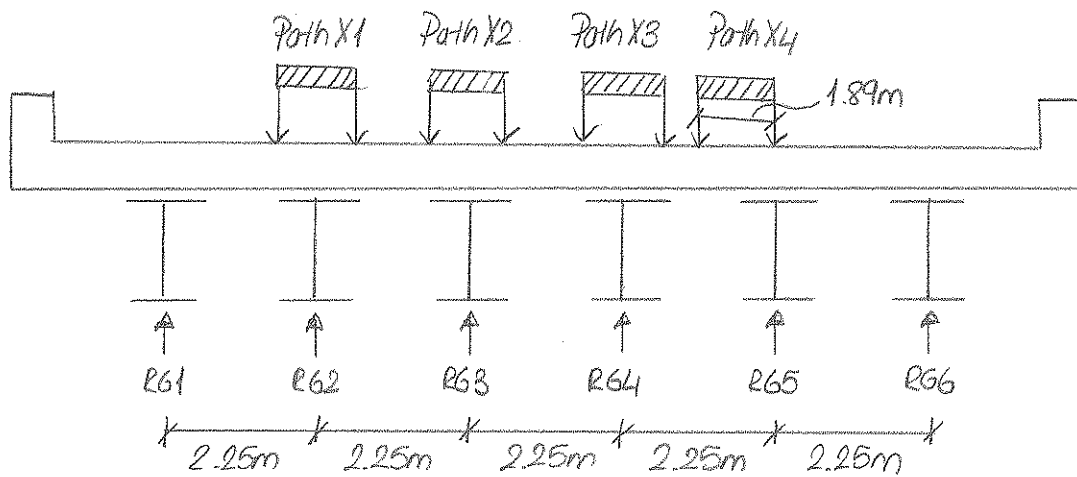
to Compute Live Load Distribution Factor

Exterior Girders;

Girder 1; $RG1 = 0.5P (0.945m / 2.25m)$ $\Rightarrow$ $DF_{GR1} = 0.21$

Girder 6; Cannot Validate

Interior Girders;

Girder 2; $RG2 = 0.5P (1.305m/2.25m) + 0.5P (1.305/2.25m) \Rightarrow DF_{GR2} = 0.58$

Truck positions same as $6R2$ for $6R3$ and $6R4$ $\Rightarrow DF_{GR3} = 0.58$

$\Rightarrow DF_{GR4} = 0.58$

Girder 5; $RG5 = 0.5P (2.25m/2.25m) + 0.5P (0.36/2.25)$ $\Rightarrow DF_{GR5} = 0.58$

Girder #	DFs	Truck Path
1	0.21	X1
2	0.58	X1
3	0.58	X2
4	0.58	X3
5	0.58	X4
6	N/A	N/A

Maximum Strain Recorded During 2010 Load Test

Girder #	Strain Gauge #	Location of SGs	Max Reading (με)	Truck Path
1	S66	Bottom Flange	70.98	X1
2	S622	" "	101.46	X1
3	S642	" "	91.66	X2
4	S661	" "	94.59	X3
5	S681	" "	84.32	X4
6	S696	" "	51.63	X4

2010 Test Truck Axle Loads;   120.34 KN   121.71 KN   86.23 KN

↓   ↓   ↓

Note; Test truck axles was weighted before the test and after the test then averaged values were used.

Girder 1	25.27 KN	25.56 KN	18.11 (KN)
Girder 2	69.8 KN	70.6 KN	50.02 KN
Girder 3	69.8 KN	70.6 KN	50.02 KN
Girder 4	69.8 KN	70.6 KN	50.02 KN
Girder 5	69.8 KN	70.6 KN	50.02 KN
Girder 6			DFs N/A.

These load applied to simple frame model in SAP2000, from the moment values the strain data (E_c) calculated.

Since strain gauges were not located at the maximum moment location, the modification factor (MF) was used.

To calculate the MF the VAB design truck HS-25 truck was used

AASHTO HS-25 Truck Axle Loads;   177.9 kN   177.9 kN   44.5 kN
                                    (40 kips) (40 kips)   (10 kips)
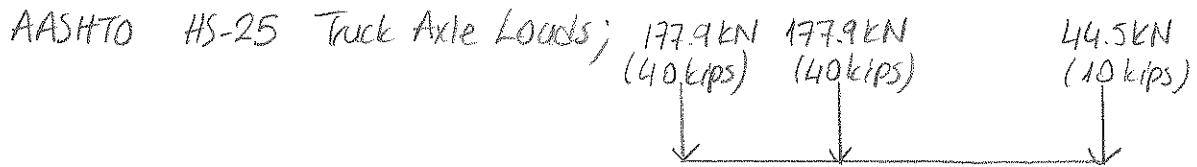
Maximum nevert caused by HS-25 ; M_{Nmax} = 1062 kNm

Maximum "   at gauges locaties by HS-25; M_{Nmax56} = 940 kNm

$$MF \, for \, all = \frac{M_{Nmax}}{M_{Nmax56}} = \frac{531.53}{470.30} = 1.13$$

Girder #	Strain Gauge #	Max Strain Reading ($\mu\varepsilon$)	MF	ε_T ($\mu\varepsilon$)
1	S66	70.98	1.13	80.21
2	S622	101.46	1.13	114.65
3	S642	91.66	1.13	103.58
4	S661	94.59	1.13	106.97
5	S681	84.32	1.13	95.28
6	S696	51.62	1.13	58.33

Calculation of E_c

$$E_c = \frac{LT}{(SF) \cdot E}$$ (AASHTO Manual, 2011 Eq. 8.8.2.3.1-3)

$E = 200 \, kN/mm^2$ $SF_{int} = 1.34 \times 10^7 \, mm^3$ $SF_{ex} = 1.937 \times 10^7 \, mm^3$

Girder 1; $\varepsilon_{Gr1} = \frac{173.72 \times 1000}{1.937 \times 10^7 \times 200} \times 10^6 = 44.84 \, \mu\varepsilon$

Girder 2; $\varepsilon_{Gr2} = \frac{479.82 \times 1000}{1.34 \times 10^7 \times 200} \times 10^6 = 179.04 \, \mu\varepsilon$

Same as for Gr3, Gr4, Gr5

$\varepsilon_{Gr3} = 179.04 \, \mu\varepsilon$

$\varepsilon_{Gr4} = 179.04 \, \mu\varepsilon$

$\varepsilon_{Gr5} = 179.04 \, \mu\varepsilon$

Girder #	$\varepsilon_T (\mu\varepsilon)$	$\varepsilon_c (\mu\varepsilon)$	$K_a = (\varepsilon_c / \varepsilon_T) - 1$
1	80.21	44.84	-0.44
2	114.65	179.04	0.56
3	103.58	179.04	0.73
4	106.97	179.04	0.67
5	95.28	179.04	0.87
6	58.33	N/A	N/A

$$K_a = \frac{\varepsilon_c}{\varepsilon_T} - 1 \qquad (AASHTO\ Manual,\ 2011\ \ Eq.\ 8.8.2.3.1-2)$$

T = result from SAP using the test truck weight

W = result from SAP using HS25 truck weight

Calculation of K_b for 2010

Girder #	T(kNm)	W(kNm)	T/W	K_b	$K = 1 + K_a K_b$
1	173.72	896.64	0.19	0	1
2	479.82	896.64	0.53	0.8	1.45
3	479.82	896.64	0.53	0.8	1.58
4	479.82	896.64	0.53	0.8	1.54
5	479.82	896.64	0.53	0.8	1.64
6	N/A	N/A	N/A	N/A	N/A

AASHTO Manual 2011 Table 8.8.2.3.1-1 used to find value of K_b.

Evaluation of Rating Factors Using 2011 NDT Data
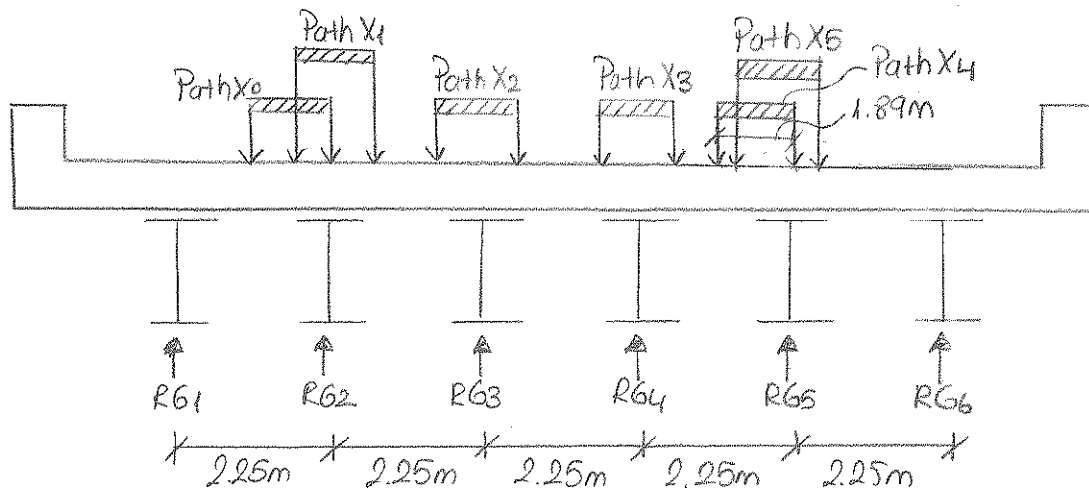
Lever Rule

to compute Live Load Distribution Factors

Exterior Girders;

Girder 1 ; $RG_1 = 0.5P \, (1.89m / 2.25m)$ $\Rightarrow$ $DFG_{R1} = 0.42$

Girder 6 ; $RG_6 = 0.5P \, (0.661m / 2.25m)$ $\Rightarrow$ $DFG_{R6} = 0.15$

Interior Girders;

Girder 2 ; $RG_2 = 0.5P(1.305m/2.25m) + 0.5P(1.305m/2.25m)$ $\Rightarrow$ $DFG_{R2} = 0.58$

Since the truck position same as G2 for G3 and G4 $\Rightarrow$ $DFG_{R3} = 0.58$

$\Rightarrow$ $DFG_{R4} = 0.58$

Girder 5 ; $RG_5 = 0.5P \, (1.229/2.25m) + 0.5P(0.661/2.25m)$ $\Rightarrow$ $DFG_{R5} = 0.42$

Girder #	DFS	Truck Path
1	0.42	X_0
2	0.58	X_1
3	0.58	X_2
4	0.58	X_3
5	0.42	X_5
6	0.15	X_5

Maximum Strain Recorded During 2011 Load Test

Girder #	Strain Gauge #	Location of SGs	Max Reading (ME)	Truck Path
1	SG6	Bottom Flange	91.25	X0
2	SG21	" "	104.56	X1
3	SG41	" "	100.20	X2
4	SG61	" "	103.46	X3
5	SG81	" "	71.02	X5
6	SG96	" "	71.12	X5

2011 Test Truck Axle Loads;
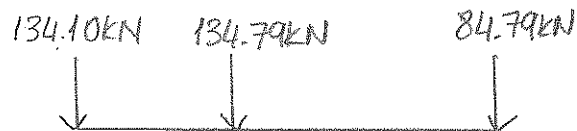
134.10kN   134.79kN   84.79kN

Note; test truck axles were weighed before the test and after the test then averaged.

Test truck axles weigh was multiplied by DFs was found in previous page.

Girder 1   56.32kN   56.62kN   35.62kN

Girder 2   77.78kN   78.18kN   49.18kN

Girder 3   77.78 kN   78.18kN   49.18 kN

Girder 4   77.78 kN   78.18kN   49.18kN

Girder 5   56.32 kN   56.62 kN   35.62kN

Girder 6   20.11 kN   20.22kN   12.72 kN

The load applied to simple frame model in SAP2000, from the newest values the strain delta (E_c) calculated.

Since strain gauges were not located, the maximum nearest location, the modification factor (MF) was used.

To calculate the MF the VAB design truck HS-25 truck was used

AASHTO HS-25 Truck Axle Loads;

177.9kN (40kips) 177.9kN (40kips) 44.5 kN (10kips)
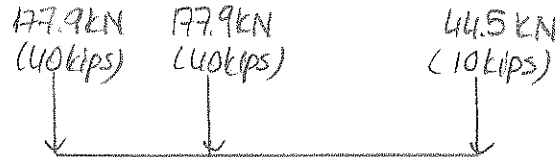
Maximum moment caused by HS-25 ; $M_{max} = 1062\,kNm$

Maximum moment at gauge location caused by HS-25; $M_{maxSG} = 940\,kN$

$$MF_{all} = \frac{M_{max}}{M_{maxSG}} = \frac{531.53}{470.30} = 1.13$$

Girder #	Strain Gauge #	Max Strain Reading ($\mu\varepsilon$)	MF	ε_T ($\mu\varepsilon$)
1	S66	91.25	1.13	103.11
2	S621	104.56	1.13	118.15
3	S641	100.20	1.13	113.23
4	S661	103.46	1.13	116.91
5	S681	71.02	1.13	80.25
6	S696	71.12	1.13	80.37

Calculation of E_c

$$E_c = \frac{LT}{(SF) \cdot E} \qquad \text{(AASHTO Manual, 2011 Eq. 8.8.2.3.1-3)}$$

$E = 200\,kN/mm^2$ $SF_{int} = 1.34 \times 10^7\,mm^3$ $SF_{ext} = 1.937 \times 10^7\,mm^3$

Girder 1; $\varepsilon_{GR1} = \dfrac{377.58 \times 1000}{1.937 \times 10^7 \times 200} \times 10^6 = 97.46\,\mu\varepsilon$

Girder 2; $\varepsilon_{GR2} = \dfrac{520.83 \times 1000}{1.34 \times 10^7 \times 200} \times 10^6 = 194.34\,\mu\varepsilon$

Girder 3; $\varepsilon_{GR3} = 194.34\,\mu\varepsilon$

Girder 4; $\varepsilon_{GR4} = 194.34\,\mu\varepsilon$

Girder 5; $\varepsilon_{Gr5} = \dfrac{364.12 \times 1000}{1.27 \times 10^7 \times 200} \times 10^6 = 143.35 \mu\varepsilon$

Girder 6; $\varepsilon_{Gr6} = \dfrac{134.83 \times 1000}{1.937 \times 10^7 \times 200} \times 10^6 = 34.80 \mu\varepsilon$

Girder #	$\varepsilon_T (\mu\varepsilon)$	$\varepsilon_c (\mu\varepsilon)$	$Ka = (\varepsilon_c/\varepsilon_T) - 1$
1	103.11	97.46	−0.055
2	118.15	194.34	0.65
3	113.23	194.34	0.72
4	116.91	194.34	0.66
5	80.25	143.35	0.79
6	80.37	34.80	−0.57

$Ka = \dfrac{\varepsilon_c}{\varepsilon_T} - 1$ (AASHTO Manual 2011   Eq. 8.8.2.3.1-2)

T = result from SAP using the test truck weight

W = result from SAP using HS25 truck weight.

Calculation of Kb for 2011

Girder #	T (kNm)	W (kNm)	T/W	Kb	K = 1 + Ka·Kb
1	377.58	896.64	0.42	0.8	1
2	520.83	896.64	0.58	0.8	1.52
3	520.83	896.64	0.58	0.8	1.58
4	520.83	896.64	0.58	0.8	1.53
5	364.12	896.64	0.41	0.8	1.63
6	134.83	896.64	0.15	0	1

AASHTO Manual 2011 Table 8.8.2.3.1-1 used to find value of Kb.

CHAPTER 6

Evaluation of Rating Factors of Powder-Mill Bridge using Calibrated Finite Element Model

The fourth and final method used in load rating comparison of the Powder-Mill Bridge was done using a calibrated finite element model to evaluate rating factors. Load rating can be improved by representing the 3D system behavior of the bridge. Therefore the calibrated finite element model is used to improve the accuracy of the rating factors.

In order to model the Powder-Mill Bridge accurately, a 3D finite element model was used, created at Tufts University (Sanayei et al., 2012). The bridge deck was modeled with solid elements and the steel girders with shell elements. The bridge deck supports were model with springs representing the neoprene pads. Due to high flexibility of these supports compared to the substructure and foundation, only the superstructure was modeled. The neutral axis of the Powder-Mill Bridge was calculated with the reinforcement and without reinforcement. Since the difference was not significant, the reinforcement was not included in the model. The bridge model was successfully calibrated and verified using the 2009 NDT truck load test data.

The calibrated FEM is used to simulate assumptions made in the hand rating calculations and obtain rating factors for the bridge. To replicate these assumptions, the bridge was loaded in two lanes with the HS25 trucks in the position to apply the greatest load to the girder of interest, according to AASHTO lane and truck specifications, Figure 6.1.
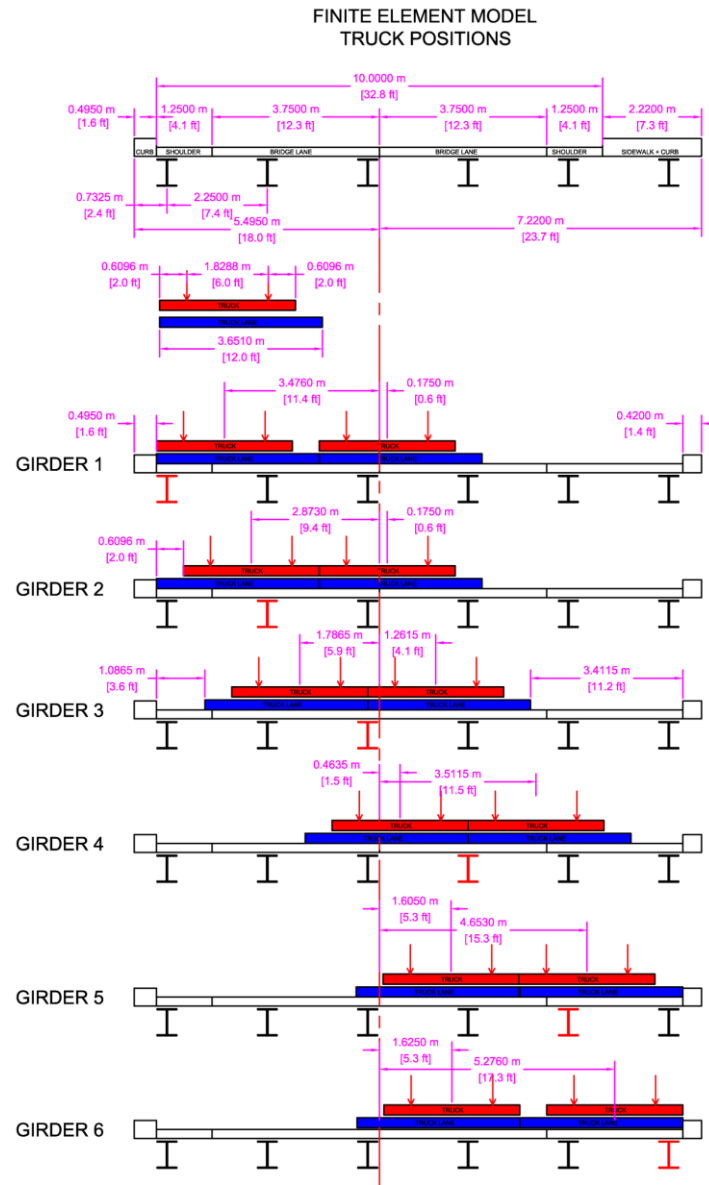
Figure 6.1 FEM Truck Load Paths

Calculated rating factors can be seen in table 6.1 and table 6.2.

Table 6.1 Rating Factor by FEM for Negative Moment Region

(a) ASD Method

Girder #	Inventory RF	Operating RF
1	3.11	4.81
2	2.59	4.10
3	2.56	4.09
4	2.34	3.79
5	2.30	3.74
6	2.45	4.25

(b) LFD Method

Girder #	Inventory RF	Operating RF
1	3.90	6.51
2	3.35	5.60
3	3.36	5.61
4	3.13	5.23
5	3.11	5.19
6	3.52	5.89

Table 6.2 Rating Factor by FEM for Positive Moment Region

(a) ASD Method
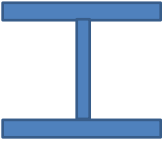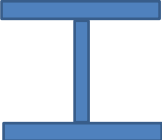
Girder #	Inventory RF	Operating RF
1	3.96	5.79
2	3.32	4.92
3	3.07	4.62
4	2.62	3.95
5	2.91	4.38
6	3.61	5.37

(b) LFD Method
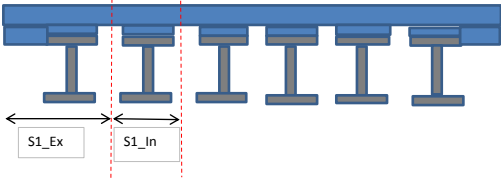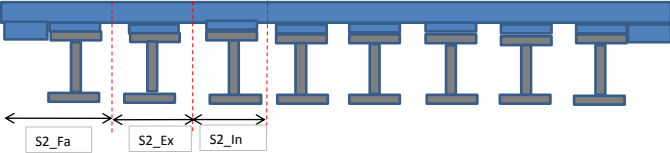
Girder #	Inventory RF	Operating RF
1	4.56	7.62
2	3.90	6.52
3	3.70	6.17
4	3.17	5.29
5	3.50	5.85
6	4.27	7.14
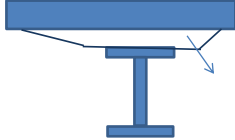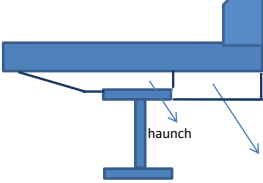
6.1 <u>**Influence of Rebars on Neutral Axis Calculations**</u>

GENERAL PROPERTIES

Ec=	24855578 KN/m^2	24.85558 KN/mm^2
Es=	199900000 KN/m^2	199.9479 KN/mm^2
n=	Es/Ec	
n=	8.04438746	

BRIDGE LENGTH	47000	mm
BRIDGE SECTION 1 (6 GIRDER)	38187	mm
BRIDGE SECTION 1 (8 GIRDER)	8813	mm
GIRDER SPACING	2250	mm
FASCIA GIRDER SPACING		
MIN	2298	mm
MAX	2460	mm
AVERAGE	2379	mm

DECK PROPERTIES

Deck Tickness=	200	mm

EXTERIOR GIRDER (W920*345)

tf=	39.878	mm
bf=	308	mm
Height=	942.34	mm
I=	6.24*10^9	mm^4
A=	43935.4	mm^2

INTERIOR GIRDER (W920*238)

tf=	25.9	mm
bf=	305	mm
Height=	914	mm
I=	4.06*10^9	mm^4
A=	30300	mm^2

FASCIA GIRDER (W920*201)

tf=	20.1	mm
bf=	305	mm
Height=	904	mm
I=	3.25*10^9	mm^4
A=	25600	mm^2

BRIDGE SECTION 1

Deck Width=	12715	mm
Overhang(from center of girder)=	732.5	mm
Overhang Width=	578.5	mm
Space 1 Interior (S1_In)=	2250	mm
Space 1 exterior (S1_Ex)=	1857.5	mm

BRIDGE SECTION 2

Deck Width=	17165	mm
Overhang(from center of girder)=	732.5	mm
Overhang Width=	578.5	mm
Space 2 Interior (S2_In)=	2250	mm
Space 2 Exterior (S2_Ex)=	2314.5	mm
Space 2 Fascia (S2_Fa)=	1922	mm

DATA FROM HAUNCH CALCULATION

INTERIOR GIRDERS (Span 1, 2 and 3)
Haunch Depth	35.0096	mm
Haunch Area	13294.22	mm^2

DATA FROM HAUNCH CALCULATION

EXTERIOR GIRDERS (Span 1 and 2)
Haunch Depth	36.449	mm
Overhang Depth	66.929	mm
Haunch Area	12089	mm^2
Overhang Area	38725	mm^2

EXTERIOR GIRDERS (Span 3)
Haunch Depth	33.528	mm
Overhang Depth	60.706	mm
Haunch Area	9181.2	mm^2
Overhang Area	35125	mm^2
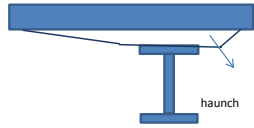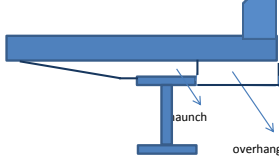
BRIDGE SECTION 1

EXTERIOR GIRDERS	A	y		Ay	
Deck Transformed=	31798.57 mm^2		100 mm	3179857 mm^3	
Haunch Transformed=	1511.125 mm^2	218.2245 mm		329764.5 mm^3	
Overhang Transformed=	19196.61 mm^2	153.4035 mm		2944828 mm^3	
Extrior Girder=	43935.4 mm^2	707.619 mm		31089524 mm^3	
Sum	96441.71 mm^2			37543973 mm^3	
N.A Axis=	389.2919 mm				
N.A from bottom=	789.4971 mm				

INTERIOR GIRDERS	A	y		Ay	
Deck Transformed=	55939.62 mm^2		100 mm	5593962 mm^3	
Haunch Transformed=	1652.608 mm^2	217.5048 mm		359450.2 mm^3	
Interior Girder=	30300 mm^2	692.0096 mm		20967891 mm^3	
Sum	87892.23 mm^2			26921303 mm^3	
N.A Axis=	306.299 mm				
N.A from bottom=	842.7106 mm				

BRIDGE SECTION 2

FASCIA GIRDERS	A	y		AY	
Deck Transformed=	33402.17 mm^2		100 mm	3340217 mm^3	
Haunch Transformed=	1141.317 mm^2	216.764 mm		247396.5 mm^3	
Overhang Transformed=	18749.1 mm^2	140.403 mm		2632429 mm^3	
Fascia Girder=	25600 mm^2	685.528 mm		17549517 mm^3	
Sum	78892.58 mm^2			23769560 mm^3	
N.A Axis=	301.2902 mm				
N.A from bottom=	836.2378 mm				

EXTERIOR GIRDERS					
Deck Transformed=	57543.23 mm^2		100 mm	5754323 mm^3	
Haunch Transformed=	1502.787 mm^2	218.2245 mm		327944.9 mm^3	
Exterior Girder=	43935.4 mm^2	707.619 mm		31089524 mm^3	
Sum	102981.4 mm^2			37171791 mm^3	
N.A Axis=	360.9563 mm				
N.A from bottom=	817.8327 mm				

INTERIOR GIRDERS					
Deck Transformed=	55939.62 mm^2		100 mm	5593962	
Haunch Transformed=	1652.608 mm^2	217.5048 mm		359450.2	
Interior Girder=	30300 mm^2	692.0096 mm		20967891	
Sum	87892.23 mm^2			26921303	
N.A Axis=	306.299 mm				
N.A from bottom=	842.7106				

145

GENERAL PROPERTIES

Ec=	24855578	KN/m^2	24.855578	KN/mm^2
Es=	199900000	KN/m^2	199.9479	KN/mm^2
n=	Es/Ec			
n=	8.0443875			

BRIDGE LENGTH	47000	mm
BRIDGE SECTION 1 (6 GIRDER)	38187	mm
BRIDGE SECTION 1 (8 GIRDER)	8813	mm
GIRDER SPACING	2250	mm
FASCIA GIRDER SPACING		
MIN	2298	mm
MAX	2460	mm
AVERAGE	2379	mm

DECK PROPERTIES

Deck Tickness=	200	mm

EXTERIOR GIRDER (W920*345)

tf=	39.878	mm
bf=	308	mm
Height=	942.34	mm
I=	6.24*10^9	mm^4
A=	43935.4	mm^2

INTERIOR GIRDER (W920*238)

tf=	25.9	mm
bf=	305	mm
Height=	914	mm
I=	4.06*10^9	mm^4
A=	30300	mm^2

FASCIA GIRDER (W920*201)

tf=	20.1	mm
bf=	305	mm
Height=	904	mm
I=	3.25*10^9	mm^4
A=	25600	mm^2

BRIDGE SECTION 1

Deck Width=	12715	mm
Overhang(from center of girder)=	732.5	mm
Overhang Width=	578.5	mm
Space 1 Interior (S1_In)=	2250	mm
Space 1 exterior (S1_Ex)=	1857.5	mm

BRIDGE SECTION 2

Deck Width=	17165	mm
Overhang(from center of girder)=	732.5	mm
Overhang Width=	578.5	mm
Space 2 Interior (S2_In)=	2250	mm
Space 2 Exterior (S2_Ex)=	2314.5	mm
Space 2 Fascia (S2_Fa)=	1922	mm

DATA FROM HAUNCH CALCULATION

INTERIOR GIRDERS (Span 1, 2 and 3)

INTERIOR GIRDERS (Span 1, 2 and	35.0096	mm
INTERIOR GIRDERS (Span 1, 2 and	13294.22	mm^2

DATA FROM HAUNCH CALCULATION

EXTERIOR GIRDERS (Span 1 and 2)

Haunch Depth	36.449	mm
Overhang Depth	66.929	mm
Haunch Area	12089	mm^2
Overhang Area	38725	mm^2

EXTERIOR GIRDERS (Span 3)

Haunch Depth	33.528	mm
Overhang Depth	60.706	mm
Haunch Area	9181.2	mm^2
Overhang Area	35125	mm^2

BRIDGE SECTION 1

EXTERIOR GIRDERS

	Ac-As		A=(Ac-As)/n	A+Ac	y		Ay	
Deck Transformed=	254787.908	mm^2	31672.75431	32684.84669	100	mm	3268484.669	mm^3
Haunch Transformed=	12089	mm^2	1502.786888	1502.786888	218.2245	mm	327944.9173	mm^3
Overhang Transformed=	154143.293	mm^2	19161.59478	19443.30203	153.4035	mm	2982670.582	mm^3
Extrior Girder=	43935.4	mm^2	43935.4	43935.4	707.619	mm	31089523.81	mm^3
Sum				97566.3356		mm^2	37668623.98	mm^3
N.A Axis=	**386.082184**	**mm**						
N.A from bottom=	**792.706816**	**mm**						

INTERIOR GIRDERS

	Ac-As		A=(Ac-As)/n	A+Ac	y		Ay	
Deck Transformed=	448219.54	mm^2	55718.29335	57498.75297	100	mm	5749875.297	mm^3
Haunch Transformed=	13294.22	mm^2	1652.608115	1652.608115	217.5048	mm	359450.1976	mm^3
Interior Girder=	30300	mm^2	30300	30300	692.0096	mm	20967890.88	mm^3
Sum				89451.36108		mm^2	27077216.37	mm^3
N.A Axis=	**302.703235**	**mm**						
N.A from bottom=	**846.306365**	**mm**						

BRIDGE SECTION 2

FASCIA GIRDERS

	Ac-As		A=(Ac-As)/n	A+Ac	y		AY	
Deck Transformed=	267636.868	mm^2	33270.01205	34333.14427	100	mm	3433314.427	mm^3
Haunch Transformed=	9181.2	mm^2	1141.317477	1141.317477	216.764	mm	247396.5416	mm^3
Overhang Transformed=	150543.293	mm^2	18714.07779	18995.78504	140.403	mm	2667065.208	mm^3
Fascia Girder=	25600	mm^2	25600	25600	685.528	mm	17549516.8	mm^3
Sum				80070.24679		mm^2	23897292.98	mm^3
N.A Axis=	**298.454094**	**mm**						
N.A from bottom=	**839.073906**	**mm**						

EXTERIOR GIRDERS

	Ac-As		A=(Ac-As)/n	A+Ac	y		AY	
Deck Transformed=	461068.501	mm^2	57315.55109	59147.05055	100	mm	5914705.055	mm^3
Haunch Transformed=	12089	mm^2	1502.786888	1502.786888	218.2245	mm	327944.9173	mm^3
Exterior Girder=	43935.4	mm^2	43935.4	43935.4	707.619	mm	31089523.81	mm^3
Sum				104585.2374		mm^2	37332173.79	mm^3
N.A Axis=	**356.954525**	**mm**						
N.A from bottom=	**821.834475**	**mm**						

INTERIOR GIRDERS

	Ac-As		A=(Ac-As)/n	A+Ac	y		AY	
Deck Transformed=	448219.54	mm^2	55718.29335	57498.75297	100	mm	5749875.297	
Haunch Transformed=	13294.22	mm^2	1652.608115	1652.608115	217.5048	mm	359450.1976	
Interior Girder=	30300	mm^2	30300	30300	692.0096	mm	20967890.88	
Sum				89451.36108		mm^2	27077216.37	
N.A Axis=	**302.703235**	**mm**						
N.A from bottom=	**846.306365**							

Bridge Section 1 Reinforcement

	Width	Number of Bars						Ac
		Top and Bottom		Piers	Bar Area			
		#13	#16	#13			#16	
Deck_ex=	1279	4.9192308		1.9676923	126.61		197.83	1012.0924
Over_deck_ex=	578.5	2.225		0				281.70725
Deck_in=	2250	8.6538462		3.4615385				1780.4596

Bridge Section 1 Reinforcement

	Width	Number of Bars						Ac
		Top and Bottom		Piers	Bar Area			
		#13	#16	#13			#16	
Deck_fas=	1343.5	5.1673077		2.0669231	126.61		197.83	1063.1322
Over_deck_fas=	578.5	2.225		0				281.70725
Deck_ex=	2314.5	8.9019231		3.5607692				1831.4995
Deck_in=	2250	8.6538462		3.4615385				1780.4596

CHAPTER 7

Processed 2011 Diagnostic Load Test Strain Data

iSite-HS 113 Address: DB0001 192.168.1.192					
Channel	**Gauge ID**	**Girder**	**Station**	**Gauge Loc.**	**Working?**
1	SG-1	1	2	Right Side Top	Yes
2	SG-2	1	2	Right Side Bottom	Yes
3	SG-3	1	4	Right Side Top	Yes
4	SG-4	1	4	Right Side Bottom	Yes
5	SG-5	1	6	Right Side Top	Yes
6	SG-6	1	6	Right Side Bottom	Yes
7	SG-7	1	8	Right Side Top	Yes
8	SG-8	1	8	Right Side Bottom	Yes
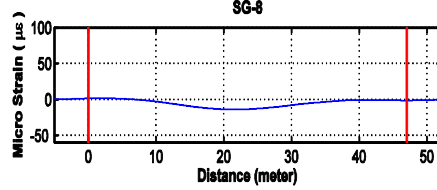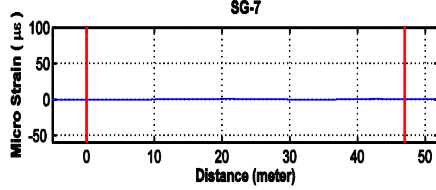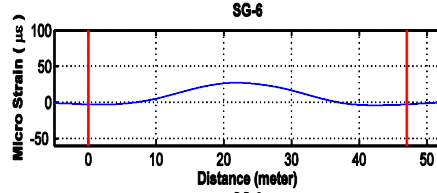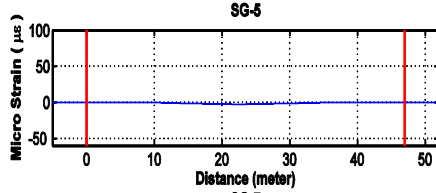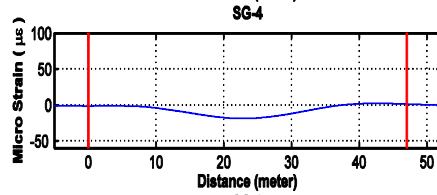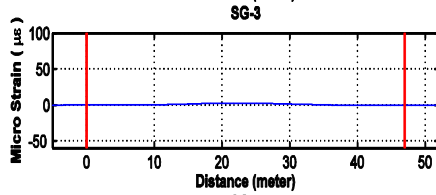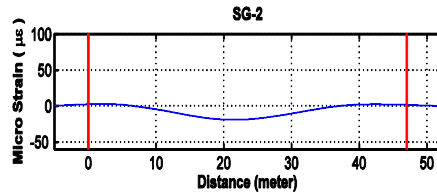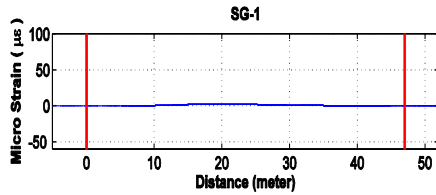
iSite-HS 112 Address: DB0099 192.168.1.191					
Channel	Gauge ID	Girder	Station	Gauge Loc.	Working?
1	SG-9	1	10	Right Side Top	Yes - 25.7 Hz Noise
2	SG-10	1	10	Right Side Bottom	Yes - 25.7 Hz Noise
3	SG-11	2	2	Left Side Top	Yes - 25.7 Hz Noise
4	SG-13	2	2	Left Side Bottom	Yes - 25.7 Hz Noise
5	SG-19	2	6	Left Side Top	Yes - 25.7 Hz Noise
6	SG-21	2	6	Left Side Bottom	Yes - 25.7 Hz Noise
7	SG-15	2	4	Left Side Top	Yes - 25.7 Hz Noise
8	SG-17	2	4	Left Side Bottom	Yes - 25.7 Hz Noise
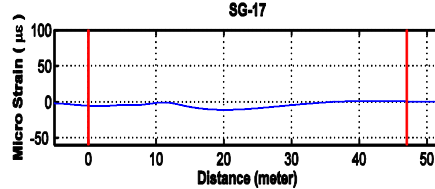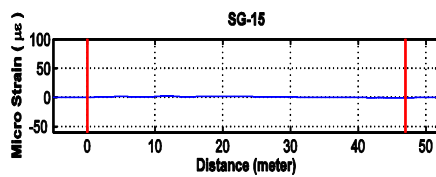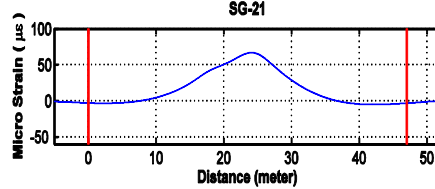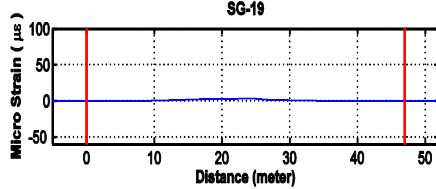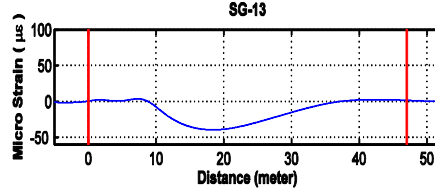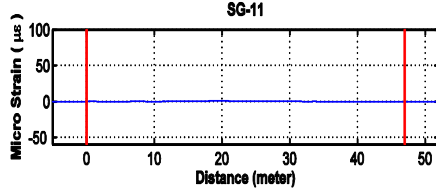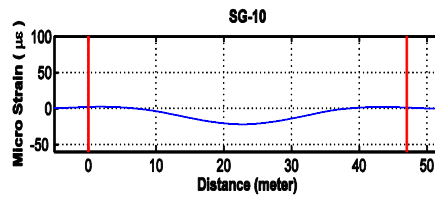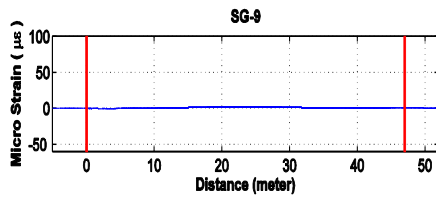
iSite-HS 111 Address: DB0098 192.168.1.190					
Channel	Gauge ID	Girder	Station	Gauge Loc.	Working?
1	SG-12	2	2	Right Side Top	Yes
2	SG-14	2	2	Right Side Bottom	Yes
3	SG-16	2	4	Right Side Top	Yes
4	SG-18	2	4	Right Side Bottom	Yes
5	SG-20	2	6	Right Side Top	Yes
6	SG-22	2	6	Right Side Bottom	Yes
7	SG-23	2	8	Left Side Top	Yes
8	SG-25	2	8	Right Side Bottom	Yes
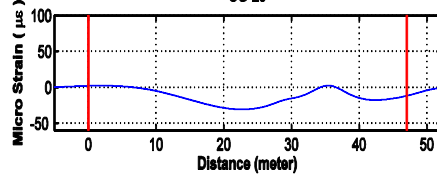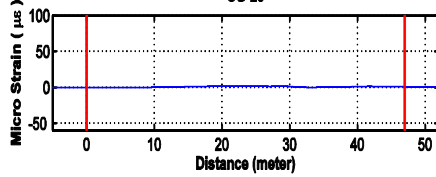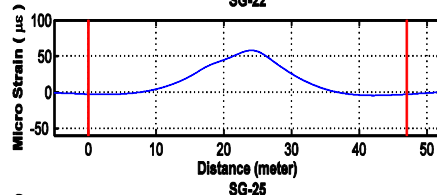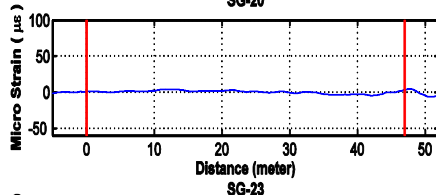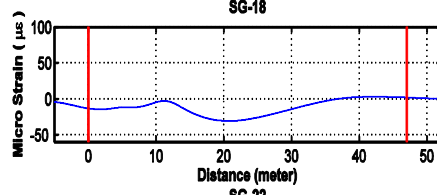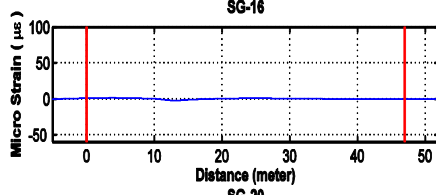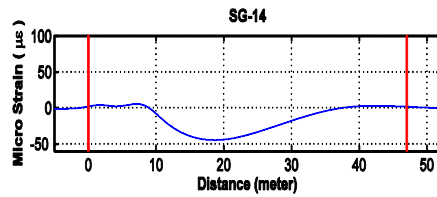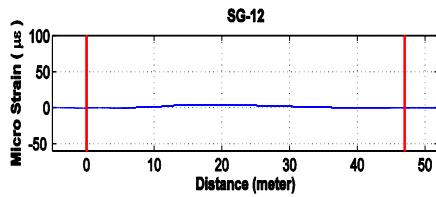
iSite-HS 110 Address: DB0097 192.168.1.189					
Channel	Gauge ID	Girder	Station	Gauge Loc.	Working?
1	SG-24	2	8	Left Side Top	Yes - 25.7 Hz Noise
2	SG-26	2	8	Left Side Bottom	Yes - 25.7 Hz Noise
3	SG-27	2	10	Left Side Top	Yes - 25.7 Hz Noise
4	SG-28	2	10	Right Side Top	Yes - 25.7 Hz Noise
5	SG-29	2	10	Left Side Bottom	Yes - 25.7 Hz Noise
6	SG-30	2	10	Right Side Bottom	Yes - 25.7 Hz Noise
7	SG-31	3	2	Left Side Top	Yes - 25.7 Hz Noise
8	SG-33	3	2	Left Side Bottom	Yes - 25.7 Hz Noise
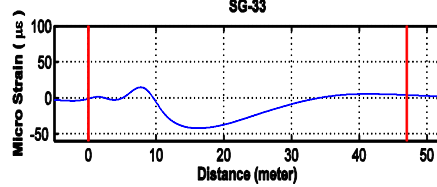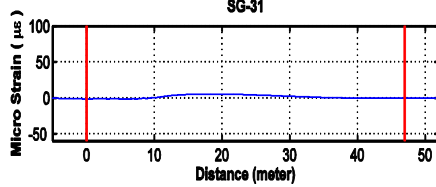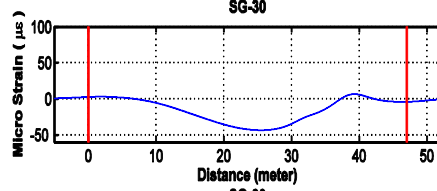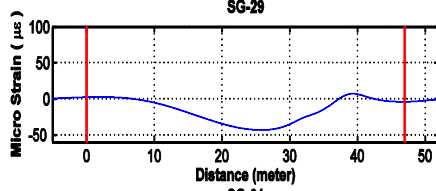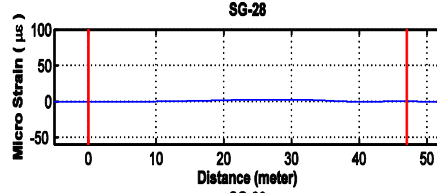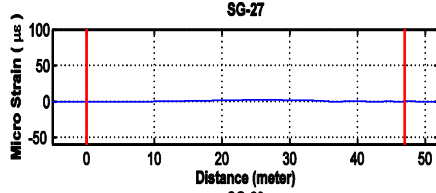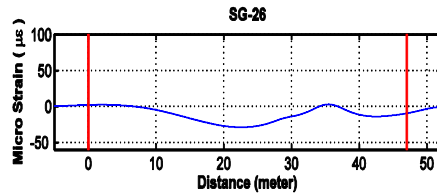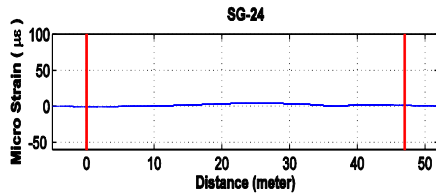
iSite-HS 109 Address: DB0096 192.168.1.188					
Channel	**Gauge ID**	**Girder**	**Station**	**Gauge Loc.**	**Working?**
1	SG-32	3	2	Right Side Top	Yes
2	SG-34	3	2	Right Side Bottom	Yes
3	SG-35	3	4	Left Side Top	Yes
4	SG-36	3	4	Right Side Top	Yes
5	SG-37	3	4	Left Side Bottom	Yes
6	SG-38	3	4	Right Side Bottom	Yes
7	SG-39	3	6	Left Side Top	Yes
8	SG-41	3	6	Left Side Bottom	Yes
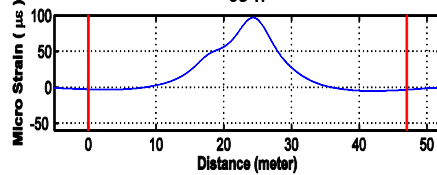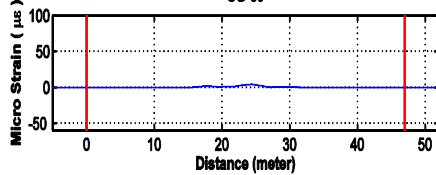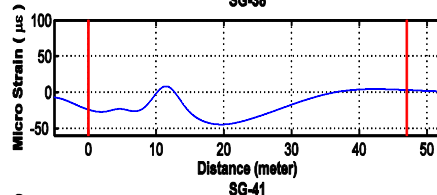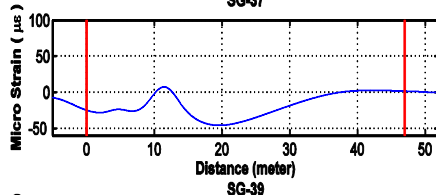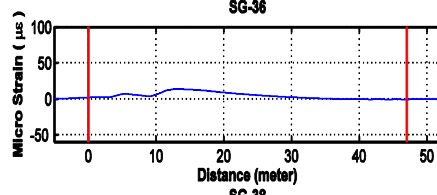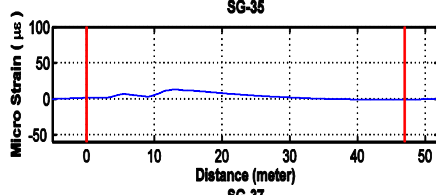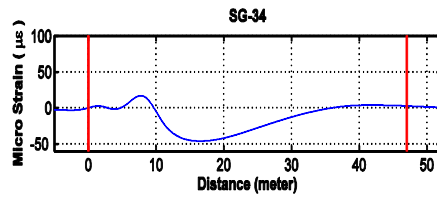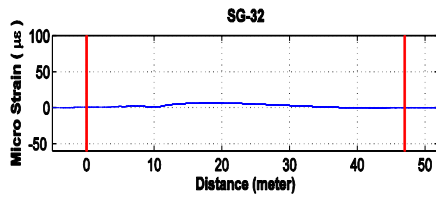
iSite-HS 108 Address: DB0095 192.168.1.187					
Channel	Gauge ID	Girder	Station	Gauge Loc.	Working?
1	SG-40	3	6	Right Side Top	Yes
2	SG-42	3	6	Right Side Bottom	Yes
3	SG-43	3	8	Left Side Top	Yes
4	SG-44	3	8	Right Side Top	Yes
5	SG-45	3	8	Left Side Bottom	Yes
6	SG-46	3	8	Right Side Bottom	Yes
7	SG-49	3	10	Left Side Bottom	Yes
8	SG-47	3	10	Left Side Top	Yes
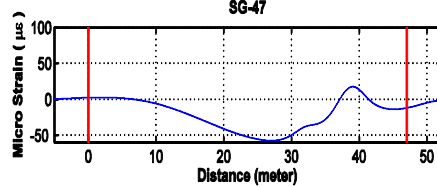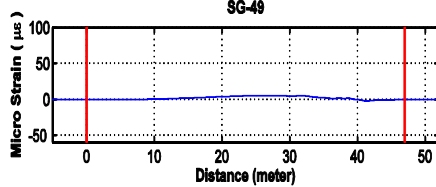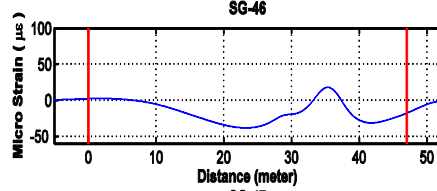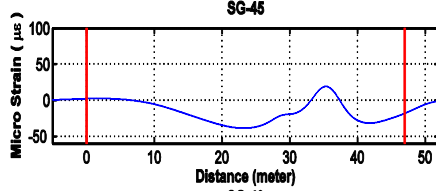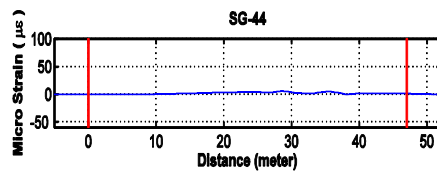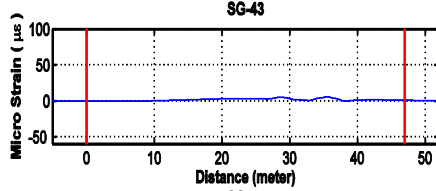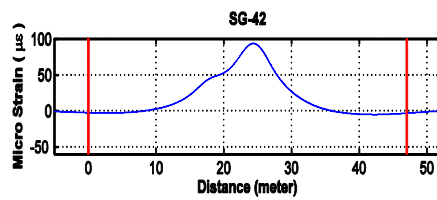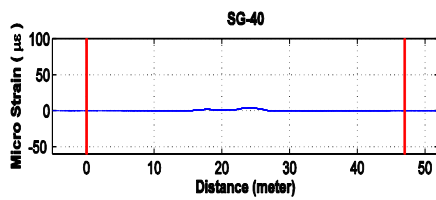
iSite-HS 107 Address: DB0094 192.168.1.186					
Channel	Gauge ID	Girder	Station	Gauge Loc.	Working?
1	SG-48	3	10	Right Side Top	Yes
2	SG-50	3	10	Right Side Bottom	Yes
3	SG-51	4	2	Left Side Top	Yes
4	SG-52	4	2	Right Side Top	Yes
5	SG-53	4	2	Left Side Bottom	Yes
6	SG-54	4	2	Right Side Bottom	Yes
7	SG-55	4	4	Left Side Top	Yes
8	SG-57	4	4	Left Side Bottom	Yes
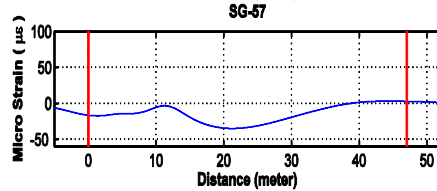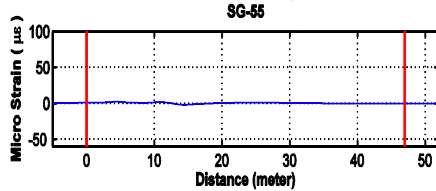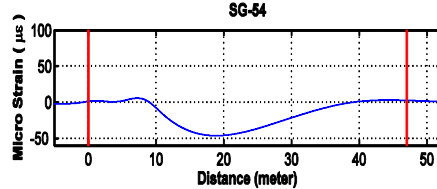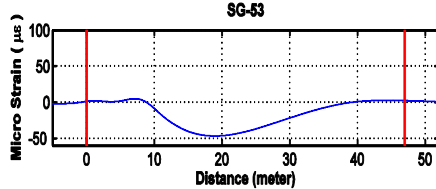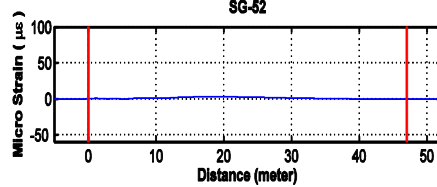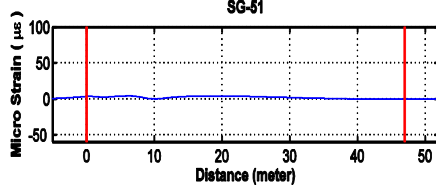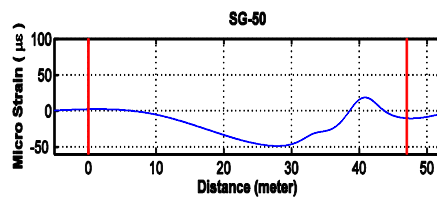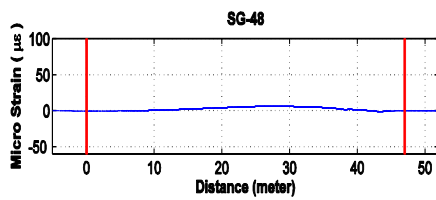
iSite-HS 106 Address: DB0093 192.168.1.185					
Channel	**Gauge ID**	**Girder**	**Station**	**Gauge Loc.**	**Working?**
1	SG-56	4	4	Right Side Top	Yes
2	SG-58	4	4	Right Side Bottom	Yes
3	Sg-59	4	6	Left Side Top	Yes
4	SG-60	4	6	Right Side Top	Yes
5	SG-61	4	6	Left Side Bottom	Yes
6	SG-62	4	6	Right Side Bottom	Yes
7	SG-63	4	8	Left Side Top	Yes
8	SG-65	4	8	Left Side Bottom	Yes
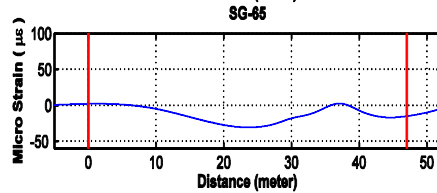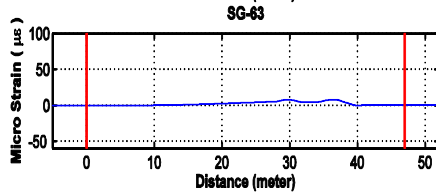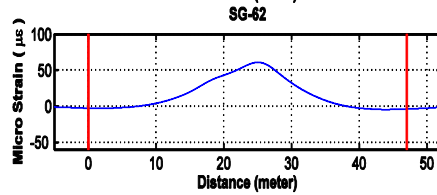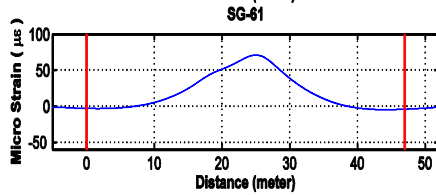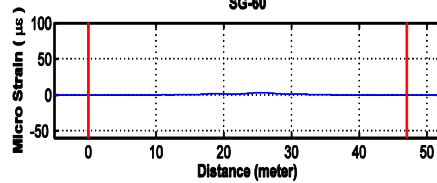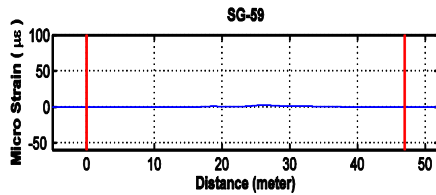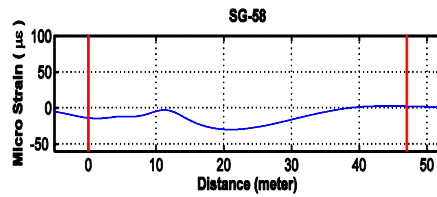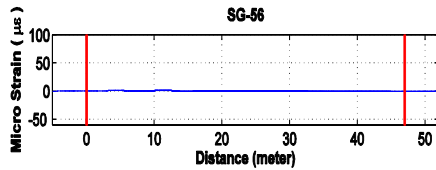
iSite-HS 105 Address: DB0092 192.168.1.184					
Channel	Gauge ID	Girder	Station	Gauge Loc.	Working?
1	SG-64	4	8	Right Side Top	Yes
2	SG-66	4	8	Right Side Bottom	Yes
3	SG-67	4	10	Left Side Top	Yes
4	SG-68	4	10	Right Side Top	Yes
5	SG-69	4	10	Left Side Bottom	Yes
6	SG-70	4	10	Right Side Bottom	Yes
7	SG-71	5	2	Left Side Top	Yes
8	SG-73	5	2	Left Side Bottom	Yes
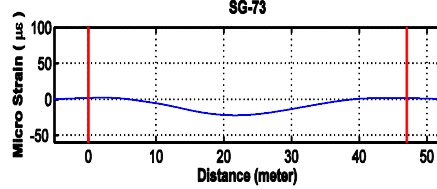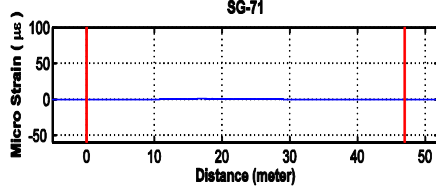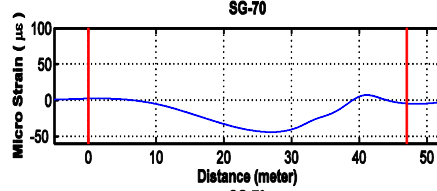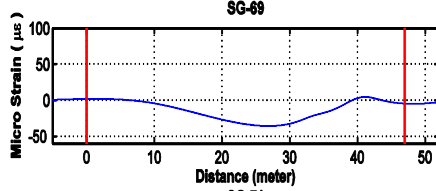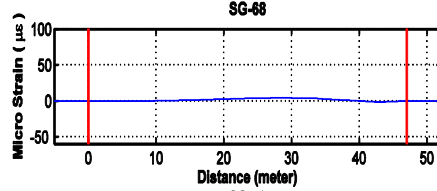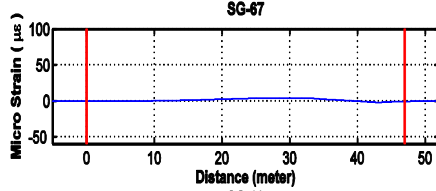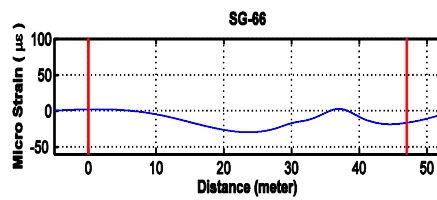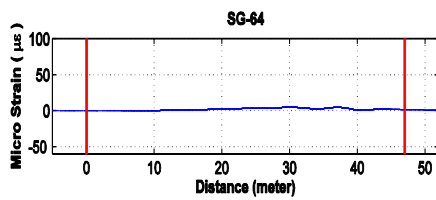
iSite-HS 104 Address: DB0091 192.168.1.183					
Channel	**Gauge ID**	**Girder**	**Station**	**Gauge Loc.**	**Working?**
1	SG-72	5	2	Right Side Top	Yes
2	Sg-74	5	2	Right Side Bottom	Yes
3	SG-75	5	4	Left Side Top	Yes
4	SG-76	5	4	Right Side Top	Yes
5	SG-77	5	4	Left Side Bottom	No
6	SG-78	5	4	Right Side Bottom	Yes
7	SG-79	5	6	Left Side Top	Yes
8	SG-81	5	6	Left Side Bottom	Yes
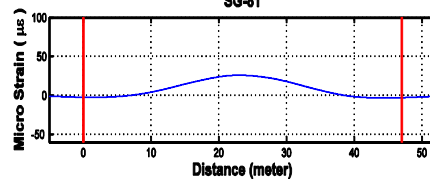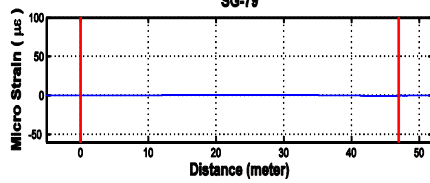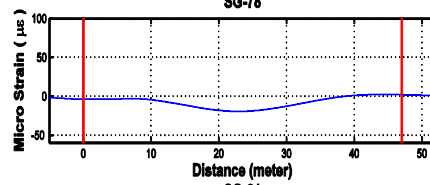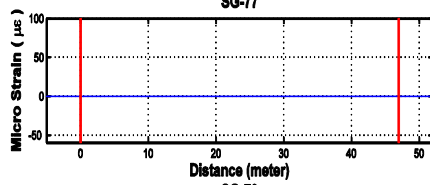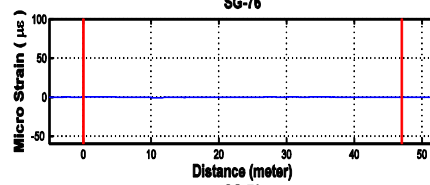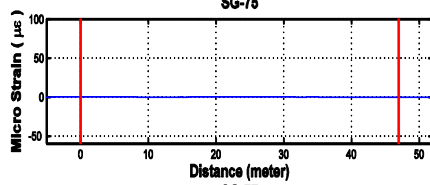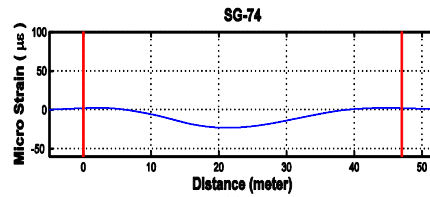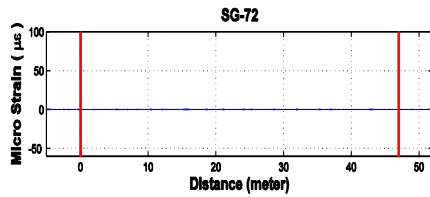
iSite-HS 103 Address: DB0090 192.168.1.182					
Channel	Gauge ID	Girder	Station	Gauge Loc.	Working?
1	SG-80	5	6	Right Side Top	Yes - Noisy
2	SG-82	5	6	Right Side Bottom	Yes - Noisy
3	SG-83	5	8	Left Side Top	Yes - Noisy
4	SG-84	5	8	Right Side Top	Yes - Noisy
5	SG-85	5	8	Left Side Bottom	Yes - Noisy
6	SG-86	5	8	Right Side Bottom	Yes - Noisy
7	SG-87	5	10	Left Side Top	Yes - Noisy
8	SG-89	5	10	Left Side Bottom	Yes - Noisy
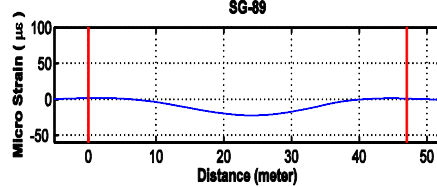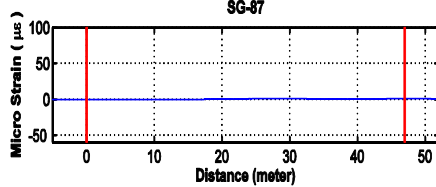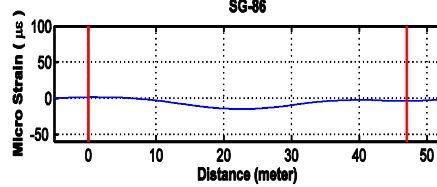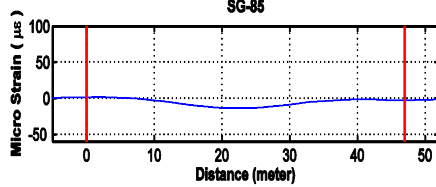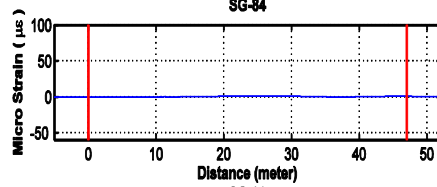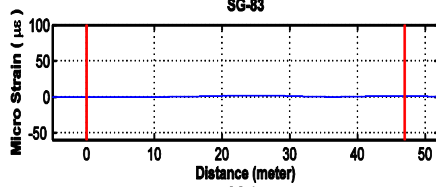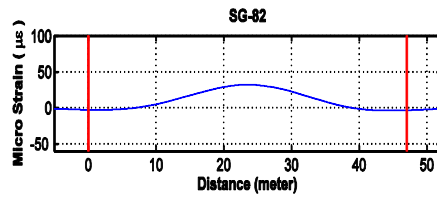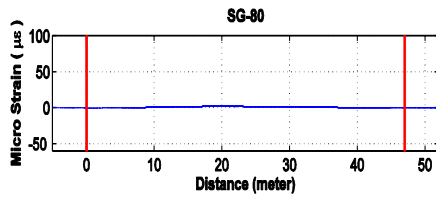
iSite-HS 102 Address: DB0089 192.168.1.181					
Channel	**Gauge ID**	**Girder**	**Station**	**Gauge Loc.**	**Working?**
1	SG-88	5	10	Right Side Top	Yes
2	SG-90	5	10	Right Side Bottom	Yes
3	SG-91	6	2	Left Side Top	Yes
4	SG-92	6	2	Left Side Bottom	Yes
5	SG-93	6	4	Left Side Top	Yes
6	SG-94	6	4	Left Side Bottom	Yes
7	SG-95	6	6	Left Side Top	Yes
8	SG-96	6	6	Left Side Bottom	Yes
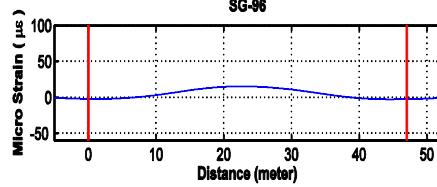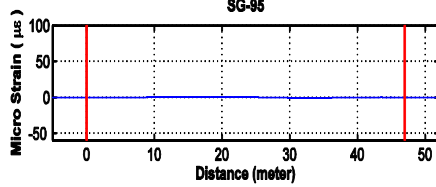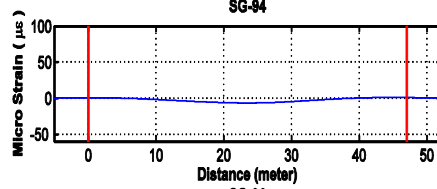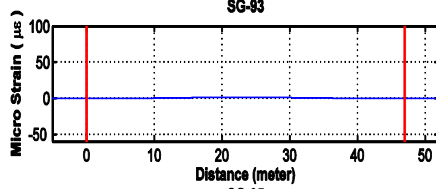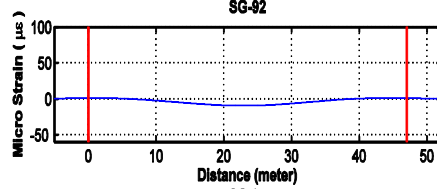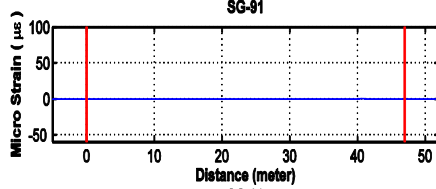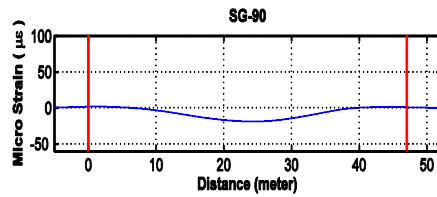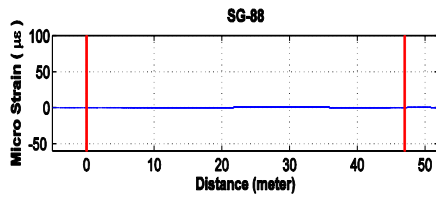
iSite-HS 101 Address: DB0088 192.168.1.180					
Channel	**Gauge ID**	**Girder**	**Station**	**Gauge Loc.**	**Working?**
1	SG-97	6	8	Left Side Top	Yes
2	SG-98	6	8	Left Side Bottom	Yes
3	SG-99	6	10	Left Side Top	Yes
4	SG-100	6	10	Left Side Bottom	No
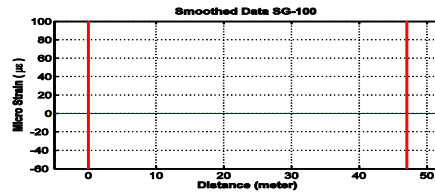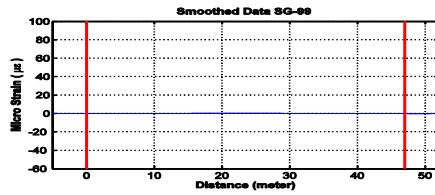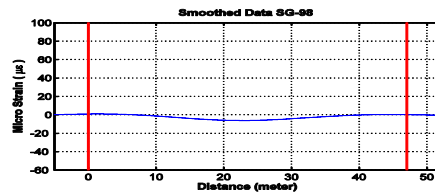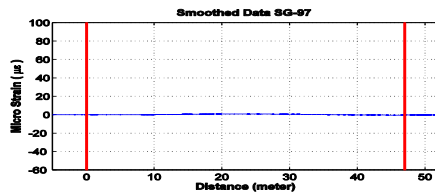
References

Alampalli, S.,Kunin, J. (2001) "Load Testing of an FRP Bridge Deck on a Truss Bridge", Special Report 137, Transportation Research and Development Bureau, New York State Department of Transportation

American Association of State Highway and Transportation Officials Virtis Opis Task Force Meeting (2011), Clearwater, FL January 12-13, 2011, accessed at http://vobug.org/Documents/Summary%20Minutes%20Virtis%20Opis%20Clearwater_Final.pdf

American Association of State Highway Officials (1931), "Standard Specifications for Highway Bridges and Incidental Structures, 1th Edition" Washington, D.C.

American Association of State Highway and Transportation Officials (2002), "Standard Specification for Highway Bridge, 17th Edition" Washington, D.C.

American Association of State Highway and Transportation Officials (2011a), "Manual for Bridge Evaluation, 2nd Edition" Washington, D.C.

American Association of State Highway and Transportation Officials (2010), "LRFD Bridge Design Specifications, 5th Edition" Washington, D.C.

American Association of State Highway and Transportation Officials (2011b), "Virtis 6.3.0, AASHTO LFD/ASD Superstructure Method of Solution Manual" Washington, D.C.

American Association of State Highway and Transportation Officials (2008), "Bridging the Gap - Restoring and Rebuilding the Nation's Bridges"

Barr, P. J., Woodward, C. B., Najera, B., and Amin, Md N.(2006), "Long-Term structural Health Monitoring of the San Ysidro Bridge", Journal of Performance of Constructed Facilities, 2006 doi:10.1061/(ASCE)0887-3828(2006)20:1(14) (7 pages)

Bridge Engineering: Construction and Maintenance, edited by Wai-Fah Chen and Lian Duan, CRC Press 2000, Section 5 – Design Philosophies for highway Bridges by John M. Kulicki

Catbas, N., Ciloglu, K., Celebioglu, A., Popovics, J. and Aktan E. (2001) "Fleet Health Monitoring of Large Populations: Aged concrete T-Beam Bridges in Pennsylvania" SPIE Conference Proceedings, 2001 doi:10.1117/12.435626

Computers and Structures Inc. (2010), "Integrated finite element analysis and design of structures" *SAP2000 v14*, Berkley, California

Computer and Structures Inc. (2011), "Modeling, analysis and design of bridge structures" *CSIBridge v15*, Berkeley, California

DeWolf, J.T., (2009) "History of Connecticut's Short-Term Strain Program for Evaluation of Steel Bridges" Report No. CT-2251-F-09-6, Connecticut Department of Transportation, http://ntl.bts.gov/lib/43000/43700/43744/01149532.pdf

Ellingwood, B. R., Zureick, H. A., Wang, N. and O'Malley, C. (2009), "Condition Assessment of Existing Bridge Structures" Georgia Institute of Technology, August 1, 2009, accessed at http://www.dot.state.ga.us/doingbusiness/research/projects/Documents/take4Report_0501bridgestructures.pdf

Emin Aktan, Daniel N. Farhey, David L. Brown, "Condition Assessment for Bridge Management", Journal of Infrastructure Systems, 1996

Federal Highway Administration (2006), "Bridge Load Ratings for the National Bridge Inventory", accessed at http://www.fhwa.dot.gov/bridge/nbis/103006.cfm

Federal Highway Administration (2011), "Our Nation's Highways: 2011", accessed at http://www.fhwa.dot.gov/policyinformation/pubs/hf/pl11028/chapter7.cfm

Gary Munkelt, HL93 Truck loads vs. HS20 Truck Loads, Business & Management, Precast INC. Magazine, July 28, 2010

Kukay, B., Barr, P., Halling, M. and Womack, K. (2010) "Determination of Residual Prestress Force of In-Service Girders using Nondestructive Testing", Structural Congress, May 12-15, 2010, Orlando, Florida

Massachusetts Highway Department, MHD (2005), "Bridge Manual, Part I and Part II" Massachusetts Department of Transportation Highway Division

Massachusetts Highway Department, MHD (2007), "Bridge Manual, Part I and Part II" Massachusetts Department of Transportation Highway Division

Massachusetts Department of Transportation Highway Division, MassDOT, 2012 Permit Limit accessed at http://www.mhd.state.ma.us/default.asp?pgid=content/permPL&sid=about

National Cooperative Highway Research Program, 1998, "Manual for Bridge Rating Through Load Testing", Washington, DC, Transportation research Board, NCHRP Research Result Digest 234

National Cooperative Highway Research Program, 2011, "A Comparison of AASHTO Bridge Load Rating Methods", Washington, DC, Transportation research Board, NCHRP Report 700

Paul J. Lefebvre, "The development and deployment of an instrumentation plan and baseline structural model of a steel girder bridge for long-term structural health monitoring and design verification", Master of Science Thesis, University of New Hampshire, May 2010

Phelps, J. E (2010), "Instrumentation, Non-destructive Testing and Finite Element Model Updating for Bridge Evaluation", Master of Science Thesis, May 2, 2010, Tufts University

Richard M. Baker, Jay Alan Puckett, Design of Highway Bridges an LRFD Approach, John Wiley & Sons, 2007

Sanayei, M., Phelps, J. E.., Sipple, J. D., Bell, E., Brenner, B. R. (2012), "Instrumentation, Nondestructive Testing, and FEM Updating for Bridge Evaluation Using Strain Measurement"

Journal of Bridge Engineering, 17, 130(2012); http://dx.doi.org/10.1061/(ASCE)BE.1943-5592.0000228

Santini-Bell, E., Lefebvre, P., Sanayei, M., Brenner, B., Sipple, J. and Peddle, J. (2012). "Objective Load Rating of a Steel Girder Bridge Using Structural Modeling and Health Monitoring", Accepted for publication in the ASCE Journal of Structural Engineering.

Schlune, H., Plos, M., Gylltoft, K. "Improved Bridge Evaluation Through Finite Element Model Updating Using Static and Dynamic Measurements", Engineering Structures, Vol. 31, Issue 7, 2009. doi http://dx.doi.org/10.1016/j.engstruct.2009.02.011

Sanayei, M., Saletnik, M J., (1996) "Parameter Estimation of Structures from Static Strain Measurements. I: Formulation" Journal of structural engineering, Vol. 122, No. 4 pp. 555-562. doi http://dx.doi.org/10.1061/(ASCE)0733-9445(1996)122:5(555)

Sanayei, M., Imbaro, R. G., McClain, A.S.J., Brown, C. L., (1997) "Structural Model Updating Using Experimental Static Measurements" Journal of Structural Engineering, Vol. 123, No. 6, pp 792. doi http://dx.doi.org/10.1061/(ASCE)0733-9445(1997)123:6(792)

Virtis 6.3 (2011), "Bridge load rating product" AASHTOWare®, July 1, 2011, Washington, D.C.

Yost, R.J., Schulz J.L. and Commander, B.C., (2005) "Using NDT Data for Finite Element Model Calibration and Load Rating of Bridges" Processing of the 2005 Structures Congress and the 2005 Forensic Engineering Symposium, doi:http://dx.doi.org/10.1061/40753(171)3

Walther, R. A., Chase, S. B. (2006), "Condition Assessment of Highway Structures Past, Present, and Future", 50 Years of Interstate Structures Past, Present and Future, Transportation Research Circular Number E – C104, September 2006 American